Unveiling some supersymmetric scenarios using tau-leptons at the Large Hadron Collider

By

Sanjoy Biswas

Harish-Chandra Research Institute, Allahabad

A Thesis submitted to the
Board of Studies in Physical Science Discipline
In partial fulfilment of the requirements
For the degree of
DOCTOR OF PHILOSOPHY
of

Homi Bhabha National Institute

June, 2011

Certificate

This is to certify that the Ph. D. thesis titled "Unveiling some supersymmetric scenarios using tau-leptons at the Large Hadron Collider" submitted by Sanjoy Biswas is a record of bonafide research work done under my supervision. It is further certified that the thesis represents independent work by the candidate and collaboration was necessitated by the nature and scope of the problems dealt with.

Date:

Biswarup Mukhopadhyaya
Thesis Adviser

Declaration

This thesis is a presentation of my original research work. Whenever contributions of others are involved, every effort is made to indicate this clearly, with due reference to the literature and acknowledgement of collaborative research and discussions.

The work is original and has not been submitted earlier as a whole or in part for a degree or diploma at this or any other Institution or University.

This work was done under the supervision of Professor Biswarup Mukhopadhyaya, at the Harish-Chandra Research Institute, Allahabad, India.

Date:

Sanjoy Biswas
Ph. D. Candidate

Dedicated to my family and friends.

Acknowledgements

First of all, I would like to take this opportunity to thank my advisor Professor Biswarup Mukhopadhyaya. He is an excellent guide and a very good friend too. The way he judges his students and guides them towards the successful completion of their PhD is a lesson to learn for me for going ahead in this field. His continuous encouragement at all levels of difficulties that appeared during the course of my PhD work inspired me to work hard. He interacts with the students quite actively and freely. I am very fortunate to have received his sincere and affectionate guidance. I have experienced very happy and enjoyable moments with him and his family during my stay at Harish-Chandra Research Institute (HRI), which I will cherish all my life.

I am also thankful to all my collaborators. I enjoyed working with Dr. Sourov Roy and Joydeep Chakrabortty. I thank Dr. Sourov Roy, who is an excellent collaborator full of enthusiasm. I have learnt various aspects of supersymmetric theories from him during our discussions. I also thank Joydeep Chakrabortty. He is not only my collaborator but also my batchmate and a very good friend, too. We started our research career together and I am very lucky to have him beside me throughout our stay at HRI. My sincere thanks are due to Professor Mihoko M. Nojiri. I have learnt quite a lot on various issues related to collider physics from her. It was a really nice experience to work with her, enjoying the hospitality in Japan. I am grateful to Dr. Subhaditya Bhattacharya. He is not only my collaborator, but a virtual guide as well. He is the first person to introduce me to the field of collider physics. I enjoyed every bit of time spent with him on various discussions. Together we shared a lot of unforgettable moments.

My work was partially supported by funding available from the Department of Atomic Energy, Government of India for the Regional Centre for Accelerator-based Particle Physics (RECAPP), Harish-Chandra Research Institute. I thank RECAPP for not only providing me with monitory support for visits at different institutes in India and abroad for academic collaborations but also for organising different schools and conferences on topical issues which have benefitted me immensely. I am grateful to the cluster computing facility of my institution where

part of my work has been carried out (`http://cluster.mri.ernet.in`).

Next, I would like to thank all the instructors who taught us during our course work. It not only strengthened my basic understanding of physics but also equipped me quite well with tools required to handle a research problem in theoretical physics. In particular, I am thankful to Professor Ashoke Sen. His way of teaching is an inspiration to me. He changed my way of thinking towards physics in general. I feel very proud and fortunate to have obtained the opportunity to attend his lectures and also to interact with him. I also thank the tutors of various courses that I took. I have benefitted a lot discussing physics with them. I thank Shamik Banerjee for helpful discussions on various physics issues. With Satyanarayan Mukhopadhyay and Nishita Deshai, two of my batchmates, I had useful discussions on various occasions.

I thank the members of the particle physics phenomenology group of HRI: Dr. Asesh K. Dutta, Professor Raj Gandhi, Professor V. Ravindran, Dr. Sandhya Choubey, Dr. Andreas Nyffeler and Dr. Kirtiman Ghosh. I had the opportunity to interact with them while doing projects which one needs to undergo before joining the group. I am also thankful to the non-academic members of HRI for their sincere cooperation. My special thanks go to Mrs. Seema Agarwal and Dr. Archan Tandon whom I always found very willing and prompt in helping me whenever the situation arose. They were really exceptional throughout my stay at HRI, extending their helping hands in resolving various non-academic issues. I also thank all the supporting staff of HRI, in particular the mess workers for providing me with good food.

I am thankful to my senior friends at HRI: Subhankar Dutta, Nabamita Banerjee, Subhaditya Bhattacharya, Arjun Bagchi, Rajesh Gupta, Soumya Das, Priyotosh Bandyopadhyay, Paramita Dey, Sudipta Das, Shamik Banerjee, Vivekanand Singh, Mohan Chintamani, Bhavin Moriya and Manimala Mitra. I thank my batchmates at HRI: Joydeep Chakrabortty, Shailesh Lal, Nishita Deshai, Dhiraj Hazra, Satyanarayan Mukhopadhyay, Jaban Meher and Mahendra Verma. I also thank my junior friends: Atri Bhattacharya, Arijit Kundu, Saurabh Niyogi, Sourav Mitra, Manoj Mandal, Ujjal Dey, Saurabh Pradhan, Arunabha Saha and Sabyasachi Tarat. I have enjoyed their company very much during my stay at HRI. The frequent get-togethers at city restaurants or daily *boithak* at midnight at the guest-house were the most enjoyable and refreshing moments of my PhD tenure. HRI is a wonderful place for the students but without their presence, life would have

been very difficult indeed.

I would like to thank Biswarup Mukhopadhyaya, Satyanarayan Mukhopadhyay, Saurabh Niyogi and Aarti Girdhar for carefully reading the thesis and providing valuable suggestions.

It's pleasure to thank all my teachers who were instrumental in this long academic journey: from the school days to the university. To name a few to whom I largely owe whatever I have been able to achieve: Pranab Sengupta, Ratan K. Das, Prakash Kundu, Narayan Kundu, Dr. Asit Chakraborty, Professor Prasanta Rudra, Professor Padmanava Dasgupta, Professor Siddhartha Roy, Late Professor Satya Biswas, Professor Arunava Chakrabarti and Professor Chirantan Niyogi. I am also grateful to Partha Bhattacharya who used to teach me during my early days of school. He continues to be my friend, philosopher and guide.

I thank two of my dearest friends Arnab Chatterjee and Avijit Paul who continue to be with me since my school days. Together we shared our successes and failures, joy and sorrow. We continue to have wonderful times during my stay at my hometown, Ranaghat.

However, all these would not have been possible without the support from my parents. I am indebted to their dedication and sacrifice which laid the foundation of this work. Their continuous encouragement and strong belief on me helped me pursue whatever I am interested in. The endless love and affection they imparted all along are truly unparalleled. I would like to express my deepest gratitude and love to them. I offer my sincere regards to my late grandfather and grandmother for their blessings. I am also very grateful to my dearest sister and my brother-in-law. Their support and love during all the ups and downs in my life are truly exceptional. Last, but not the least, I must mention my sweet niece, Sneha, who has brought a lot of joy to our lives. My love and best wishes to her.

List of Publications

(The thesis is based on those marked with asterisk)

* 1) S. Biswas and B. Mukhopadhyaya, "*Neutralino reconstruction in supersymmetry with long-lived staus*", Phys. Rev. **D79:115009**, (2009), arXiv:0902.4349 [hep-ph]

* 2) S. Biswas and B. Mukhopadhyaya, "*Chargino reconstruction in supersymmetry with long-lived staus*", Phys. Rev. **D81:015003**, (2010), arXiv:0910.3446 [hep-ph]

* 3) S. Biswas, "*Reconstruction of the left-chiral tau-sneutrino in supersymmetry with a right-sneutrino as the lightest supersymmetric particle*", Phys. Rev. **D82:075020**, (2010), arXiv:1002.4395 [hep-ph].

4) S. Biswas, J. Chakrabortty and S. Roy, "*Multi-photon signal in supersymmetry comprising non-pointing photon(s) at the LHC*", Phys. Rev. **D83:075009**, (2011), arXiv:1010.0949 [hep-ph]

* 5) S. Bhattachrya, S. Biswas, B. Mukhopadhyaya and M. M. Nojiri, "*Signatures of supersymmetry with non-universal Higgs mass at the Large Hadron Collider*", arXiv:1105.3097 [hep-ph]

Synopsis

- **Name: Sanjoy Biswas**
- **Thesis Title: Unveiling some supersymmetric scenarios using tau-leptons at the Large Hadron Collider.**
- **Supervisor: Professor Biswarup Mukhopadhyaya**
- **Submitted to Homi Bhaba National Institute (HBNI)**

The Standard Model (SM) of particle physics is incomplete in various senses. To list a few, the Higgs mass is unstable under the quantum correction, the SM can't provide a viable dark matter candidate, the observed baryon asymmetry of the Universe remains unexplained and moreover the evidences of non-vanishing neutrino masses and mixing are unexplained. Therefore, there are ample reasons to look for physics beyond the Standard Model.

The Supersymmetric (SUSY) extension of the SM is one of the most popular and theoretically well motivated framework for physics beyond the SM. It not only solves the problem of quadratic divergence appearing in the quantum correction of Higgs mass but also provide a viable candidate for dark matter in terms of the weakly interacting stable massive particle in its $\mathcal{R}$-parity conserving form (with $\mathcal{R}$- parity defined by $\mathcal{R} = (-)^{3B+L+2S}$).

Searches for supersymmetry at the collider experiments and currently at the Large Hadron Collider (LHC) are largely based on signals with missing transverse energy ($\not{E}_T$) due to the pair production of invisible lightest supersymmetric particles (LSP) which go undetected at the collider.

However, $\not{E}_T$ is not a unique signal of SUSY. Scenarios with quasi-stable charged particles are also viable possibilities within SUSY. Such a scenario can arise when the next-to-lightest SUSY particle (NLSP) is a charged particle and the decay of the NLSP to the LSP is suppressed due to very small coupling or when the NLSP and LSP are degenerate in masses. For example, one can have a gravitino LSP in a supergravity (SUGRA) model. They can be envisioned in gauge-mediated SUSY breaking theories as well. In the MSSM, too, one can have the so-called co-annihilation region of dark matter, where a stau and the neutralino LSP are closely degenerate, leading to a quasi-stable character of the former. One

can also have a scenario, the one we have worked with, in which the minimal supersymmetric standard model (MSSM) is augmented with a right-chiral neutrino superfield for each generation, motivated by the non-vanishing neutrino masses and mixing. The essence of SUSY signal lies not in $\not{E}_T$ but in charged tracks due to massive particles, seen in the muon chambers. From the kinematics of these charged particles and a detailed study of the momenta of the final state particles, which often include tau produced in association with charged tracks, one is able to reconstruct the masses of various superparticle.

The thesis aims at looking at the possibilities of reconstructing the masses of various superparticles in such scenarios. We have suggested some techniques for reconstruction of the masses of the neutralino, the lightest chargino and the left-chiral tau-sneutrino in this long-lived stau scenario.

- To reconstruct the neutralino we have considered pair production of neutralinos in SUSY cascades. It further decays into a $\tilde{\tau}\tau$ pair. The final state consists of $2\tau_j + 2\tilde{\tau} + \not{E}_T + X$, where, X comprises of all the hard jets arising from SUSY cascades. Reconstruction of the neutralino requires the knowledge of four-momenta of tau as well as stau. We first reconstruct the two taus in the final state from the knowledge of total $\not{E}_T$ of that event. The four momenta of the stau (which shows up as a charged track in the muon chamber) are not completely known. From the bending of the track only its three momenta can be measured. To measure the mass of the particle (lighter stau) associated with the charged track we have prescribed a method of extracting it on a event-by-event basis. Then the mass of the neutralino can be obtained from the invariant mass distribution of the $\tilde{\tau}\tau$ pair.

- The chargino has been reconstructed considering the associated production of it with the neutralinos in SUSY cascades. The chargino further decays into a $\tilde{\tau}\nu_\tau$ pair and the neutralino on the other side decays into a $\tilde{\tau}\tau$ pair. The final state in this case consists of $\tau_j + 2\tilde{\tau} + \not{E}_T + X$. However, this final state can be faked by other SUSY processes. We have suggested a way of reducing these SUSY backgrounds imposing various cuts. The chargino mass, can then be found from the transverse mass distribution of the $\tilde{\tau}\nu_\tau$-pair, where we have also prescribed a way to find the transverse component of the four-momenta of the neutrino out of a chargino decay.

- The left-chiral tau sneutrino ($\tilde{\nu}_{\tau_L}$) has been reconstructed in a way similar to

that for the chargino. $\tilde{\nu}_{\tau_L}$ is predominantly produced in SUSY cascade via the decay of second lightest neutralino or the chargino and it further decays into a $\tilde{\tau}W$ pair. Therefore, we have an additional W in the final state in addition to that considered for chargino case, namely, $\tau_j + W + 2\tilde{\tau} + \not{E}_T + X$. We have suggested two different methods for reconstructing the mass of the left-chiral tau sneutrino. One of them is independent of the mass of the other SUSY particles whereas, the other one is more model dependent but has better signal to background ratio.

In each of the above cases, we have also addressed the possible SM backgrounds and suggested various cuts for their elimination. The method of reconstruction that we have suggested is not limited to the scenario with right-handed sneutrino LSP alone. In fact it can be applied to all those cases where the stau is long-lived.

The thesis also focuses on aspects of theories with non-universal Higgs mass (NUHM). One of the most striking feature of this theory is that the lighter stau mass eigenstate is dominated by the left-chiral stau component owing to the large negative value of $m^2_{H_u} - m^2_{H_d}$ where, $m^2_{H_u}$ and $m^2_{H_d}$ are the mass squared value of the Higgs doublets which give masses to the up-type and down-type quarks respectively. This is rather difficult to obtain in an mSUGRA scenario where, the lighter stau mass eigenstate is dominantly right-chiral. Hence, the tau produced in the SUSY cascade in such a scenario will be left polarised as long as the lighter chargino and first and second neutralino are gaugino-like. We have shown that studying the polarisation of the tau, it is possible to distinguish the NUHM scenario from mSUGRA in the same sign di-tau channel at the LHC for a substantial region in the $m_0 - m_{1/2}$ plane. In addition, we have studied a charge asymmetry in the jet-lepton invariant mass distribution, arising from decay chains of squarks leading to leptons of the first two families. Using these two types of discriminators, we conclude that it is indeed possible to identify NUHM scenario at the LHC.

Contents

Part I

Introduction

Chapter 1

The Standard Model of Particle Physics: Outline

1.1 Introduction

The standard model (SM) of particle physics is a successful quantum field theory, which describes the interactions among elementary particles [1]. In nature, all the known phenomena observed so far, can be described in terms of the following four fundamental interactions:

- Strong interaction
- Weak interaction
- Electromagnetic interaction
- Gravitational interaction

Among the four fundamental forces, only the first three are correctly described by the SM. Gravity is irrelevant at the highest energy scale of particle accelerator experiment achieved till date, and therefore its non-inclusion does

not affect the explanation of whatever has been observed so far in the world of elementary particles.

To outline the basic construction of the SM, all the matter particles are spin-1/2 fermions which are further classified into quarks and leptons. They occur in three families carrying identical quantum numbers but with progressively higher masses. The interactions among the particles are introduced by demanding the invariance of the matter Lagrangian under a local $SU(3)_C \otimes SU(2)_L \otimes U(1)_Y$ gauge group [2,3]. And this is achieved by introducing new vector fields, known as gauge fields. The quanta which are the spin-1 excitations of these fields, are called gauge bosons and play the role of force carriers.

In Table 1.1 we tabulate the transformation properties of the fields corresponding to particles of the first family under the SM gauge-group:

Fermion	$SU(3)_C$	Hypercharge, Y	Isospin	T_3	EM Charge, Q
$\bar{d}_R$	$\bar{3}$	$-\frac{2}{3}$	0	0	$-\frac{1}{3}$
$\bar{u}_R$	$\bar{3}$	$+\frac{4}{3}$	0	0	$\frac{2}{3}$
$Q = \begin{pmatrix} u \\ d \end{pmatrix}_L$	3	$+\frac{1}{3}$	$\frac{1}{2}$	$+\frac{1}{2}$ $-\frac{1}{2}$	$+\frac{2}{3}$ $-\frac{1}{3}$
e_R^-	singlet	-2	0	0	-1
$L = \begin{pmatrix} \nu_e \\ e^- \end{pmatrix}_L$	singlet	-1	$\frac{1}{2}$	$+\frac{1}{2}$ $-\frac{1}{2}$	0 -1

Table 1.1: *Standard model fermions of the first family and their gauge quantum numbers.*

The table replicates itself for the other two generations of fermions. The gauge fields belong to the adjoint representation of the SM gauge-group. The strongly interacting sector contains eight massless vector fields G_μ^a ($a = 1, 2, .., 8$), known as the gluon fields corresponding to the $SU(3)_C$ gauge group. Only the quarks which transform under the $SU(3)_C$ gauge group non-trivially (see Table 1.1) in-

teract with these gluon fields with a strength g_c. In addition, the gluons also have self-interactions (both trilinear and quartic), since they posses non-trivial $SU(3)_C$ charges. The gauge bosons corresponding to the $SU(2)_L$ gauge group are the three vector fields W^i_μ ($i = 1, 2, 3$), which couple to the weak isospin current with coupling constant g. The vector field B_μ is associated with the $U(1)_Y$ group, which couples to the weak hypercharge current with strength conventionally taken as $g'/2$. The fields $W^\pm = \frac{1}{\sqrt{2}}(W^1_\mu \mp iW^2_\mu)$ describe the charged bosons $W^\pm$. From Table 1.1 it is clear that the gauge bosons W^i_μ couple to the left-chiral fermions only and the right-chiral fermions are singlets under this gauge interaction, a feature together with different hypercharge assignments of the left- and right-handed fermions lead to violation of parity in the SM.

Origin of mass: Higgs mechanism

The particle spectrum of the SM described above is still incomplete. So far, we have only considered the interactions among the particles which is a consequence of local gauge invariance. However, invariance under $SU(2)_L \otimes U(1)_Y$ implies that all the fermions as well as the gauge bosons have to be massless. Explicitly introducing masses for them threatens the good features of the theory, such as renormalisability and unitarity [4].

The way out of this, is to introduce the mass term in the Lagrangian by breaking the gauge symmetry spontaneously [5].

To break the gauge symmetry spontaneously, in the minimal form, one needs to introduce a complex scalar field (H), known as Higgs field, a doublet under $SU(2)_L$ and carrying a hypercharge +1 [6]:

$$H = \begin{pmatrix} h^+ \\ h^0 \end{pmatrix} \tag{1.1}$$

with

$$h^+ = \frac{1}{\sqrt{2}}(h_1 + ih_2) \tag{1.2}$$

$$h^0 = \frac{1}{\sqrt{2}}(h_3 + ih_4) \tag{1.3}$$

The $SU(2)_L \otimes U(1)_Y$ invariant Lagrangian corresponding to this field is given by-

$$\mathcal{L} = |(i\partial_\mu - gT \cdot W_\mu - g'Y/2B_\mu)H|^2 - V(H^\dagger H) \tag{1.4}$$

where,

$$V(H^\dagger H) = \mu^2 H^\dagger H + \lambda (H^\dagger H)^2 \qquad (\text{with } \mu^2 < 0 \text{ and } \lambda > 0). \tag{1.5}$$

One can also write a set of interaction terms of the fermions with this Higgs field, the so called Yukawa interaction in a gauge invariant way:

$$y_\ell H L \bar{e}_R \tag{1.6}$$

for the leptons and similar terms can be written for the quarks as well.

There exists a set of points at which $V(H^\dagger H)$ is minimised. If we choose the real part of the neutral component of the Higgs field to acquire a nonvanishing vacuum expectation value (VEV), in the following form

$$< H >= \frac{1}{\sqrt{2}} \begin{pmatrix} 0 \\ v \end{pmatrix} \tag{1.7}$$

the effect is the spontaneous breakdown of $SU(2)_L \otimes U(1)_Y$ to $U(1)_{em}$. The above mechanism generates masses of the gauge bosons and the fermions. The former acquires masses from the kinetic energy terms of the Higgs field 1.4, and the latter from the Yukawa interaction terms 1.6, once the Higgs field acquires a VEV.

If $SU(2)_L \otimes U(1)_Y$ is broken, the neutral fields W^3_μ and B_μ mix in such a way that the mass eigenstates are:

$$A_\mu = B_\mu \cos\theta_W + W^3_\mu \sin\theta_W \qquad (\text{massless}) \tag{1.8}$$

$$Z_\mu = -B_\mu \sin\theta_W + W^3_\mu \cos\theta_W \qquad (\text{massive}) \tag{1.9}$$

where θ_W is called the Weinberg angle or weak mixing angle. The gauge bosons ($W^\pm, Z$) become massive. The massless vector field A_μ corresponds to the photon field that couples to the matter fields with electromagnetic coupling constant e, the electronic charge. And it is related to the $SU(2)_L$ and $U(1)_Y$ coupling constants in the following way:

$$g \sin\theta_W = g' \cos\theta_W = e \tag{1.10}$$

The theory based on this spontaneously broken gauge symmetry is renormalisable, which means that it is possible to systematically cancel divergences

to all orders of quantum corrections. That a spontaneously broken gauge theory preserves this feature was demonstrated by t' Hooft and Veltman [4]. This theory has been tested rather precisely by experiments and no significant deviation has been found so far apart from the hint of small neutrino masses, while in the SM they are massless.

However, the Higgs boson which is a crucial component of the SM is yet to be observed in experiments. The mass of the Higgs boson (m_H) is a free parameter in the SM; however precision measurements suggest that m_H should be $\sim$ 114.4-166 GeV with 95% confidence level [7]. The search for Higgs at the LEP experiment sets a lower bound on Higgs mass which is 114.4 GeV at 95% confidence level [8]. The Large Hadron Collider [9] at CERN, Geneva, which has already started running, is largely dedicated to the search for this essential component of the SM.

1.2 Need for new physics

Despite its immense success, the SM of particle physics is yet to be regarded as the ultimate theory of nature. And there are ample reasons, both theoretical and experimental, to look for physics beyond the SM. We list below some points which indicate that the SM is, after all, somewhat incomplete:

- The SM suffers from a large number of free parameters ($\sim$ 20). All the masses, couplings and also the mixing at the quark sector are described by some free parameters of the theory and can only be fixed by experiments.
- The masses of the fermions are generated in an *ad hoc* basis. There is no explanation why we should have such a large hierarchy in the fermion masses, ranging from 0.5 MeV (mass of the electron) to as large as 175 GeV (mass of the top quark). Also, there is no explanation of the family structure of the fermions within the SM.
- The evidences of non-vanishing neutrino masses and mixing also lead us towards physics beyond the standard model [10–12]. There is no explanation of why the mixing pattern are so different in the lepton and quark sectors.
- Cosmological observations tell us that the universe is made of more matter than what is visible to us. In fact, only 4.6% of the universe consists of visible matter and rest consists of dark matter and dark energy. The rotation

curve of spiral galaxies and recent experiments have indicated that there should be some non-luminous matter amounting to about 24% of the energy of universe [13]. Within the SM there is no such particle which can account for this large amount of dark matter density.

- SM can not explain the observed baryon asymmetry of the universe, namely why we have more matter than antimatter.
- The Higgs mass is unstable under quantum corrections. For example, correction due to top quark contribution shifts the mass of the Higgs boson from its tree level value by

$$\Delta m_H^2 \;=\; -\frac{|y_t|^2}{4\pi^2}\Lambda^2 \tag{1.11}$$

  where Λ is some cut off scale up to which SM is well behaved and beyond which new physics starts intervening and y_t is the top Yukawa coupling due to which the correction is largest. Now if $\Lambda \sim M_P$, where M_P is the Planck scale ($\sim 10^{19}$ GeV) then the correction to the Higgs mass is $\sim 10^{38}$ GeV^2. Therefore, in order to achieve a Higgs mass consistent with electroweak precision measurements and also to maintain the perturbative nature of the theory, we need to add counter-terms to the Higgs mass-squared so that the divergences cancel out. And this requires a high degree of fine tuning of the counter-terms in the Lagrangian [14].
- In the SM, it is difficult to achieve the gauge coupling unification, the so called grand unification (GUT). The running of the strong and electroweak gauge couplings are such that the couplings hardly unify at any given energy scale [15].
- One of the fundamental forces, namely Gravity which becomes important at around Planck scale, is not incorporated in the SM. SM may be treated as an effective theory up to some scale and new physics should appear at that scale.

Bibliography

[1] For introduction, see, for example, F. Halzen and A.D. Martin, *Quarks and Leptons: An introductory course in modern particle physics*, (Ed. John Wiley, 1984); G. Kane, *Modern Elementary Particle Physics*, (Addison-Wesley, NY, 1993) T. D. Lee, *Particle Physics and Introduction to Field Theory*, (Harwood Academic Publisher, 1981) C. Quigg, *Gauge Theories of the Strong, Weak and Electromagnetic Interactions*, (Westview Press 1997); T.P. Cheng and L.F. Li, *Gauge theory of elementary particle physics*, (Oxford Univ. Press, 1991).

[2] M. Gell-Mann, Phys. Lett. **8**, 214 (1964); O. W. Greenberg, Phys. Rev. Lett. **13**, 598 (1964); D. J. Gross and F. Wilczek, Phys. Rev. Lett. **30**, 1343 (1973); H. D. Politzer, Phys. Rev. Lett. **30**, 1346 (1973).

[3] S. L. Glashow, Nucl. Phys. **22**, 579 (1961); S. Weinberg, Phys. Rev. Lett. **19**, 1264 (1967); A. Salam, Proceedings of 8th Nobel Symposium, Ed. N. Svartholm (1968).

[4] G. 't Hooft, Nucl. Phys. B **35**, 167 (1971); G. 't Hooft and M. J. G. Veltman, Nucl. Phys. B **44**, 189 (1972).

[5] Y. Nambu and G. Jona-Lasinio, Phys. Rev. **122**, 345 (1961). Y. Nambu and G. Jona-Lasinio, Phys. Rev. **124**, 246 (1961); J. Goldstone, Nuovo cimento **19**, 154 (1961) J. Goldstone, A. Salam and S. Weinberg, Phys. Rev. **127**, 965 (1962)

[6] F. Englert and R. Brout, Phys. Rev. Lett. **13**, 321 (1964); P. W. Higgs, Phys. Rev. Lett. **13**, 508 (1964); G. S. Guralnik, C. R. Hagen and T. W. B. Kibble, Phys. Rev. Lett. **13**, 585 (1964); P. W. Higgs, Phys. Rev. **145**, 1156 (1966); T. W. B. Kibble, Phys. Rev. **155**, 1554 (1967).

[7] S. Dittmaier, D. Schildknecht, Phys. Lett. **B391**, 420-428 (1997) [hep-ph/9609488]; J. H. Field, Phys. Rev. **D61**, 013010 (2000) [hep-ph/9810288];

P BRenton, Rept. Prog. Phys. **65**, 1271-1330 (2002). [hep-ph/0206231]; J. Erler, AIP Conf. Proc. **870**, 228-231 (2006) [hep-ph/0606148]; J. Alcaraz *et al.* [ALEPH Collaboration and DELPHI Collaboration and L3 Collaboration and], arXiv:hep-ex/0612034; M. W. Grunewald, [arXiv:0710.2838 [hep-ex]]; M. Goebel and f. t. G. Group, PoS **ICHEP2010**, 570 (2010) [arXiv:1012.1331 [hep-ph]].

[8] LEP Higgs Working Group, arXiv:hep-ex/0107030; R. Barate *et al.* [LEP Working Group for Higgs boson searches], Phys. Lett. B **565**, 61 (2003) [arXiv:hep-ex/0306033].

[9] The LHC Study Group, Large Hadron Collider, The Accelerator Project, CERN/AC/93-03 (LHC); The LHC Study Group, P. Lefevre and T. Pettersson (editors), The Large Hadron Collider, Conceptual Study, CERN/AC/95-05 (LHC); (http://lhc.web.cern.ch/lhc/).

[10] R. N. Mohapatra *et al.*, Rept. Prog. Phys. **70**, 1757 (2007) [arXiv:hep-ph/0510213]; A. Y. Smirnov, J. Phys. Conf. Ser. **136**, 012002 (2008) [arXiv:0810.2668 [hep-ph]]; A. Y. Smirnov, arXiv:0910.1778.

[11] B. Kayser, Phys. Rev. D**24**, 110 (1981); F. Boehm and P. Vogel, Physics of Massive Neutrinos (Cambridge University Press, Cambridge, 1987) p. 87; C. Giunti, C. Kim, and U. Lee, Phys. Rev. D**44**, 3635 (1991); J. Rich, Phys. Rev. D**48**, 4318 (1993); H. Lipkin, Phys. Lett. B**348**, 604 (1995); A. Bandyopadhyay, S. Choubey, S. Goswami and D. P. Roy, Phys. Lett. B **540**, 14 (2002) [arXiv:hep-ph/0204286].

[12] S. Fukuda *et al.* [Super-Kamiokande Collaboration], Phys. Lett. B **539**, 179 (2002) [arXiv:hep-ex/0205075]; S. N. Ahmed *et al.* [SNO Collaboration], Phys. Rev. Lett. **92**, 181301 (2004) [arXiv:nucl-ex/0309004]; T. Araki *et al.* [KamLAND Collaboration], Phys. Rev. Lett. **94**, 081801 (2005) [arXiv:hep-ex/0406035]; E. Aliu *et al.* [K2K Collaboration], Phys. Rev. Lett. **94**, 081802 (2005) [arXiv:hep-ex/0411038]; Y. Ashie *et al.* [Super-Kamiokande Collaboration], Phys. Rev. D **71**, 112005 (2005) [arXiv:hep-ex/0501064].

[13] E. Komatsu *et al.* [WMAP Collaboration], Astrophys. J. Suppl. **192**, 18 (2011), [arXiv:1001.4538 [astro-ph.CO]].

[14] S. Weinberg, Phys. Rev. D **13**, 974 (1976), Phys. Rev. D **19**, 1277 (1979); E. Gildener, Phys. Rev. D **14**, 1667 (1976); L. Susskind, Theory," Phys. Rev. D **20**, 2619 (1979); G. 't Hooft, in *Recent developments in gauge theories*, Pro-

ceedings of the NATO Advanced Summer Institute, Cargese 1979, (Plenum, 1980).

[15] See for example, *Grand Unified Theories* by G. Ross(1984), Westview Press; H. Georgi and S. L. Glashow, Phys. Rev. Lett. **32**, 438 (1974); J. C. Pati and A. Salam, Phys. Rev. D **10**, 275 (1974) [Erratum-ibid. D **11**, 703 (1975)]; P. Langacker, "Grand Unified Theories And Proton Decay," Phys. Rept. **72** (1981) 185.

Chapter 2

Supersymmetry: A prototype of physics beyond the standard model

2.1 Introduction

Supersymmetry (SUSY) [1, 2] is a symmetry between bosonic and fermionic degrees of freedom. In the presence of SUSY, for each particle there exists another particle with spin differing by half unit. Supersymmetry for a four dimensional field theory was introduced by Wess and Zumino in 1974 [3] (also by Salam and Strathdee, 1974 [4]), and later applied to the $SU(2) \otimes U(1)$ model by Fayet in 1975 [5].

In the next section we describe the motivations of $\mathcal{N}$=1 global SUSY, followed by its basic formalism in section 2.3. In section 2.4 we briefly mention a realistic supersymmetric version of the standard model, proposed by Howard Georgi and Savas Dimopoulos [6], which is called the minimal supersymmetric standard model (MSSM). Some aspects of SUSY breaking and its embedding in a larger setting have been discussed in section 2.5. Search for supersymmetry at

collider experiments is discussed in section 2.6.

2.2 $\mathcal{N}$=1 global supersymmetry: Motivation

The role of SUSY in TeV scale physics has far reaching consequences than its original motivation of introduction in string theories.

- SUSY broken at TeV scale is one of the leading contenders for solving the naturalness problem mentioned in section 1.2. For example, the top quark contribution to the Higgs self-energy correction is given by [2]

$$-i(\Delta m_H^2)_t \;=\; (-1)N_c(-iy_t)^2 \int \frac{d^4k}{(2\pi)^4} Tr\left(\frac{i}{\not{k}-m_t}\frac{i}{\not{k}-m_t}\right) \tag{2.1}$$

where, -1 is due to fermion-loop, $N_c = 3$ is the number of colour states that contribute and $y_t = m_t/v$, m_t is the mass of the top quark and v is the Higgs' VEV (see equation 1.10).

On simplification the quadratically divergent part comes out to be

$$(\Delta m_H^2)_t \;\approx\; -\frac{N_c(y_t)^2}{4\pi^2}\Lambda^2 \tag{2.2}$$

where, Λ is the ultra-violet cut-off scale of the theory, as mentioned in section 1.2, and can be of the order of M_P (Planck scale).

Now suppose, there are two complex colour triplet scalar fields $\tilde{f}_r,\ r = 1, 2$ with mass and couplings to H given by

$$\mathcal{L}_{\tilde{f}H} = \lambda_{\tilde{f}_r} H^2 \tilde{f}_r^\dagger \tilde{f}_r + \kappa_{\tilde{f}_r} H \tilde{f}_r^\dagger \tilde{f}_r + m_r^2 \tilde{f}_r^\dagger \tilde{f}_r \tag{2.3}$$

The quantum corrections at one-loop level to Higgs squared mass parameters m_H^2 due to these new fields are given by (Figure 2.1)

$$\begin{aligned} -i(\Delta m_H^2)_{\tilde{f}_r} \;=\; & -2N_c(-i\lambda_{\tilde{f}_r}) \int \frac{d^4k}{(2\pi)^4} \frac{i}{k^2 - m_r^2} \\ & + N_c(-i\kappa_{\tilde{f}_r})^2 \int \frac{d^4k}{(2\pi)^4} \left(\frac{i}{k^2 - m_r^2}\frac{i}{k^2 - m_r^2}\right) \end{aligned} \tag{2.4}$$

The quadratically divergent contribution comes from the first integral and is given by

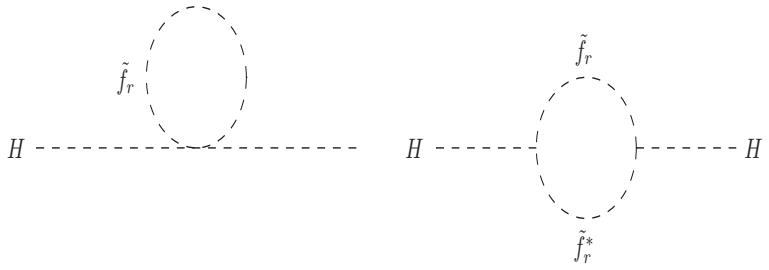

Figure 2.1: One-loop quantum corrections to the Higgs squared mass parameter m_H^2, due to the scalars $\tilde{f}_{1,2}$.

$$(\Delta m_H^2)_{\tilde{f}_r} \approx \frac{N_c \lambda_{\tilde{f}_r}}{8\pi^2}\Lambda^2 \tag{2.5}$$

Comparing equations 2.2 and 2.5, one finds that the quadratic divergences cancel if we choose

$$\lambda_{\tilde{f}_1} = \lambda_{\tilde{f}_2} = -(y_t)^2 \tag{2.6}$$

However, there is no reason to believe that the coupling constant relation in equation 2.6 holds to all order in perturbation theory. This would be a remarkable accident if not enforced by some symmetry. Fortunately in supersymmetric extension of the SM the systematic cancellation of dangerous quadratic divergences occurs rather naturally. If $\tilde{f}_{1,2}$ are the scalar superpartners of the t_L and t_R, respectively, then the necessary coupling constant relation is ensured by SUSY.

In fact, in the exact SUSY limit one also has that $\kappa_{\tilde{f}_r} = 2v(y_t)^2$ and $m_r^2 = m_t^2$, which implies that the logarithmically divergent contributions to m_H^2 also cancel exactly. However, no evidence of superpartners has been found yet. Therefore, one has to assume that SUSY is not an exact symmetry of nature, and must be broken softly (in a sense to be explained later), so that the quadratic divergences remain under control.

- SUSY also removes one of the most arbitrary aspects of the SM, namely the arbitrariness associated with the quartic Higgs self-coupling constant λ. In SUSY theories this role is played by the gauge couplings and sets a theoretical upper bound on the mass of the lightest neutral Higgs. The fact that the quartic couplings thus determined turn out to be positive in

supersymmetric theories, goes a long way in ensuring that the Higgs scalar potential is bounded from below.

- In many SUSY theories electroweak symmetry breaking (EWSB) is achieved rather naturally. As we know, EWSB is most easily accomplished for a negative value of the Higgs squared-mass which is an *ad hoc* assumption in the SM. A positive Higgs squared-mass at high-scale can be driven negative down at low-scale by the renormalisation group evolution (RGE) of the squared- mass parameter. This is known as radiative EWSB, a beautiful feature of SUSY.

- Another strong theoretical motivation for SUSY theories is that of gauge coupling unification. It is possible to construct models in which the three fundamental interactions of nature, i.e., strong, weak and electromagnetic interactions are unified at some scale and can be represented by a single gauge group. This is difficult to achieve within the SM. The RGE's of the SM gauge couplings (g_1, g_2, g_3) at one-loop level are given by

$$\frac{d}{dt}g_a = \frac{1}{16\pi^2} b_a g_a^3 \tag{2.7}$$

where $t = \ln(Q/Q_0)$, with Q the RG scale, and Q_0 is the reference scale and

$$(b_1, b_2, b_3) = \begin{cases} (41/10,\ -19/6,\ -7) & \text{Standard Model} \\ (33/5,\ 1,\ -3) & \text{Minimal SUSY SM above} \\ & \text{the SUSY breaking scale.} \end{cases} \tag{2.8}$$

The quantities $\alpha_a = g_a^2/4\pi$ have the nice property that their reciprocals run linearly with RG scale at one-loop order:

$$\frac{d}{dt}\alpha_a^{-1} = -\frac{b_a}{2\pi} \qquad (a = 1, 2, 3) \tag{2.9}$$

The running of α_a's are depicted in Figure 2.2. For the minimal supersymmetric extension of the SM (MSSM) one achieves unification at a scale $\sim 10^{16}$ GeV, if SUSY breaking takes place at around a TeV.

- SUSY can provide a solution to the dark matter problem of the universe, as mentioned in section 1.2. Observations related to DM search experiments suggest that the DM candidates must be weakly interacting and their masses are in between 10 GeV to a few TeV. SUSY with a discrete Z_2 symmetry, implies that the lightest SUSY particle (LSP) is stable and it turns out

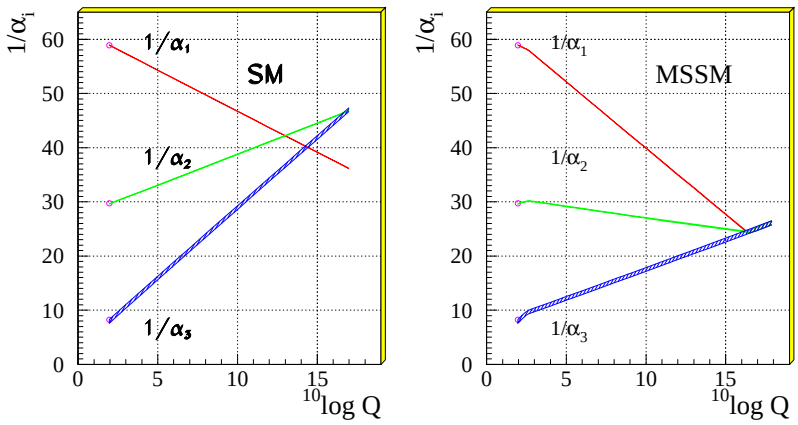

Figure 2.2: *Evolution of the inverse gauge couplings in the SM (left) and in the MSSM (right) [7], with SUSY broken at around a TeV.*

that the LSP can be neutral and weakly interacting over a large region of the SUSY parameter space. This weakly interacting massive particle can be a viable candidate for the observed DM of the universe.

2.3 Formalism

2.3.1 SUSY algebra

In a celebrated theorem, Coleman and Mandula showed that under certain assumptions, the symmetry group of a consistent four dimensional quantum field theory can not be extended beyond the group of symmetry containing the direct product of an internal symmetry group and the Poincaré group [8]. The introduction of a different symmetry algebra, the supersymmetry algebra (by Haag, Lopuszanski and Sohnius in 1975 [9]) offered a way to bypass the above theorem. The idea is to generalise the concept of symmetries in terms of generators having both commutation and anticommutation relations. The generators of the extended Poincaré group which includes SUSY are the following: the energy-momentum operators P^{μ}, the generators of space-time translation; the generators of homogeneous Lorentz group, $M^{\mu\nu}$; and a finite number of fermionic operators

Q^i (i=1,2,..,N), generators of SUSY, all of which commute with P^μ and transform like a spinor of rank 1 under the homogeneous Lorentz group. Using the spinor notation, the generators of SUSY can be divided into two sets, Q^i_α (α=1,2) and their conjugates $\bar{Q}^i_{\dot{\alpha}} \equiv (Q^i_\alpha)^\dagger$, indicating the different transformation property under Lorentz transformation by dotted and undotted indices. The generators of the extended Poincaré group give rise to an algebra, known as graded Lie algebra which is a generalisation of Lie algebra. We summarise below the algebra of $N = 1$ SUSY:

$$
\begin{aligned}
[P^\mu, P^\nu] &= 0 && \text{(2.10a)}\\
[M^{\mu\nu}, P^\rho] &= i(g^{\nu\rho}P^\mu - g^{\mu\rho}P^\nu) && \text{(2.10b)}\\
[M^{\mu\nu}, M^{\rho\sigma}] &= i(g^{\nu\rho}M^{\mu\sigma} + g^{\mu\sigma}M^{\nu\rho} - g^{\mu\rho}M^{\nu\sigma} - g^{\nu\sigma}M^{\mu\rho}) && \text{(2.10c)}
\end{aligned}
$$

$$
\begin{aligned}
[Q_\alpha, P_\mu] &= [\bar{Q}_{\dot{\alpha}}, P_\mu] = 0 && \text{(2.11a)}\\
\{Q_\alpha, Q_\beta\} &= \{\bar{Q}_{\dot{\alpha}}, \bar{Q}_{\dot{\beta}}\} = 0 && \text{(2.11b)}\\
[M^{\mu\nu}, Q_\alpha] &= -i(\sigma^{\mu\nu})_\alpha{}^\beta Q_\beta && \text{(2.11c)}\\
\left[M^{\mu\nu}, \bar{Q}^{\dot{\alpha}}\right] &= -i(\bar{\sigma}^{\mu\nu})^{\dot{\alpha}}{}_{\dot{\beta}}\bar{Q}^{\dot{\beta}} && \text{(2.11d)}\\
\{Q_\alpha, \bar{Q}_{\dot{\beta}}\} &= 2\sigma^\mu{}_{\alpha\dot{\beta}}P_\mu && \text{(2.11e)}
\end{aligned}
$$

where the following conventions have been followed: $g_{\mu\nu} = g^{\mu\nu} = diag(1, -1, -1, -1)$, $\sigma^\mu = (\mathbf{1}, \sigma_i)$, $\bar{\sigma}^\mu = (\mathbf{1}, -\sigma_i)$ with σ_i being the 2×2 Pauli matrices. $\sigma^{\mu\nu} = \frac{i}{4}(\sigma^\mu\bar{\sigma}^\nu - \sigma^\nu\bar{\sigma}^\mu)$ and $\bar{\sigma}^{\mu\nu} = \frac{i}{4}(\bar{\sigma}^\mu\sigma^\nu - \bar{\sigma}^\nu\sigma^\mu)$ are the spinor representations of the generators of the Lorentz group.

The non-vanishing commutators of the supersymmetry generators with $M^{\mu\nu}$ indicates that SUSY connects states of different spin and statistics, i.e;

$$
Q_\alpha|Boson> = |Fermion> \qquad\qquad Q_\alpha|Fermion> = |Boson> \qquad \text{(2.12)}
$$

The single-particle states of a supersymmetric theory form an irreducible representation of the SUSY algebra, called supermultiplets. Each supermultiplet contains both fermionic and bosonic states, which are often called superpartners of each other. It can be shown that each supermultiplet has equal number of

bosonic and fermionic degrees of freedom. In addition, since the SUSY generators commute with the momentum generators (see equation 2.11), they in turn also commute with the mass-squared operator $P^2 = P^\mu P_\mu$. Hence, the particles within the same supermultiplet must have the same mass. The SUSY generators also commute with the generators of gauge transformations. Therefore, particles in the same supermultiplet must also be in the same representation of the gauge group, and so must have the same electric charges, weak isospin, and colour degrees of freedom.

2.3.2 Ingredients of building a SUSY model

Superspace and superfields

In order to construct a SUSY model, it is useful to introduce the concept of superspace and superfields. A superspace is an extension of the four dimensional space-time coordinates x^μ into a larger space, involving two additional anticommuting (Grassmann) coordinates θ_α, with $\alpha = 1, 2$ and their conjugates $\bar{\theta}_{\dot{\alpha}} \equiv (\theta_\alpha)^\dagger$. A SUSY transformation can then be thought of as a translation in superspace, defined as

$$G(a, \epsilon, \bar{\epsilon}) = e^{i(\epsilon Q + \bar{\epsilon}\bar{Q} + a \cdot P)} \tag{2.13}$$

generated by

$$P_\mu = i\partial_\mu \tag{2.14a}$$

$$Q_\alpha = -i\frac{\partial}{\partial\theta^\alpha} - \sigma^\mu_{\alpha\dot{\alpha}}\bar{\theta}^{\dot{\alpha}}\partial_\mu \tag{2.14b}$$

$$\bar{Q}_{\dot{\alpha}} = i\frac{\partial}{\partial\bar{\theta}^{\dot{\alpha}}} + \theta^\alpha\sigma^\mu_{\alpha\dot{\alpha}}\partial_\mu \tag{2.14c}$$

where a^μ is a Lorentz four-vector and ϵ, $\bar{\epsilon}$ are anticommuting Grassmann variables.

We can generalise the notion of an ordinary field to a superfield which is an operator $S(x, \theta, \bar{\theta})$, function of the superspace coordinates. One can expand $S(x, \theta, \bar{\theta})$ in powers of θ and $\bar{\theta}$, going up to terms bilinear in each of θ and $\bar{\theta}$. The advantage of introducing a superfield is that the coefficients of various powers of θ and $\bar{\theta}$ can be identified as the components of a supermultiplet. The most general

Lorentz invariant superfield can be expanded in the following way:

$$\begin{aligned} S(x,\theta,\bar{\theta}) &= \phi(x) + \sqrt{2}\theta\xi(x) + \sqrt{2}\bar{\theta}\bar{\chi}(x) + \theta\theta F(x) + \bar{\theta}\bar{\theta}G(x) + \theta\sigma^{\mu}\bar{\theta}A_{\mu}(x) \\ &\quad + \theta\theta\bar{\theta}\bar{\lambda}(x) + \bar{\theta}\bar{\theta}\theta\kappa(x) + \frac{1}{2}\theta\theta\bar{\theta}\bar{\theta}D(x) \end{aligned} \tag{2.15}$$

where ϕ, F, G, and D are Lorentz scalar functions of x; ξ, $\bar{\chi}$, κ, and $\bar{\lambda}$ are Weyl spinors; and A_{μ} is a vector.

The SUSY transformation of a superfield is given by

$$S(x,\theta,\bar{\theta}) \rightarrow e^{i(\epsilon Q + \bar{\epsilon}\bar{Q} + a\cdot P)} S(x,\theta,\bar{\theta}) \tag{2.16}$$

A general superfield, $S(x,\theta,\bar{\theta})$, belongs to a reducible representation of the SUSY algebra. However, irreducible representations of this algebra can be obtained by imposing further constraints on the superfields, covariant under the SUSY transformation. The simplest constraint that one can apply to a superfield is the reality condition:

$$S^{\dagger} = S \quad \text{vector superfield} \tag{2.17}$$

Let us define two fermionic derivatives which anticommute with the generators of SUSY algebra and transform covariantly, as

$$D_{\alpha} = \frac{\partial}{\partial\theta^{\alpha}} + i\sigma^{\mu}_{\alpha\dot{\alpha}}\bar{\theta}^{\dot{\alpha}}\partial_{\mu} \tag{2.18a}$$

$$\bar{D}_{\dot{\alpha}} = -\frac{\partial}{\partial\bar{\theta}^{\dot{\alpha}}} - i\theta^{\alpha}\sigma^{\mu}_{\alpha\dot{\alpha}}\partial_{\mu} \tag{2.18b}$$

The operators D_{α} and $\bar{D}_{\dot{\alpha}}$ can be used to impose covariant constraints on superfields:

$$\bar{D}_{\dot{\alpha}} S = 0 \quad \text{left} - \text{chiral superfield} \tag{2.19a}$$

$$D_{\alpha} S^{\dagger} = 0 \quad \text{right} - \text{chiral superfield} \tag{2.19b}$$

Chiral superfields

A left-chiral superfield $\Phi(x^{\mu},\theta,\bar{\theta})$ which satisfies equation 2.19a, can be expanded in terms of the Grassmann variables θ and $\bar{\theta}$ as

$$\begin{aligned} \Phi(x^{\mu},\theta,\bar{\theta}) &= \phi(x) + \sqrt{2}\theta\psi(x) + \theta\theta F(x) + i\partial_{\mu}\phi(x)\theta\sigma^{\mu}\bar{\theta} \\ &\quad - \frac{i}{\sqrt{2}}\theta\theta\partial_{\mu}\psi(x)\sigma^{\mu}\bar{\theta} - \frac{1}{4}\partial^{\mu}\partial_{\mu}\phi(x)\theta\theta\bar{\theta}\bar{\theta} \end{aligned} \tag{2.20}$$

The component fields include a Weyl spinor ψ, and a complex scalar field ϕ. The field F is an auxiliary field that ensures the closure of the SUSY algebra even under off-shell condition and can be eliminated using the equations of motion. The component fields of a left chiral superfield transform in the following way under the SUSY transformations:

$$\delta\phi = \sqrt{2}\xi\psi \tag{2.21a}$$

$$\delta\psi = \sqrt{2}\xi F - i\sqrt{2}\partial_\mu\phi\sigma^\mu\bar{\xi} \tag{2.21b}$$

$$\delta F = i\sqrt{2}\partial_\mu\psi\sigma^\mu\bar{\xi} \tag{2.21c}$$

This can be obtained from equation 2.16 with $a = 0$. A right-chiral superfield can be obtained by taking Hermitian conjugate of $\Phi(x, \theta, \bar{\theta})$. The coefficient of the $\theta\theta$ term is known as the F-term. Equation(2.21c) shows that the change, under the SUSY transformations, of the F-term is a total derivative.

Let us consider how to construct the Lagrangian for the chiral superfields. This can be done by taking products of chiral superfields. In particular, the product of two left chiral superfields is also a left chiral superfield. Hence the F-term of a product of left chiral superfields can be used to give a suitable term in the Lagrangian. The product of a left and a right chiral superfield gives a vector superfield. The D-term (the coefficient of $\theta\theta\bar{\theta}\bar{\theta}$) of the product of a left and a right chiral superfield can therefore also be used to give a term in the Lagrangian. The simplest example of this is a single left chiral superfield. We can form the product of this field with its hermitian conjugate and take the D-term. This gives

$$[\Phi\Phi^\dagger]_{\theta\theta\bar{\theta}\bar{\theta}} = FF^\dagger + \partial_\mu\phi^*\partial^\mu\phi + i\bar{\psi}\bar{\sigma}^\mu\partial_\mu\psi \tag{2.22}$$

which, after eliminating the auxiliary field F using the equations of motion, gives the final Lagrangian.

The most general set of renormalisable interaction terms for these fields consistent with SUSY, can be introduced elegantly using the notion of superpotential, which is an analytic function of the scalar fields ϕ's. For example, in a theory with only one chiral superfield,

$$\mathbf{W}(\Phi) = \frac{m}{2}\Phi\Phi + \frac{y}{3}\Phi\Phi\Phi \tag{2.23}$$

In general we can only include terms which are at most cubic in the superfields in

order for the theory to be renormalisable. This gives the interaction Lagrangian

$$\begin{aligned}\mathcal{L} &= [W(\Phi)]_{\theta\theta} + \text{h.c.} && (2.24)\\ &= m(\phi F - \frac{1}{2}\psi\psi) + y(\phi^2 F - \phi\psi\psi) + \text{h.c.} && (2.25)\end{aligned}$$

We can then write the full Lagrangian for this theory eliminating the auxiliary field F, using the equation of motion:

$$F^\dagger = -m\phi - \lambda\phi^2 \tag{2.26}$$

On substitution of F we get

$$\begin{aligned}\mathcal{L}_{chiral} &= [\Phi\Phi^\dagger]_{\theta\theta\bar{\theta}\bar{\theta}} + ([W(\Phi)]_{\theta\theta} + \text{h.c.}) && (2.27)\\ &= \partial_\mu\phi^*\partial^\mu\phi + i\bar{\psi}\bar{\sigma}^\mu\partial_\mu\psi - |\lambda\phi^2 + m\phi|^2 \\ &\qquad - \left(\frac{m}{2}\psi\psi + \lambda\psi\psi\phi + \text{h.c.}\right) && (2.28)\end{aligned}$$

Vector superfields

A vector superfield which is defined by equation 2.17, can be expanded in powers of θ and $\bar{\theta}$ as,

$$\begin{aligned}V(x^\mu,\theta,\bar{\theta}) &= C(x) + i\theta\chi(x) - i\bar{\theta}\bar{\chi}(x) + \frac{i}{2}\theta\theta\left[M(x) + iN(x)\right] \\ &\quad -\frac{i}{2}\bar{\theta}\bar{\theta}\left[M(x) - iN(x)\right] + \theta\sigma^\mu\bar{\theta}V_\mu(x) \\ &\quad +i\theta\theta\bar{\theta}\left[\bar{\lambda}(x) + \frac{i}{2}\bar{\sigma}^\mu\partial_\mu\chi(x)\right] - i\bar{\theta}\bar{\theta}\theta\left[\lambda(x) + \frac{i}{2}\sigma^\mu\partial_\mu\bar{\chi}(x)\right] \\ &\quad +\frac{1}{2}\theta\theta\bar{\theta}\bar{\theta}\left[D(x) - \frac{1}{2}\partial_\mu\partial^\mu C(x)\right] \qquad (2.29)\end{aligned}$$

where C, M, N, and D are the real scalar fields; χ, and λ are the Weyl fermions; and V_μ is a real gauge field.

Using the supersymmetric $U(1)$ gauge transformation

$$V(x,\theta,\bar{\theta}) \to V(x,\theta,\bar{\theta}) + i(\Phi(x,\theta,\bar{\theta}) - \Phi^\dagger(x,\theta,\bar{\theta})) \tag{2.30}$$

the component fields C, M, N and χ can be eliminated by a particular choice of Φ, leaving the gauge field V_μ and its superpartner gaugino field λ, and the auxiliary field D. In this gauge, the vector superfield has the following form

$$V_{WZ}(x,\theta,\bar{\theta}) = \theta\sigma^{\mu}\bar{\theta}V_{\mu}(x) + i\theta\theta\bar{\theta}\bar{\lambda}(x) - i\bar{\theta}\bar{\theta}\theta\lambda(x) + \frac{1}{2}\theta\theta\bar{\theta}\bar{\theta}D(x)$$

This particular choice of Φ is known as the Wess-Zumino gauge which is in some sense analogous to the unitary gauge in the SM. The component fields of a vector superfield transform in the following way under the SUSY transformations:

$$\begin{aligned}
\delta\lambda_{\alpha} &= -iD\xi_{\alpha} - \frac{1}{2}(\sigma^{\mu}\bar{\sigma}^{\nu})_{\alpha}{}^{\beta}\xi_{\beta}\left(\partial_{\mu}V_{\nu} - \partial_{\nu}V_{\mu}\right) && \text{(2.31a)}\\
\delta V^{\mu} &= i\left(\xi\sigma^{\mu}\bar{\lambda} - \lambda\sigma^{\mu}\bar{\xi}\right) - \partial^{\mu}\left(\xi\chi + \bar{\xi}\bar{\chi}\right) && \text{(2.31b)}\\
\delta D &= \partial_{\mu}\left(-\xi\sigma^{\mu}\bar{\lambda} + \lambda\sigma^{\mu}\bar{\xi}\right) && \text{(2.31c)}
\end{aligned}$$

Here the variation of the coefficient of the $\theta\theta\bar{\theta}\bar{\theta}$ term, the D-term, is a total derivative.

The construction of the kinetic energy terms for V_{μ} and λ is rather involved. It is possible to construct a supersymmetric derivative of V which contains the field strength $F_{\mu\nu}$ and a derivative of λ. The F-term of the contraction of this field with itself yields the gauge kinetic terms

$$\mathcal{L}_{\text{gauge}} = -\frac{1}{4}F^{a}_{\mu\nu}F^{\mu\nu a} + i\lambda^{\dagger a}\overline{\sigma}^{\mu}D_{\mu}\lambda^{a} + \frac{1}{2}D^{a}D^{a} \qquad (2.32)$$

The auxiliary field D^a has dimension of $[mass]^2$ and has no kinetic term. Therefore it can be eliminated using equation of motion, just like the auxiliary field in case of chiral superfields. However, as we shall see below, it can be non-trivial if one switches on interactions between chiral and vector supermultiplets.

With both chiral and vector supermultiplets present in a scenario, it is possible to write down their interaction terms that are renormalisable (of mass dimension ≤ 4), namely

$$(\phi^{*}T^{a}\psi)\lambda^{a}, \qquad \lambda^{\dagger a}(\psi^{\dagger}T^{a}\phi), \qquad \text{and} \qquad (\phi^{*}T^{a}\phi)D^{a}. \qquad (2.33)$$

After some algebra one can now fix the coefficients for the terms in equation 2.33, with the result that the full Lagrangian density for a renormalisable supersymmetric theory is

$$\mathcal{L} = \mathcal{L}_{\text{chiral}} + \mathcal{L}_{\text{gauge}} - \sqrt{2}g(\phi^{*}T^{a}\psi)\lambda^{a} - \sqrt{2}g\lambda^{\dagger a}(\psi^{\dagger}T^{a}\phi) + g(\phi^{*}T^{a}\phi)D^{a} \qquad (2.34)$$

where $\mathcal{L}_{\text{chiral}}$ means the chiral supermultiplet Lagrangian and $\mathcal{L}_{\text{gauge}}$ is the one related to the gauge supermultiplet as mentioned above (equations 2.28 and 2.32).

The first two interaction terms represent direct couplings of gauginos to matter fields; this can be thought of as the "supersymmetrisation" of the usual gauge boson couplings to matter fields. It is also to be noted that SUSY invariance of the gauge (gaugino) interaction requires the superpotential to be gauge invariant. The last term combines with the term $D^a D^a/2$ in $\mathcal{L}_{\text{gauge}}$ to provide an equation of motion

$$D^a = -g(\phi^* T^a \phi). \tag{2.35}$$

Thus, like the auxiliary fields F_i and F^{*i}, the D^a are expressible purely in terms of the scalar fields and their gauge quantum numbers. Replacing the auxiliary fields in equation (2.34) using equation (2.35), one finds that the complete scalar potential is (recall that $\mathcal{L}$ contains $-V$):

$$V(\phi, \phi^*) = F^{*i} F_i + \frac{1}{2}\sum_a D^a D^a = W_i^* W^i + \frac{1}{2}\sum_a g_a^2 (\phi^* T^a \phi)^2. \tag{2.36}$$

The two types of terms in this expression are known as "F-term" and "D-term", respectively. Since $V(\phi, \phi^*)$ is a sum of squares, it is always positive semi-definite. It is a unique feature of supersymmetric theories that the SUSY invariant scalar potential is completely determined by the *other* interactions in the theory.

2.3.3 Making a SUSY model realistic: SUSY breaking

In order to make a SUSY theory realistic, any phenomenological version of it must contains SUSY breaking [10], as superpartners are yet to be observed in experiments. To provide a solution to the naturalness problem in presence of SUSY breaking, the coupling constant relations (such as equation 2.6) which hold in unbroken SUSY theory must still be maintained after SUSY breaking terms are introduced. From a theoretical perspective, we therefore expect SUSY to be broken in masses and couplings of positive mass dimension, not in dimensionless couplings. This implies that the effective Lagrangian will consist of

$$\mathcal{L} = \mathcal{L}_{SUSY} + \mathcal{L}_{soft} \tag{2.37}$$

where, $\mathcal{L}_{SUSY}$ is SUSY conserving Lagrangian which includes gauge and Yukawa interactions, and, $\mathcal{L}_{soft}$ contains only (SUSY violating) soft mass terms and coupling parameters with positive mass dimension. The possible Lagrangian containing the soft SUSY breaking terms can be parametrised by [11]

$$\mathcal{L}_{soft} = -(\frac{1}{2}M_a \lambda^a \lambda^a + \frac{1}{6}y^{ijk}\phi_i\phi_j\phi_k + \frac{1}{2}b^{ij}\phi_i\phi_j + t^i\phi_i) + \text{c.c.} - (m^2)^i_j \phi^{j\star}\phi_i \tag{2.38}$$

which consists of gaugino masses M_a for each gauge group, scalar squared-mass terms $(m^2)^j_i$ and b^{ij}, and (scalar)^3 couplings y^{ijk}, and "tadpole" couplings t^i. The last of these can only occur if ϕ_i is a gauge singlet. An attempt to address the possible origin of such a plethora of new terms, however, will be described in section 2.5.

2.4 The minimal supersymmetric standard model

In the SUSY extension of the SM [6, 12], the particle spectrum becomes almost doubled due to the fact that for each SM particle one has its superpartners. The SM fermions belong to the chiral supermultiplets. This is because the right and left handed component of SM fermions transform differently under gauge transformation which is consistent if the fermions belong to chiral supermultiplets. The superpartners of the SM fermions are generically named as *sfermions* and the symbols for them are same as for the corresponding fermions, except for an additional tilde (˜) which is used to denote the superpartners of the SM fermions. For example, the superpartner of electron is known as selectron: $\tilde{e}_L$, $\tilde{e}_R$. The same is true for all other leptons and quarks. The only scalar in SM is the Higgs boson which gives masses to charged leptons, quarks and also to gauge bosons. Being a scalar, it must reside in a chiral supermultiplet. However, in SUSY extension of the SM, one has to include two chiral supermultiplets due to the following two reasons: first is due to the holomorphic nature of the superpotential. It implies that, a field and its complex conjugate can not appear simultaneously in the superpotential. Hence to give masses to both the up (having third component of isospin, $T_3 = +\frac{1}{2}$) and down ($T_3 = -\frac{1}{2}$) type of quarks one needs two Higgs supermultiplets, with equal and opposite hypercharges. The second reason can be traced back to the fact that, with only one Higgs chiral supermultiplet the gauge symmetry will become anomalous which can be avoided by the introduction of two chiral Higgs supermultiplets. In this case, the contributions to triangle anomaly due to the two fermionic members of the Higgs chiral supermultiplets cancel each other if they have equal and opposite hypercharges. They are denoted by H_u (hypercharge, $Y = \frac{1}{2}$) and H_d ($Y = -\frac{1}{2}$). The vector bosons and their spin-1/2 superpartners belong to the gauge or vector supermultiplets of the MSSM. The name of the fermionic superpartners of the SM particles commonly come with a suffix '-ino' attached to their SM name. Table 2.1 and 2.2 describe the

Names		spin 0	spin 1/2	$SU(3)_C$, $SU(2)_L$, $U(1)_Y$
squarks, quarks	Q	$(\widetilde{u}_L \;\; \widetilde{d}_L)$	$(u_L \;\; d_L)$	$(\mathbf{3}, \mathbf{2}, \frac{1}{6})$
	$\overline{u}$	$\widetilde{u}_R^*$	$u_R^\dagger$	$(\overline{\mathbf{3}}, \mathbf{1}, -\frac{2}{3})$
	$\overline{d}$	$\widetilde{d}_R^*$	$d_R^\dagger$	$(\overline{\mathbf{3}}, \mathbf{1}, \frac{1}{3})$
sleptons, leptons	L	$(\widetilde{\nu} \;\; \widetilde{e}_L)$	$(\nu \;\; e_L)$	$(\mathbf{1}, \mathbf{2}, -\frac{1}{2})$
	$\overline{e}$	$\widetilde{e}_R^*$	$e_R^\dagger$	$(\mathbf{1}, \mathbf{1}, 1)$
Higgs, higgsinos	H_u	$(H_u^+ \;\; H_u^0)$	$(\widetilde{H}_u^+ \;\; \widetilde{H}_u^0)$	$(\mathbf{1}, \mathbf{2}, +\frac{1}{2})$
	H_d	$(H_d^0 \;\; H_d^-)$	$(\widetilde{H}_d^0 \;\; \widetilde{H}_d^-)$	$(\mathbf{1}, \mathbf{2}, -\frac{1}{2})$

Table 2.1: Chiral supermultiplets in the Minimal Supersymmetric Standard Model. The spin-0 fields are complex scalars, and the spin-1/2 fields are left-handed two-component Weyl fermions.

particle content together with their gauge quantum numbers, corresponding to the chiral and vector supermultiplets of the MSSM respectively. Table 2.1 replicates itself for other two generations of quark and lepton supermultiplets.

Having described the particle content of the MSSM, the next thing is to specify the superpotential and soft SUSY breaking terms which completely describe the model. The superpotential for the MSSM is given by

$$W_{\text{MSSM}} = \hat{\overline{u}}\mathbf{y_u}\hat{Q}\hat{H}_u - \hat{\overline{d}}\mathbf{y_d}\hat{Q}\hat{H}_d - \hat{\overline{e}}\mathbf{y_e}\hat{L}\hat{H}_d + \mu\hat{H}_u\hat{H}_d\,. \tag{2.39}$$

suppressing all the family and gauge indices. Here, the hat ($\hat{}$) implies that the above objects appearing in the superpotential are superfields corresponding to the chiral supermultiplets. The first three term are the Yukawa terms and the last term is the mass term for the two Higgs doublets, also known as the μ-term.

The terms that appear in the MSSM superpotential, are not the only possible terms that can be written down in a renormalisable and gauge invariant way. In fact one can also add some lepton and baryon number violating bilinear and trilinear terms to the superpotential in a renormalisable and gauge invariant manner. However they are seriously constrained by the non-observation of lep-

Names	spin 1/2	spin 1	$SU(3)_C$, $SU(2)_L$, $U(1)_Y$
gluino, gluon	$\widetilde{g}$	g	(**8**, **1** , 0)
winos, W bosons	$\widetilde{W}^{\pm}$ $\widetilde{W}^0$	$W^{\pm}$ W^0	(**1**, **3** , 0)
bino, B boson	$\widetilde{B}^0$	B^0	(**1**, **1** , 0)

Table 2.2: Gauge supermultiplets in the Minimal Supersymmetric Standard Model.

ton and baryon number violating processes, for example proton decay. To avoid these terms one postulates a discrete symmetry, called $\mathcal{R}$-parity, defined as

$$\mathcal{R} = (-1)^{3B+L+2s} \tag{2.40}$$

If $\mathcal{R}$-parity is conserved only terms even under it are allowed. All the SM particles and Higgs bosons have $\mathcal{R} = +1$, while their supersymmetric counterparts have $\mathcal{R} = -1$. With this assignment only terms written in equation 2.39 are allowed. One immediate consequence of this is that the lightest supersymmetric particle (LSP) is stable. In addition if it is neutral and weakly interacting, it can be a viable dark matter candidate.

The soft SUSY breaking terms of the MSSM are given by

$$\begin{aligned}
\mathcal{L}_{\text{soft}} \;=\; & -\frac{1}{2}\left(M_1\tilde{B}\tilde{B} + M_2\tilde{W}_a\tilde{W}^a + M_3\tilde{g}_\alpha\tilde{g}^\alpha + \text{c.c.}\right) \\
& - \left(A^L_{ij}\tilde{L}^a_i H^b_d \tilde{E}^*_j + A^D_{ij}\tilde{Q}^a_i H^b_d \tilde{D}^*_j + A^U_{ij}\tilde{Q}^b_i H^a_u \tilde{U}^*_j + \text{c.c.}\right) \\
& - - M^2_{\tilde{L},ij}\tilde{L}^*_{ia}\tilde{L}^a_j - M^2_{\tilde{E},ij}\tilde{E}^*_i\tilde{E}_j \\
& - M^2_{\tilde{Q},ij}\tilde{Q}^*_{ia}\tilde{Q}^a_j - M^2_{\tilde{U},ij}\tilde{U}^*_i\tilde{U}_j - M^2_{\tilde{D},ij}\tilde{D}^*_i\tilde{D}_j \\
& - m^2_{H_d}H^*_{da}H^a_d - m^2_{H_u}H^*_{ua}H^a_u - \left(bH^a_d H^b_u + \text{c.c.}\right).
\end{aligned} \tag{2.41}$$

In equation (2.41), M_3, M_2, and M_1 are the gluino, wino, and bino mass terms ($a = 1,2,3; \alpha = 1,2..,8$). The next set of terms in equation 2.41 contains the (scalar)^3 couplings. Each of A^L_{ij}, A^D_{ij}, A^U_{ij} is a complex 3×3 matrix in family space, with dimensions of [mass]. They are in one-to-one correspondence with the Yukawa couplings of the superpotential. Q, L, U, D, E are all three-component column vectors containing all the fermion families. Q, L are quark and lepton doublet

superfields respectively while U, D, E are singlets. Terms in the next two lines of equation 2.41 consist of squark and slepton mass terms of the form $(m^2)^j_i \phi^{*i} \phi_j$. Each of $M^2_{\tilde{L},ij}$, $M^2_{\tilde{E},ij}$, $M^2_{\tilde{Q},ij}$, $M^2_{\tilde{U},ij}$, $M^2_{\tilde{D},ij}$ is a 3×3 matrix in family space, having in general complex entries, but they must be hermitian so that the Lagrangian is real. Finally, in the last line of equation 2.41 we have supersymmetry-breaking contributions to the Higgs potential; $m^2_{H_d}$ and $m^2_{H_u}$ are squared-mass terms of $(m^2)^j_i$ type, while b is the only bilinear squared-mass term that can occur in MSSM with terms of $(m^2)^{ij} \phi_i \phi_j$ type. In order to have a successful cure of the naturalness problem, we expect

$$M_1,\, M_2,\, M_3,\, A^L_{ij},\, A^D_{ij},\, A^D_{ij} \;\sim\; m_{\text{soft}}, \tag{2.42}$$

$$M^2_{\tilde{L},ij},\, M^2_{\tilde{E},ij},\, M^2_{\tilde{Q},ij},\, M^2_{\tilde{U},ij},\, M^2_{\tilde{D},ij},\, m^2_{H_u},\, m^2_{H_d},\, b \;\sim\; m^2_{\text{soft}}, \tag{2.43}$$

with a characteristic mass scale m_{soft} that is not much larger than 1000 GeV.

Electroweak symmetry breaking in the MSSM

The classical scalar potential for the Higgs scalar fields ($H_u = (H^+_u,\, H^0_u)$ and $H_d = (H^0_d,\, H^-_d)$) in the MSSM is given by

$$\begin{aligned} V \;=\; & (|\mu|^2 + m^2_{H_u})(|H^0_u|^2 + |H^+_u|^2) + (|\mu|^2 + m^2_{H_d})(|H^0_d|^2 + |H^-_d|^2) \\ & + [b\,(H^+_u H^-_d - H^0_u H^0_d) + \text{c.c.}] + \frac{1}{8}(g^2 + g'^2)(|H^0_u|^2 + |H^+_u|^2 - |H^0_d|^2 \\ & - |H^-_d|^2)^2 + \frac{1}{2} g^2 |H^+_u H^{0*}_d + H^0_u H^{-*}_d|^2. \end{aligned} \tag{2.44}$$

where terms proportional to $|\mu|^2$ come from F-terms and those proportional to g^2 and g'^2 are the D-term contributions. The remaining terms are the soft SUSY breaking terms appearing in equation 2.41. The full scalar potential of the theory also includes terms involving the squark and slepton fields. However for the discussion of EWSB, we can ignore them, as long as they do not get VEVs. To break the electroweak symmetry spontaneously the following inequalities must be satisfied:

$$2b < 2|\mu|^2 + m^2_{H_u} + m^2_{H_d}. \tag{2.45}$$

$$b^2 > (|\mu|^2 + m^2_{H_u})(|\mu|^2 + m^2_{H_d}). \tag{2.46}$$

where the first one reflects the fact that the potential is bounded from below and the later one ensures that one linear combination of H^0_u and H^0_d will have negative

squared-mass in order to break the electroweak symmetry. The neutral components of the two Higgs doublets can then acquire non-zero VEV's

$$v_u = \langle H_u^0 \rangle, \qquad v_d = \langle H_d^0 \rangle. \tag{2.47}$$

and generate masses for the $(W^{\pm}, Z)$-bosons. v_u and v_d are related to the SM VEV v as $v = \sqrt{v_u^2 + v_d^2}$ and their ratio is defined as

$$\tan\beta \equiv v_u / v_d. \tag{2.48}$$

The Higgs scalar fields in the MSSM consist of two complex $SU(2)_L$-doublets, or eight real, scalar degrees of freedom. When the electroweak symmetry is broken, three of them, which are the would-be Nambu-Goldstone bosons, become the longitudinal modes of the Z^0 and $W^{\pm}$ massive vector bosons, leaving us with 5 physical scalars.

Mass spectrum

The mass spectrum of the MSSM can be described as follows:

- Higgs scalar mass eigenstates consist of two CP-even neutral scalars h^0 and H^0, one CP-odd neutral scalar A^0, and a pair of charged scalar H^+ and its conjugate H^-. At the tree level, the lighter CP-even neutral scalar h^0 must satisfy the relation $m_{h^0} \leq m_Z$. However, higher order corrections to the scalar potential allows m_{h^0} to be pushed up at around 135 GeV [2].
- The mass eigenstates of the sleptons for each family is denoted by $\tilde{l}_{1,2}$ ($l = e,\ \mu,\ \tau$) which are linear combinations of the left- and right-chiral states. The left-right mixing for the first two families are very small, mainly driven by the electron and muon Yukawa coupling. Hence, the mass eigenstates are the same as the chiral states. However, there is a substantial mixing in the third family and the mixing is proportional to the tau Yukawa coupling and $\tan\beta$ (defined in equation 2.48).
- The same is true in the squark sector as well, except the fact that here one has both up- and down-type of squarks for each family. The squarks mass eigenstates are denoted by $\tilde{q}_{1,2}$.
- The mass of the gluino is denoted by $m_{\tilde{g}}$.

- The neutral gauginos ($\tilde{B}, \tilde{W}_3^0$) and the neutral Higgsinos ($\tilde{H}_u^0, \tilde{H}_d^0$) mix to form the mass eigenstates, known as neutralinos χ_i^0 $(i = 1, .., 4)$.
- The combination of charged higgsinos ($\tilde{H}_u^+, \tilde{H}_d^-$) and the charged gauginos (winos) ($\tilde{W}^+, \tilde{W}^-$) form the mass eigenstates, known as charginos with charge ± 1, $\chi_i^\pm$ $(i = 1, 2)$.

2.5 High-scale SUSY breaking as an organising principle

The arbitrary values of the soft SUSY breaking parameters introduced in the previous section equation 2.41 can be restricted by various precision measurements and low energy constraints such as : flavour violating processes ($\mu \to e\gamma$, $\tau \to e\gamma, etc.$); anomalous magnetic moment of muon and rare decay of B mesons (e.g. $B \to s\gamma$, $B \to s\ell^-\ell^+$). In addition, there are also constraints on the CP-violating phases coming from electric dipole moment of electron and neutron [13–19]. To avoid these constraints arising from flavour mixings, flavour-changing neutral current effects in the MSSM, one normally assumes SUSY braking to be flavour blind and all the squark and slepton squared-mass matrices and trilinear scalar couplings are diagonal in the flavour basis, i.e.,

$$\mathbf{m_Q^2} = m_Q^2\mathbf{1}, \quad \mathbf{m_{\bar{u}}^2} = m_{\bar{u}}^2\mathbf{1}, \quad \mathbf{m_{\bar{d}}^2} = m_{\bar{d}}^2\mathbf{1}, \quad \mathbf{m_L^2} = m_L^2\mathbf{1}, \quad \mathbf{m_{\bar{e}}^2} = m_{\bar{e}}^2\mathbf{1}. \tag{2.49}$$

$$\mathbf{a_u} = A_{u0}\,\mathbf{y_u}, \qquad \mathbf{a_d} = A_{d0}\,\mathbf{y_d}, \qquad \mathbf{a_e} = A_{e0}\,\mathbf{y_e}, \tag{2.50}$$

In addition one also assumes there are no CP-violating phases in the theory other than that coming from CKM phase of SM. This implies

$$\arg(M_1),\ \arg(M_2),\ \arg(M_3),\ \arg(A_{u0}),\ \arg(A_{d0}),\ \arg(A_{e0}) \ = \ 0 \text{ or } \pi, \tag{2.51}$$

The next question is to ask whether spontaneous breaking of SUSY tells us something about the soft terms and whether it is possible to generate the pattern given in equations 2.49, 2.50 and 2.51.

Spontaneous breaking of SUSY

Spontaneous SUSY breaking means that the vacuum state is not invariant under the SUSY transformations although the Lagrangian is. In other words, the

vacuum state $|0\rangle$ should not be annihilated by at least one of the SUSY generators, i.e.,

$$Q_\alpha|0\rangle \neq 0 \quad \text{or} \quad \bar{Q}_{\dot{\alpha}}|0\rangle \neq 0 \tag{2.52}$$

for some α or$\dot{\alpha}$. In global SUSY the Hamiltonian operator H and SUSY generators are related through SUSY algebra and H takes the form (equation 2.11e):

$$H = P^0 = \frac{1}{4}(Q_1Q_1^\dagger + Q_1^\dagger Q_1 + Q_2Q_2^\dagger + Q_2^\dagger Q_2) \tag{2.53}$$

This implies that the vacuum state has zero energy if SUSY is unbroken. Conversely, the vacuum has non-zero positive energy in a spontaneously broken SUSY theory. If the space-time dependent effects and fermion condensate effects can be neglected, then one can write

$$\langle 0|H|0\rangle = \langle 0|V|0\rangle \tag{2.54}$$

where V is the scalar potential of the SUSY theory at tree level, given by (equation 2.36)

$$V(\phi, \phi^\star) = F^i F^{i\star} + \frac{1}{2}D^a D^a \tag{2.55}$$

Hence, SUSY will be spontaneously broken if F_i and/or D^a does not vanish in the ground state. To break SUSY, either the VEV of F-term of a chiral superfield has to be non-zero (known as F-term SUSY breaking [20]) or the VEV of D-term of a vector superfield should be non-vanishing (known as D-term SUSY breaking [21]). There is also a possibility of breaking SUSY dynamically [22]. But we will not consider it here and concentrate only on the spontaneous breaking aspects of SUSY.

One of the consequences of spontaneous breaking of a global SUSY is the generation of a massless neutral Weyl fermion, which is known as goldstino, having the same quantum numbers as that of the broken symmetry generator. Goldstino is a potential problem of spontaneously broken global SUSY theories, just like Goldstone bosons in case of ordinary global symmetries. Another potential problem with spontaneously broken SUSY is due to the *supertrace* theorem. It states that, the weighted sum of tree level squared-masses (m_j^2) over all particles of spin j is zero, i.e.,

$$STr(m^2) = \Sigma_j(-)^{2j}(2j+1)Tr(m^2{}_j) = 0 \tag{2.56}$$

This theorem is valid when SUSY is broken spontaneously via renormalisable interactions, which implies that the superpartners of light fermions will be much

lighter than the masses of the light fermions themselves and therefore phenomenologically quite unsatisfactory.

It is therefore clear that spontaneous breaking of SUSY in the visible sector can not lead us to phenomenologically acceptable predictions. Hence we need to look for a different SUSY breaking sector (hidden sector) and SUSY breaking will be then transmitted to the MSSM sector (visible sector) by some mechanism. The guidelines for such a mechanism are the following:

- SUSY breaking to the visible sector must be transmitted either via non-renormalisable interactions or via loops.
- In addition, it will be of phenomenological interest if the interaction is flavour blind, so that it is possible to achieve the pattern given in equations (2.49-2.51)
- The SUSY breaking at the hidden sector must take place at some scale consistent with m_{soft}.

There are many competing models depending on various SUSY breaking mechanisms at the hidden sector and also the mechanism for mediation to the visible sector. *Supergravity* or gravity mediated SUSY breaking is the most popular among them and we describe it below.

Supergravity

In the supergravity framework [23] SUSY transformation is no longer global, instead the transformation parameters become space-time dependent, i.e., it is now a local transformation. SUSY breaking is transmitted to the MSSM sector by gravitational interaction suppressed by Planck mass (M_P). The following set of non-renormalisable interaction terms can be written:

$$\begin{aligned}\mathcal{L}_{\text{Nonrenm. int.}} &= -\frac{1}{M_P}F\left(\frac{1}{2}f_a\lambda^a\lambda^a + \frac{1}{6}y'^{ijk}\phi_i\phi_j\phi_k + \frac{1}{2}\mu'^{ij}\phi_i\phi_j\right) + \text{c.c.} \\ &\quad -\frac{1}{M_P^2}FF^*\,k^i_j\phi_i\phi^{*j} \end{aligned} \tag{2.57}$$

where F is the auxiliary field for a chiral supermultiplet in the hidden sector, and ϕ_i and λ^a are the scalar and gaugino fields in the MSSM, and f^a, y'^{ijk}, and k^i_j are dimensionless couplings. The full Lagrangian for supergravity is much more complicated and the details are beyond the scope of this thesis. Once the

auxiliary field F gets a VEV, all the MSSM soft terms mentioned in equation 2.41 are generated. By dimensional analysis,

$$m_{soft} \sim \frac{< F >}{M_P} \tag{2.58}$$

and in order to get a correct order of magnitude for the m_{soft}, the SUSY breaking scale $\sqrt{< F >}$ should be $\sim 10^{11}$ GeV.

The large set of parameters f_a, k^i_j, y'^{ijk} and μ'^{ij} in $\mathcal{L}_{\text{Nonrenm. int.}}$, which are to be determined by the underlying theory, make it inconvenient for phenomenological purpose. This problem simplifies considerably in the minimal form, where one assumes a common $f_a = f$ for the three gauginos; $k^i_j = k\delta^i_j$ is the same for all scalars; and the other couplings are proportional to the corresponding superpotential parameters, so that $y'^{ijk} = \alpha y^{ijk}$ and $\mu'^{ij} = \beta\mu^{ij}$ with universal dimensionless constants α and β. Then the soft terms in $\mathcal{L}^{\text{MSSM}}_{\text{soft}}$ are all determined by just four parameters:

$$m_{1/2} = f\frac{\langle F\rangle}{M_P}, \qquad m_0^2 = k\frac{|\langle F\rangle|^2}{M_P^2}, \qquad A_0 = \alpha\frac{\langle F\rangle}{M_P}, \qquad B_0 = \beta\frac{\langle F\rangle}{M_P}. \tag{2.59}$$

In terms of these, the parameters appearing in equation 2.41 are:

$$M_3 = M_2 = M_1 = m_{1/2}, \tag{2.60}$$

$$\mathbf{m_Q^2} = \mathbf{m_{\bar{u}}^2} = \mathbf{m_{\bar{d}}^2} = \mathbf{m_L^2} = \mathbf{m_{\bar{e}}^2} = m_0^2\,\mathbf{1}, \qquad m^2_{H_u} = m^2_{H_d} = m_0^2, \tag{2.61}$$

$$\mathbf{a_u} = A_0\mathbf{y_u}, \qquad \mathbf{a_d} = A_0\mathbf{y_d}, \qquad \mathbf{a_e} = A_0\mathbf{y_e}, \tag{2.62}$$

$$b = B_0\mu \tag{2.63}$$

at a renormalisation scale $Q \approx M_P$ and all the MSSM soft parameters can then be obtained by RGEs of the soft parameters from the unified high-scale boundary conditions down to low energy. Though the unification of parameters does not follow from any symmetry principle, nevertheless, with this assumptions the phenomenology of such a theory becomes more tractable.

Besides the aforementioned scenario, there are also other SUSY breaking frameworks. For example, in gauge-mediated SUSY breaking (GMSB) model, where the SUSY breaking to the visible sector is transmitted via gauge interactions and the MSSM soft terms are generated via loops involving some messenger particles [24]. Another possibility is anomaly-mediated SUSY breaking (AMSB), where the MSSM soft terms arise due to the anomalous violation of the local superconformal invariance [25].

2.6 Search for supersymmetry at colliders

The SUSY extension of the SM comes with a proliferation of new particles. SUSY with conserved $\mathcal{R}$-parity implies that SUSY particles (or sparticles) are produced in pair at the colliding beam experiments and the decay of a sparticle must associate another sparticle. Therefore the LSP becomes stable and all the SUSY cascade should culminate in pair production of the LSP's. Now, the LSP is required to be neutral and weakly interacting from the cosmological observations. Hence, the LSP goes undetected at the detector, resulting in large amount of missing energy and momentum carried away by it. This is a canonical signal of SUSY. However, if $\mathcal{R}$ -parity is not conserved then the LSP will decay into the SM particles, increasing lepton or jet multiplicities in the final state, and the missing energy will only be due to the neutrinos.

In the next section we describe the limits or constraints on various SUSY models.

2.6.1 SUSY search at the LEP and the Tevatron

The large e^+e^- collider, LEP was in operation from 1989 to 2000 at CERN. Initially it started running at a center-of-mass energy near the Z-pole (91.2 GeV) and then progressively moved up to a center-of-mass energy of 209 GeV. In e^+e^- colliders, missing energy can be directly inferred from the knowledge of center-of-mass energy ($\sqrt{s}$) and total visible energy (E). Four detectors, ALEPH, DELPHI, L3, and OPAL, each collected a total of about 1 fb^{-1} of data [26].

On the otherhand, the Tevatron is a $p\bar{p}$-collider at Fermilab. Its first run at a center-of-mass energy 1.8 TeV, ended in 1996. In hadron collider , however, the initial momenta of the partons along the beam direction are unknown. Hence, missing transverse energy, rather than missing energy, obtained by balancing the visible momenta in the transverse plane, is a useful variable. During its first phase of run the CDF and DØ detectors collected about 110 pb^{-1} of data each. Run-II of Tevatron began in 2001 at a center-of-mass energy 1.96 TeV. By 2009 over 6 fb^{-1} of data had been accumulated by each experiment [27].

The models studied are the mSUGRA inspired MSSM, with conserved $\mathcal{R}$-parity. The LSP in such a scenario is the lightest neutralino; GMSB model, where the LSP is the gravitino and the NLSP is the lightest neutralino or lighter stau; and

various $\mathcal{R}$-parity violating models. The observations of hardly any SUSY events at both the colliders, set some lower limits on the mass of the superparticles. We list them below:

- $m_{\tilde{g}} > 390$ GeV at 95 % confidence level (CL) assuming $m_{\tilde{q}} = m_{\tilde{g}}$. The limit is 308 GeV for any values of squark masses. These limits in addition, assume GUT unification of gaugino masses and gauge couplings and weakly depends on $\tan\beta$.
- $m_{\tilde{q}} > 379$ GeV with 95% CL. Although this is specifically for $\mu < 0$ and $\tan\beta = 2$, this limit is weakly sensitive to these parameters. Limits on third generation squarks are lower.
- Limits on sleptons are also around 100 GeV. Same is the case for lighter chargino.

2.6.2 Search for SUSY at the Large Hadron Collider

The Large Hadron Collider (LHC) [28] which is a pp-collider at CERN, started running in 2009. Six different detectors, namely, ATLAS, CMS, ALICE, LHCb, TOTEM and LHCf are built for various physics purposes [29]. Among these the ATLAS and CMS detectors are specially dedicated for issues in SM (for example top physics, Higgs search, etc.) and they also look for signals of various new physics scenarios. The other detectors are made for studying B-physics, flavour physics, heavy ion collision, physics in the extreme forward region etc. We shall concentrate on the various physics issues that have already been addressed or will be addressed in near future at these two detectors. In September, 2008, the proton beams were successfully circulated in the ring of LHC for the first time, but were halted due to some major technical problems. In 2009, the proton beams were again circulated and the the first proton-proton collision was recorded at a center-of-mass energy of 450 GeV three days later. Figure 2.3 depicts a typical LHC detector and a schematic diagram of proton-proton collision is shown in Figure 2.4.

One major disadvantage of LHC, like the Tevatron is the lack of knowledge of partonic center-of-mass motion. Hence, it is difficult to reconstruct the missing momentum along the beam direction. Therefore, in LHC one works with the transverse component of missing momentum. The environment is less clean compared to that of the e^+e^--collider. Processes consisting of hadronic final states

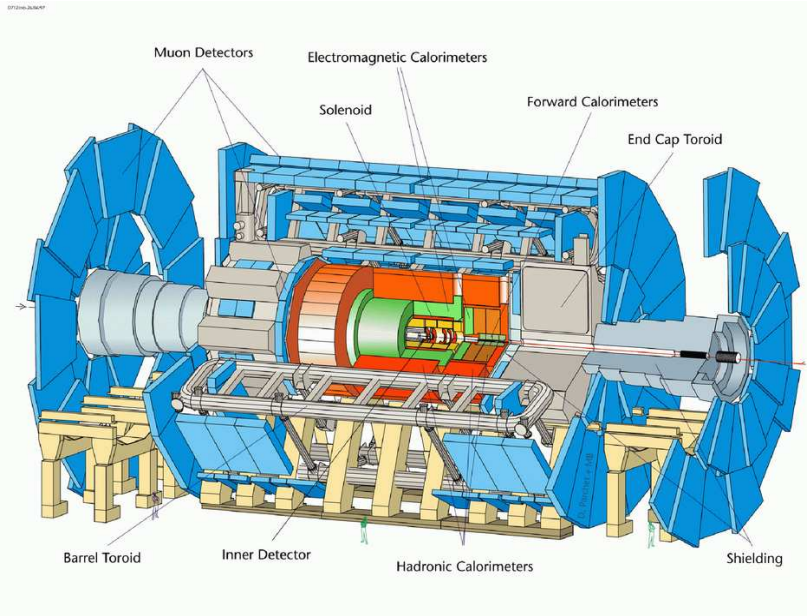

Figure 2.3: A typical LHC detector [30].

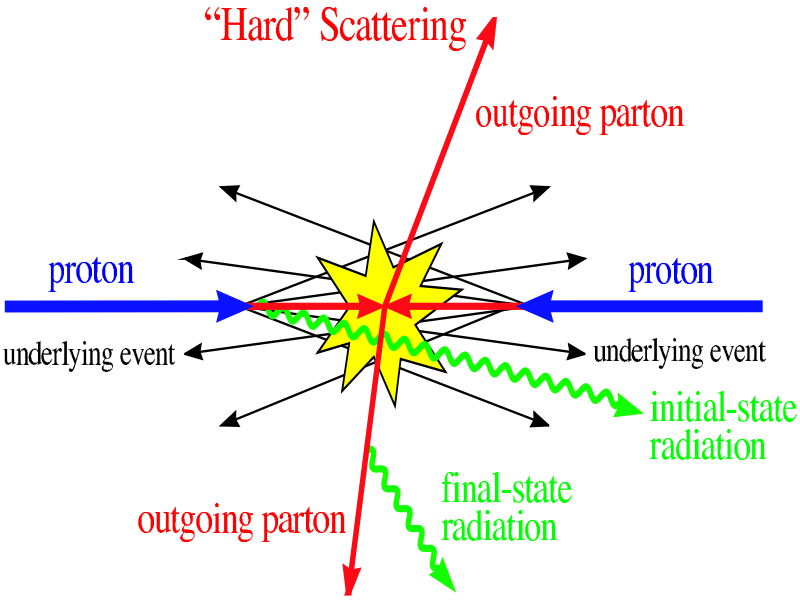

Figure 2.4: An illustrative event in pp-collision at the LHC [31].

e.g., $q\bar{q}$, qg, gg, $t\bar{t}$ have huge cross-section at the LHC and are of serious concern as the background of new physics signals. Also a large number of underlying and pile-up events are expected to be present.

The LHC being a hadron collider, it is dominated by the strong production and if SUSY exists at the TeV scale, squarks and gluinos will be copiously produced at LHC. The generic search channel at the LHC consists of $n\ leptons + m\ jets + \not{E}_T$. Jets are a cluster of hadrons defined within a certain cone with a minimum transverse energy. In Table 2.3 we summarise the various search channels at the LHC.

In 2010, LHC started running with center-of-mass energy of 7 TeV and when this thesis is being written the CMS and ATLAS collaborations have already collected and analysed 35 pb^{-1} of data. The analyses have been done both model dependent and model independent way. In the first case, the model mainly studied is the minimal supergravity and constrained MSSM (CMSSM). Some new bounds have been obtained with an extension of the exclusion limit in the $m_0 - m_{1/2}$-plane (see Figure 2.5, 2.6). This in turn puts some lower bounds on the masses of the squarks and gluinos (roughly, $m_{\tilde{g}} \gtrsim 600$ GeV and $m_{\tilde{g}} \gtrsim 650$ GeV), though, the amount of data obtained is still insufficient to make any kind of conclusive statement. Moreover, relaxation of the conditions of universal gaugino and scalar masses at high scale can open up many additional allowed region of the SUSY parameter space.

Hopefully, the LHC will reach its design center-of-mass energy (14 TeV) and luminosity in the near future, and one may either end up discovering SUSY at the LHC or set some strong limit on the mass ($\geq 1 - 3$ TeV) of the superparticles. In the latter case, our understanding of the Higgs mass stabilization mechanism needs to be reviewed.

Production	The main decay modes	Signature
• $\tilde{g}\tilde{g}, \tilde{q}\tilde{q}, \tilde{g}\tilde{q}$	$\left.\begin{array}{l} \tilde{g} \to q\bar{q}\tilde{\chi}_1^0 \\ q\bar{q}'\tilde{\chi}_1^\pm \\ g\tilde{\chi}_1^0 \end{array}\right\} m_{\tilde{q}} > m_{\tilde{g}}$ $\left.\begin{array}{l} \tilde{q} \to q\tilde{\chi}_i^0 \\ \tilde{q} \to q'\tilde{\chi}_i^\pm \end{array}\right\} m_{\tilde{g}} > m_{\tilde{q}}$	$\not{E}_T +$ multijets (+leptons)
• $\tilde{\chi}_1^\pm \tilde{\chi}_2^0$	$\tilde{\chi}_1^\pm \to \tilde{\chi}_1^0 \ell^\pm \nu,\ \tilde{\chi}_2^0 \to \tilde{\chi}_1^0 \ell\ell$	trilepton + $\not{E}_T$
	$\tilde{\chi}_1^\pm \to \tilde{\chi}_1^0 q\bar{q}', \tilde{\chi}_2^0 \to \tilde{\chi}_1^0 \ell\ell,$	dileptons + jet + $\not{E}_T$
• $\tilde{\chi}_1^+ \tilde{\chi}_1^-$	$\tilde{\chi}_1^+ \to \ell\tilde{\chi}_1^0 \ell^\pm \nu$	dilepton + $\not{E}_T$
• $\tilde{\chi}_i^0 \tilde{\chi}_i^0$	$\tilde{\chi}_i^0 \to \tilde{\chi}_1^0 \ell\ell, \tilde{\chi}_i^0 \to \tilde{\chi}_1^0 q\bar{q}$	dilepton+jet + $\not{E}_T$
• $\tilde{t}_1 \tilde{t}_1$	$\tilde{t}_1 \to c\tilde{\chi}_1^0$	2 noncollinear jets + $\not{E}_T$
	$\tilde{t}_1 \to b\tilde{\chi}_1^\pm, \tilde{\chi}_1^\pm \to \tilde{\chi}_1^0 q\bar{q}'$	single lepton + $\not{E}_T + b's$
	$\tilde{t}_1 \to b\tilde{\chi}_1^\pm, \tilde{\chi}_1^\pm \to \tilde{\chi}_1^0 \ell^\pm \nu,$	dilepton + $\not{E}_T + b's$
• $\tilde{l}\tilde{l}, \tilde{l}\tilde{\nu}, \tilde{\nu}\tilde{\nu}$	$\tilde{\ell}^\pm \to \ell^\pm \tilde{\chi}_i^0, \tilde{\ell}^\pm \to \nu_\ell \tilde{\chi}_i^\pm$	dilepton + $\not{E}_T$
	$\tilde{\nu} \to \nu\tilde{\chi}_1^0$	single lepton + $\not{E}_T$

Table 2.3: *Production of superpartners and the main decay modes. Courtesy A. V. Gladyshev et. al. [7].*

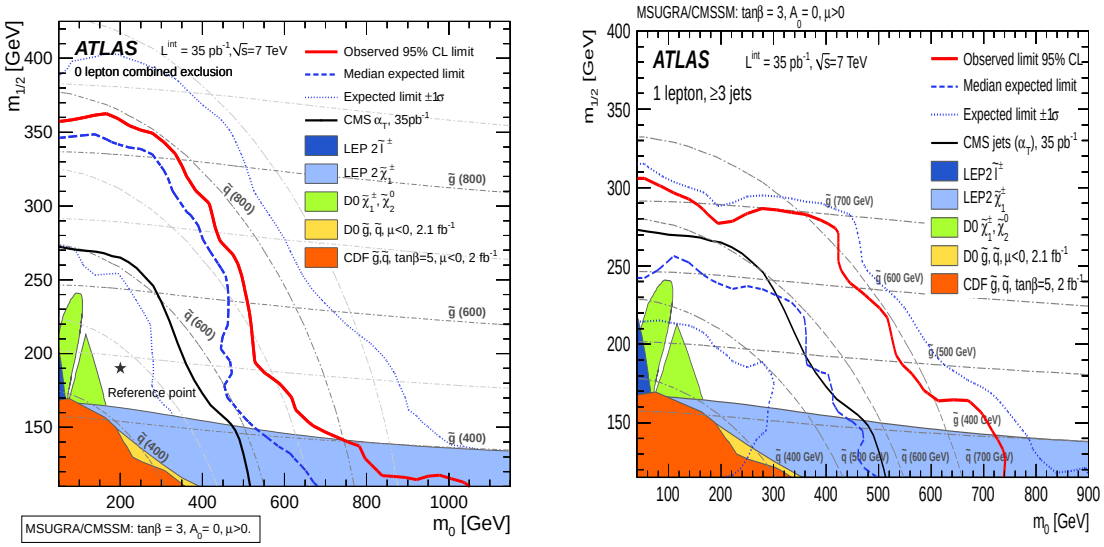

Figure 2.5: The LHC data. The exclusion limit in the $m_0 - m_{1/2}$-plane of mSUGRA/CMSSM in the a) $jets + \not{E}_T$ channel (left) and b) $\ell + jets + \not{E}_T$ channel (right). Courtesy ATLAS collaboration [32].

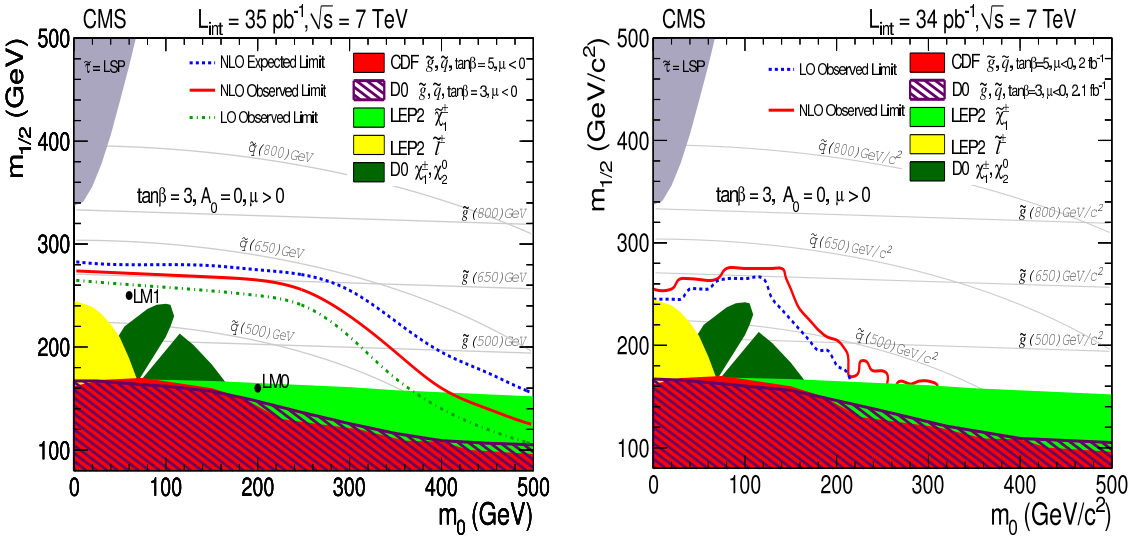

Figure 2.6: The LHC data. The exclusion limit in the $m_0 - m_{1/2}$-plane of mSUGRA/CMSSM in the a) $jets + \not{E}_T$ channel (left) and b) $\ell^+\ell^- + jets + \not{E}_T$ channel (right). Courtesy CMS collaboration [33].

Bibliography

[1] For introductry reviews see, for example, H. P. Nilles, Phys. Rept. **110**, 1 (1984); J. Wess and J. Bagger, *Supersymmetry and Supergravity*, (Princeton Univ. Press, 1992). P.C. West, *Introduction to Supersymmetry and Supergravity*, (World Scientific, 1990); D. Bailin and A. Love, *Supersymmetric Gauge Field Theory and String Theory*, (Institute of Physics Publishing, 1994); M. Drees, R. Godbole and P. Roy, *Theory and Phenomenology of Sparticles*, (World Scientific, 2004); H. Baer and X. Tata *Weak Scale Supersymmetry From Superfields to Scattering Events*, (Cambridge University Press, 2006).

[2] For reviews see, for example, H. E. Haber and G. L. Kane, Phys. Rept. **117**, 75 (1985); *Perspectives on Supersymmetry* by G. Kane(ed), (World Scientific, 1998) and articles therein; M. Drees and S.P. Martin, [hep-ph/9504324]; M. Drees, arXiv:hep-ph/9611409; J.D. Lykken, TASI-96 lectures, [hep-th/9612114]; S. P. Martin, arXiv:hep-ph/9709356, and references therein; J.F. Gunion, [hep-ph/9704349], M. E. Peskin, arXiv:0801.1928 [hep-ph].

[3] J. Wess and B. Zumino, Nucl. Phys. B **70**, 39 (1974). J. Wess and B. Zumino, Phys. Lett. B **49**, 52 (1974). J. Wess and B. Zumino, Nucl. Phys. B **78**, 1 (1974). J. Wess and B. Zumino, Phys. Lett. B **74**, 51 (1978).

[4] A. Salam and J. A. Strathdee, Phys. Lett. B **51**, 353 (1974). A. Salam and J. A. Strathdee, Nucl. Phys. B **76**, 477 (1974). A. Salam and J. A. Strathdee, Nucl. Phys. B **80**, 499 (1974). A. Salam and J. A. Strathdee, Nucl. Phys. B **87**, 85 (1975).

[5] P. Fayet, Phys. Lett. B **58**, 67 (1975). P. Fayet, Nucl. Phys. **B90**, 104 (1975). P. Fayet, Nuovo Cim. A **31**, 626 (1976). P. Fayet, Phys. Lett. B **64**, 159 (1976). P. Fayet and S. Ferrara, Phys. Rept. **32**, 249 (1977).

[6] S. Dimopoulos, H. Georgi, Nucl. Phys. **B193**, 150 (1981).

[7] A. V. Gladyshev and D. I. Kazakov, Phys. Atom. Nucl. **70**, 1553 (2007) [arXiv:hep-ph/0606288].

[8] S. R. Coleman and J. Mandula, Phys. Rev. **159**, 1251 (1967);

[9] R. Haag, J. Lopuszanski, and M. Sohnius, Nucl. Phys. B **88**, 257 (1975).

[10] M. E. Peskin, Prog. Theor. Phys. Suppl. **123**, 507 (1996) [arXiv:hep-ph/9604339].

[11] L. Girardello and M.T. Grisaru Nucl. Phys. B **194**, 65 (1982); D.J.H. Chung et al., Phys. Rept. **407**, 1 (2005) [hep-ph/0312378]; M.A. Luty, [hep-th/0509029].

[12] X. Tata, [hep-ph/9706307]; I. Aitchison,[hep-ph/0505105].

[13] J. Ellis and D.V. Nanopoulos, Phys. Lett. B **110**, 44 (1982); R. Barbieri and R. Gatto, Phys. Lett. B **110**, 211 (1982); B.A. Campbell, Phys. Rev. D **28**, 209 (1983); J.F. Donahue, H.P. Nilles and D. Wyler, Phys. Lett. B **128**, 55 (1983); A. Bouquet, J. Kaplan and C.A. Savoy, Phys. Lett. B **148**, 69 (1984); M. Dugan, B. Grinstein and L.J. Hall, Nucl. Phys. B **255**, 413 (1985); F. Gabbiani and A. Masiero, Nucl. Phys. B **322**, 235 (1989); J. Hagelin, S. Kelley and T. Tanaka, Nucl. Phys. B **415**, 293 (1994); M. Misiak, S. Pokorski and J. Rosiek, "Supersymmetry and FCNC effects," [hep-ph/9703442].

[14] L.J. Hall, V.A. Kostalecky and S. Raby, Nucl. Phys. B **267**, 415 (1986); F. Gabbiani and A. Masiero, Phys. Lett. B **209**, 289 (1988); R. Barbieri and L.J. Hall, Phys. Lett. B **338**, 212 (1994) [hep-ph/9408406]; R. Barbieri, L.J. Hall and A. Strumia, Nucl. Phys. B **445**, 219 (1995) [hep-ph/9501334].

[15] J. Ellis, S. Ferrara and D.V. Nanopoulos, Phys. Lett. B **114**, 231 (1982); W. Buchmüller and D. Wyler, Phys. Lett. B **121**, 321 (1983); J. Polchinski and M.B. Wise, Phys. Lett. B **125**, 393 (1983); F. del Aguila, M.B. Gavela, J.A. Grifols and A. Méndez, Phys. Lett. B **126**, 71 (1983) [Erratum-ibid. B **129**, 473 (1983)]; D.V. Nanopoulos and M. Srednicki, Phys. Lett. B **128**, 61 (1983).

[16] S. Bertolini, F. Borzumati, A. Masiero and G. Ridolfi, Nucl. Phys. B **353**, 591 (1991); R. Barbieri and G.F. Giudice, Phys. Lett. B **309**, 86 (1993) [hep-ph/9303270].

[17] F. Gabbiani, E. Gabrielli, A. Masiero and L. Silvestrini, Nucl. Phys. B **477**, 321 (1996) [hep-ph/9604387]; Y. Grossman, Y. Nir and R. Rattazzi, [hep-

ph/9701231]; S. Pokorski, J. Rosiek and C. A. Savoy, Nucl. Phys. B **570**, 81 (2000) [hep-ph/9906206]; S. Abel, S. Khalil and O. Lebedev, Nucl. Phys. B **606**, 151 (2001) [hep-ph/0103320]; S. Khalil, T. Kobayashi and A. Masiero, Phys. Rev. D **60**, 075003 (1999) [hep-ph/9903544].

[18] P.H. Chankowski and L. Slawianowska, Phys. Rev. D **63**, 054012 (2001) [hep-ph/0008046]; T. Besmer, C. Greub and T. Hurth, Nucl. Phys. B **609**, 359 (2001) [hep-ph/0105292]; A.J. Buras, P.H. Chankowski, J. Rosiek and L. Slawianowska, Nucl. Phys. B **659**, 3 (2003) [hep-ph/0210145]; M. Ciuchini, E. Franco, A. Masiero and L. Silvestrini, Phys. Rev. D **67**, 075016 (2003) [Erratum-ibid. D **68**, 079901 (2003)] [hep-ph/0212397].

[19] M.L. Brooks *et al.* [MEGA Collaboration], Phys. Rev. Lett. **83**, 1521 (1999) [hep-ex/9905013], Phys. Rev. D **65**, 112002 (2002) [hep-ex/0111030].

[20] L. O'Raifeartaigh, Nucl. Phys. **B96**, 331 (1975).

[21] P. Fayet and J. Illiopoulos, Phys. Lett. B **51**, 461 (1974); P. Fayet, Nucl. Phys. **B90**, 104 (1975).

[22] E. Witten, Nucl. Phys. **B202**, 253 (1982); I. Affleck, M. Dine and N. Seiberg, Nucl. Phys. **B241**, 493 (1981).

[23] A. H. Chamseddine, R. Arnowitt and P. Nath, Phys. Rev. Lett. **49**, 970 (1982); R. Barbieri, S. Ferrara and C. A. Savoy, Phys. Lett. B **119**, 343 (1982); L. J. Hall, J. Lykken and S. Weinberg, Phys. Rev. D **27**, 2359 (1983); P. Nath, R. Arnowitt and A. H. Chamseddine, Nucl. Phys. B **227**, 121 (1983); N. Ohta, Prog. Theor. Phys. **70**, 542 (1983).

[24] M. Dine, A. E. Nelson, Phys. Rev. D **48**, 1277 (1993) [hep-ph/9303230]; M. Dine, A.E. Nelson, Y. Shirman, Phys. Rev. D **51**, 1362 (1995) [hep-ph/9408384]; M. Dine, A.E. Nelson, Y. Nir, Y. Shirman, Phys. Rev. D **53**, 2658 (1996) [hep-ph/9507378].

[25] L. Randall and R. Sundrum, Nucl. Phys. B **557**, 79 (1999) [hep-th/9810155]; G.F. Giudice, M.A. Luty, H. Murayama and R. Rattazzi, JHEP **9812**, 027 (1998) [hep-ph/9810442].

[26] H. Baer, M. Drees and X. Tata, Phys. Rev. D **41**, 34143420 (1990); The LEP SUSY Working Group (LEPSUSYWG), `http://www.cern.ch/lepsusy`.

[27] H. Baer, C. Kao and X. Tata, Phys. Rev. D **48**, 51755180 (1993); M. Carena, R. Culbertson, H. Frisch, S. Eno and S. Mrenna, Rev. Mod. Phys. **71**, 937981

(1999); The Tevatron Run II studies on supersymmetry: S. Abel *et al.* [SUGRA Working Group Collaboration], [hep-ph/0003154]; S. Ambrosanio *et al.* [MSSM Working Group Collaboration], [hep-ph/0006162]; R. Culbertson *et al.* [SUSY Working Group Collaboration], [hep-ph/0008070].

[28] The LHC Study Group, Large Hadron Collider, The Accelerator Project, CERN/AC/93-03 (LHC); The LHC Study Group, P. Lefevre and T. Pettersson (editors), The Large Hadron Collider, Conceptual Study, CERN/AC/95-05 (LHC); (http://lhc.web.cern.ch/lhc/).

[29] ATLAS Technical proposal, CERN/LHCC/94-43. CMS Technical proposal, CERN/LHCC/94-38. ALICE Technical Proposal, CERN/LHCC/95-71. LHCb Technical Proposal, CERN-LHCC-98-04. TOTEM Technical Proposal, CERN/LHCC/99-07. LHCf Technical Proposal, CERN-LHCC-05-32.

[30] ATLAS detector, ATLAS-TDR-017, CERN-LHCC-2005-022, (http://scipp.ucsc.edu/personnel/atlas.html).

[31] T. Han, arXiv:hep-ph/0508097.

[32] ATLAS Collaboration, arXiv:1102.5290 [hep-ex]; arXiv:1102.2357 [hep-ex].

[33] CMS Collaboration, arXiv:1101.1628 [hep-ex]; arXiv:1104.3168 [hep-ex].

Chapter 3

SUSY with right-chiral sneutrino and long-lived stau

3.1 Introduction

In the last chapter we have seen that the search for SUSY is largely based on the large amount of $\not{E}_T$ in association with hard jets and/or leptons due to a pair of invisible LSP in an R-parity conserving scenario. However, within the MSSM or in some small variant of it, there is a possibility that the LSP is produced outside the detector in a collider experiment, owing to the fact that the decay of all other MSSM particles to the LSP is highly suppressed. This may occur due to very small coupling involved between them, so that the decay width is small, or due to very small mass splitting, so that decay of NLSP into the LSP is kinematically suppressed. Though all other MSSM particles will cascade down to the NLSP in several steps, the NLSP will turn out to be stable at the length scale of the detector in such cases. In cases where the NLSP is a charged particle, the signal for SUSY lies in a pair of charged tracks due to massive particles at the muon chamber.

In the framework of general MSSM (see section 2.4), one can in principle have such a possibility and any charged sparticle can be a candidate for long-lived charged NLSP [1]. An interesting scenario here is that of a light stop NLSP [2–5], as motivated by electroweak baryogenesis [6, 7]. In this scenario non-universal squark mass terms are used to arrange a small mass difference between the $\tilde{t_1}$ and the lightest neutralino which is the LSP. One can also have a $\tilde{\tau}_1$ NLSP for small slepton masses and/or large $\tan\beta$ and/or large A_τ or, the less likely case of a $\tilde{b}_1$ NLSP for small squark masses and large $\tan\beta$ and/or very large $A_b >> A_t$ nearly degenerate with the LSP.

In models motivated by various SUSY breaking mechanisms, a long-lived charged massive NLSP appears very naturally [1]. And more often than not the charged NLSP turns out to be the lighter charged slepton of third generation ($\tilde{\tau}$). There are a number of situations where such a long-lived $\tilde{\tau}$-NLSP may occur. For example,

- In supergravity models with gravitino LSP and stau NLSP, the stau can be long-lived due to the gravitational coupling involved between them, which is suppressed by ($M_{Planck} \approx 2.4 \times 10^{18}$ GeV) [8].
- In Gauge Mediated SUSY Breaking (GMSB) Models with gravitino LSP, where the SUSY breaking at the hidden sector can in principle takes place at very low scale (10-1000 TeV) and is mediated to the MSSM sector by guage interactions, one can have a long-lived stau as the NLSP [9, 10].
- MSSM with a right-chiral neutrino superfield, motivated by the non-vanishing neutrino masses and mixings [11, 12] can eminently lead to a situation in which the $\tilde{\nu}_R$ is the LSP and $\tilde{\tau}$ is the NLSP. The stau can be quasi-stable if the neutrinos only interact via neutrino Yukawa coupling [13, 14].

In this chapter we will concentrate on this last possibility and will describe in the next section how one can achieve this possibility in a high-scale framework of SUSY breaking namely, mSUGRA.

3.2 Right-chiral sneutrino LSP in an mSUGRA framework

As has been already stated, the most simple-minded extension of the MSSM, accommodating neutrino masses, is the addition of one right-handed neutrino superfield per family. If the neutrinos are of Majorana type, the smallness of the

neutrino mass can be explained by the seesaw mechanism introducing heavy Majorana mass (larger than the electroweak scale) for the right-handed neutrinos [15–17]. In that case the mass of the right-handed sneutrino is governed by the same term in addition to the SUSY breaking mass term and it is difficult to obtain a right-chiral sneutrino LSP in such a case.

On the other hand, if the neutrinos have purely Dirac mass, then the right-handed sneutrinos receive masses dominantly from SUSY breaking terms. As a result, there is a possibility that the $\tilde{\nu}_R$ can be the LSP for well-motivated values of the SUSY breaking parameters.

The superpotential of such an extended MSSM becomes (suppressing family indices) [13, 14],

$$W_{MSSM} = y_l \hat{L} \hat{H}_d \hat{E}^c + y_d \hat{Q} \hat{H}_d \hat{D}^c + y_u \hat{Q} \hat{H}_u \hat{U}^c + \mu \hat{H}_d \hat{H}_u + y_\nu \hat{H}_u \hat{L} \hat{\nu}^c_R \tag{3.1}$$

where $\hat{H}_d$ and $\hat{H}_u$, respectively, are the Higgs superfields that give masses to the $T_3 = -1/2$ and $T_3 = +1/2$ fermions, and $y's$ are the strengths of Yukawa interaction. $\hat{L}$ and $\hat{Q}$ are the left-handed lepton and quark superfields respectively, whereas $\hat{E}^c$, $\hat{D}^c$ and $\hat{U}^c$, in that order, are the right handed charged lepton, down-type and up-type quark superfields. $\hat{\nu}^c$ is the right-chiral gauge singlet neutrino superfield and μ is the Higgsino mass parameter.

The neutrino masses are typically given by,

$$m_\nu = y_\nu \left\langle H^0_u \right\rangle = y_\nu v \, \sin\beta \tag{3.2}$$

The right-handed sneutrinos interact via only the neutrino Yukawa coupling (y_ν) and the small Diarc masses of the neutrinos, induced by very small Yukawa couplings imply that y_ν are quite small ($\lesssim 10^{-13}$).

It is a common practice to attempt reduction of free parameters in the theory and at the same time suggest consistent SUSY breaking schemes, by embedding the MSSM in a high-scale framework. The most commonly adopted scheme is based on N = 1 mSUGRA (see section 2.5). There SUSY breaking in the hidden sector at high scale is manifested in universal soft masses for scalars (m_0) and gauginos ($m_{1/2}$), together with the trilinear (A) and bilinear (B) SUSY breaking parameters in the scalar sector. The bilinear parameter B is determined by the

electroweak symmetry breaking (EWSB) conditions. So is the parameter μ, up to a sign. All the scalar and gaugino masses at low energy obtained by renormalisation group evolution (RGE) of the universal mass parameters m_0 and $m_{1/2}$ from high-scale values [18]. Thus one generates all the squark, slepton, and gaugino masses as well as all the mass parameters in the Higgs sector. The Higgsino mass parameter μ (up to a sign), too is determined from EWSB conditions. All one has to do in this scheme is to specify the high scale ($m_0, m_{1/2}, A_0$, together with $sign(\mu)$ and $\tan\beta = \langle H_u \rangle / \langle H_d \rangle$) where, $\tan\beta$ is the ratio of the vacuum expectation values of the two Higgs doublets that give masses to the up-and down-type quarks respectively.

With the inclusion of the right-chiral neutrino superfields as a minimal extension, it makes sense to assume that the masses of their scalar components, too, originate in the same parameter m_0. The evolution of all other parameters practically remain the same in this scenario as in the MSSM, while the right-chiral sneutrino mass parameter evolves at the one-loop level [19] as

$$\frac{dM^2_{\tilde{\nu}_R}}{dt} = \frac{2}{16\pi^2} y_\nu^2 \; A_\nu^2 \; . \tag{3.3}$$

where A_ν is obtained by the running of the trilinear soft SUSY breaking term A and is responsible for left-right mixing in the sneutrino mass matrix.

It follows from above that the value of $M_{\tilde{\nu}_R}$ remains practically frozen at m_0, thanks to the extremely small Yukawa couplings, whereas the other sfermion masses are enhanced at the electroweak scale. Thus, for a wide range of values of the gaugino masses, one naturally ends up with a sneutrino LSP ($\tilde{\nu}_1$), dominated by the right-chiral state. This is because the mixing angle is controlled by the neutrino Yukawa couplings:

$$\tilde{\nu}_1 = -\tilde{\nu}_L \sin\theta + \tilde{\nu}_R \cos\theta \tag{3.4}$$

where the mixing angle θ is given by,

$$\tan 2\theta = \frac{2 y_\nu v \sin\beta |\cot\beta\mu - A_\nu|}{m^2_{\tilde{\nu}_L} - m^2_{\tilde{\nu}_R}} \tag{3.5}$$

Of the three charged sleptons, the amount of left-right mixing is always the largest in the third family, and hence the lighter stau ($\tilde{\tau}_1$) often turns out to be the NLSP in such a scenario. There are regions in the parameter space the three lighter sneutrino states corresponding to the three flavours act virtually as co-LSP's. It is, however, sufficient for illustrating our points to consider the lighter

sneutrino mass eigenstate of the third family, as long as the state ($\tilde{\tau}_1$) is the lightest among the charged sleptons. Thus the addition of a right-chiral sneutrino superfield, for each family, which is perhaps the most minimal input to explain neutrino masses and mixing, can eminently turn a mSUGRA theory into one with a stau NLSP and a sneutrino LSP.

3.3 Right-chiral sneutrino as dark matter of the universe

The dark matter relic density in the present universe has been precisely determined by the Wilkinson Microwave Anisotropy Probe (WMAP) [20]:

$$\Omega_{\rm DM} h^2 = 0.105^{+0.007}_{-0.013}\,, \tag{3.6}$$

where $h \simeq 0.73$ is the present Hubble constant in units of 100km/sec/Mpc [21]. Any candidate for dark matter must account for this observed relic density. It turns out that the right-chiral sneutrino can be a viable candidate for it. The next crucial question then arises how are they produced in the early universe in order to have the correct relic abundance that we observe today?

In the early universe these sneutrinos were never thermalised due to their extremely small neutrino Yukawa coupling. One possibility is then that they were produced either via the decay of MSSM superparticles or via decays of the MSSM-LSP after freeze out, assuming the initial abundance of $\tilde{\nu}_R$ is zero. The decay of the MSSM-LSP into $\tilde{\nu}_R$ is extremely suppressed due to very small neutrino Yukawa coupling and the lifetime of the MSSM-LSP is long enough so that the decay of the MSSM-LSP occurs sufficiently after its freeze out [13, 22].

In a minimal supergravity framework, three right-handed sneutrinos have similar fate, i.e., they are almost degenerate in masses. The mass differences mainly come from the effects of RG evolution through y_ν, and hence they are very small. Consequently, all the three right-handed sneutrinos are stable within the age of the universe and contribute to the dark-matter density.

The density parameter of $\tilde{\nu}_R$ from the decay of the MSSM-LSP after freeze out is given by [13]

$$\Omega^{\rm FO}_{\tilde{\nu}_R} = \frac{m_{\tilde{\nu}_R}}{m_{\text{MSSM-LSP}}}\,\Omega_{\text{MSSM-LSP}}\,, \tag{3.7}$$

where $\Omega_{\text{MSSM-LSP}}$ is the (would-be) present density parameter of the MSSM-LSP for the case where it is stable. $\Omega_{\text{MSSM-LSP}}$ is estimated using conventional method since the neutrino Yukawa coupling constants are very small.

$\tilde{\nu}_R$ can account for the present dark-matter density if $\Omega^{\text{FO}}_{\tilde{\nu}_R} = \Omega_{\text{DM}}$. We note here that $\Omega^{\text{FO}}_{\tilde{\nu}_R}$ is insensitive to the reheating temperature T_R after inflation as long as T_R is higher than T_F, where T_F is the freeze-out temperature which is roughly given by $T_F \sim m_{\text{MSSM-LSP}}/20$.

Based on equation 3.7, $\tilde{\nu}_R$-CDM is realised with some choice of MSSM parameters which satisfies the following relation:

$$\Omega_{\text{MSSM-LSP}} = \frac{m_{\text{MSSM-LSP}}}{m_{\tilde{\nu}_R}} \Omega_{\text{DM}} \,. \tag{3.8}$$

Since $m_{\text{MSSM-LSP}} \neq m_{\tilde{\nu}_R}$, this implies that the MSSM parameters realizing $\tilde{\nu}_R$-CDM are different from those for the conventional scenario where the MSSM-LSP, say the lightest neutralino, becomes CDM. Furthermore, $\tilde{\nu}_R$-CDM is possible even if the MSSM-LSP is an electrically charged and/or coloured superparticle, and hence the $\tilde{\nu}_R$-CDM is realised in a wider parameter range compared with the MSSM-LSP dark matter [13].

3.4 Collider phenomenology

The presence of a right chiral sneutrino superfield for each generation in the MSSM particle spectrum can lead to a situation in which the LSP is dominated by the right-chiral sneutrino states. Since the right-chiral sneutrino has no gauge interaction, the only way it can interact with matter is via neutrino Yukawa coupling, the strength of which is very small. It should be emphasized that the physical LSP state can have (a) Yukawa couplings proportional to the neutrino mass, and (b) gauge coupling with the small left-chiral admixture in it, driven by left-right mixing which is again proportional to y_ν. Thus the decay of any particle (particularly the NLSP) into the LSP will always be a very slow process, not taking place within the detector. Under such circumstances, the quintessential SUSY signal is not $\not{E}_T$ anymore, but a pair of charged tracks left by the quasi-stable NLSP which often found to be the lighter mass eigen-state of the scalar tau.

Such stable charged particles can in principle be distinguished from muons through a number of techniques. These include the measurement of time delay

between the inner tracking chamber and the muon chamber, the degree of ionisation, and also more exotic proposals such as the absorption of the stable particles in a chamber which can be subsequently emptied underground to observe the decays [2, 10, 23]. While these are all of sufficient importance and interest, it has been shown in earlier works [14, 24] that there are some very good kinematic discriminators for such stable charged particles, which make the signals practically background-free. Event selection criteria based on the transverse momentum (p_T) of the tracks, in conjunction with quantities such as the scalar sum of all visible transverse momenta and the invariant mass of track pairs, are found to be useful in this respect.

The kinematic information available from this charged track helps one to reconstruct the mass of the superparticles, which is otherwise difficult in the usual SUSY scenarios, where, $\not{E}_T$ is the only signature of SUSY. In addition to this, it is also possible to analyse the polarisations of the final state particles [25] in such a scenario which, may in turn give us the hint about the spin of these sparticles.

Bibliography

[1] M. Fairbairn, A. C. Kraan, D. A. Milstead, T. Sjostrand, P. Z. Skands and T. Sloan, Phys. Rept. **438**, 1 (2007) [arXiv:hep-ph/0611040].

[2] C. L. Chou and M. E. Peskin, Phys. Rev. D **61**, 055004 (2000), [arXiv:hep-ph/9909536].

[3] S. Kraml and A. R. Raklev, Phys. Rev. D **73**, 075002 (2006) [arXiv:hep-ph/0512284].

[4] B. C. Allanach *et al.*, arXiv:hep-ph/0602198.

[5] A. de Gouvea, S. Gopalakrishna and W. Porod, JHEP **0611**, 050 (2006) [arXiv:hep-ph/0606296].

[6] M. S. Carena, D. Choudhury, R. A. Diaz, H. E. Logan and C. E. M. Wagner, Phys. Rev. D **66**, 115010 (2002) [arXiv:hep-ph/0206167].

[7] C. Balazs, M. S. Carena and C. E. M. Wagner, Phys. Rev. D **70**, 015007 (2004) [arXiv:hep-ph/0403224].

[8] J. L. Feng, A. Rajaraman and F. Takayama, Phys. Rev. Lett. **91**, 011302 (2003), [arXiv:hep-ph/0302215]; J. L. Feng, A. Rajaraman and F. Takayama, Phys. Rev. D **68**, 063504 (2003), [arXiv:hep-ph/0306024]; J. R. Ellis, K. A. Olive, Y. Santoso and V. C. Spanos, Phys. Lett. B **588**, 7 (2004), [arXiv:hep-ph/0312262]; J. L. Feng, S. Su and F. Takayama, Phys. Rev. D **70**, 075019 (2004), [arXiv:hep-ph/0404231]; A. Ibarra and S. Roy, JHEP **0705**, 059 (2007), [arXiv:hep-ph/0606116].

[9] S. Dimopoulos, M. Dine, S. Raby and S. D. Thomas, Phys. Rev. Lett. **76**, 3494 (1996), [arXiv:hep-ph/9601367]. D. A. Dicus, B. Dutta and S. Nandi, Phys. Rev. Lett. **78**, 3055 (1997), [arXiv:hep-ph/9701341]; S. Ambrosanio, G. D. Kribs and S. P. Martin, Phys. Rev. D **56**, 1761 (1997), [arXiv:hep-ph/9703211]; D. A. Dicus, B. Dutta and S. Nandi, Phys. Rev. D **56**, 5748 (1997), [arXiv:hep-ph/9704225]; K. M. Cheung, D. A. Dicus, B. Dutta and

S. Nandi, Phys. Rev. D **58**, 015008 (1998), [arXiv:hep-ph/9711216]; J. L. Feng and T. Moroi, Phys. Rev. D **58**, 035001 (1998), [arXiv:hep-ph/9712499]; P. G. Mercadante, J. K. Mizukoshi and H. Yamamoto, Phys. Rev. D **64**, 015005 (2001), [arXiv:hep-ph/0010067].

[10] S. Ambrosanio, G. D. Kribs and S. P. Martin, Phys. Rev. D **56**, 1761 (1997), [arXiv:hep-ph/9703211]; A. V. Gladyshev, D. I. Kazakov and M. G. Paucar, Mod. Phys. Lett. A **20**, 3085 (2005), [arXiv:hep-ph/0509168]; T. Jittoh, J. Sato, T. Shimomura and M. Yamanaka, Phys. Rev. D **73**, 055009 (2006), [arXiv:hep-ph/0512197].

[11] R. N. Mohapatra *et al.*, Rept. Prog. Phys. **70**, 1757 (2007), [arXiv:hep-ph/0510213].

[12] T. Schwetz, M. Tortola and J. W. F. Valle, New J. Phys. **10**, 113011 (2008), [arXiv:0808.2016 [hep-ph]]. G. L. Fogli *et al.*, Phys. Rev. D **78**, 033010 (2008), [arXiv:0805.2517 [hep-ph]]. A. Bandyopadhyay, S. Choubey, S. Goswami, S. T. Petcov and D. P. Roy, arXiv:0804.4857 [hep-ph].

[13] T. Asaka, K. Ishiwata and T. Moroi, Phys. Rev. D **73**, 051301 (2006), [arXiv:hep-ph/0512118]. T. Asaka, K. Ishiwata and T. Moroi, Phys. Rev. D **75**, 065001 (2007), [arXiv:hep-ph/0612211].

[14] S. K. Gupta, B. Mukhopadhyaya and S. K. Rai, Phys. Rev. D **75**, 075007 (2007), [arXiv:hep-ph/0701063].

[15] See, for example, P. Minkowski, Phys. Lett. **B67**, 421 (1977); T. Yanagida, in *Proceedings of the Workshop on the Unified Theory and the Baryon Number in the Universe*, O. Sawada and A. Sugamoto *(eds.)*, KEK, Tsukuba, Japan, 1979, p. 95; M. Gell-Mann, P. Ramond and R. Slansky, *Supergravity*, P. van Nieuwenhuizen *et al. (eds.)*, North Holland, Amsterdam, 1980, p. 315; R.N. Mohapatra and G. Senjanovic, Phys. Rev. Lett. **44**, 912 (1980).

[16] See, for example, R.N. Mohapatra, A. Perez-Lorenzana and C.A. de Sousa Pires, Phys. Lett. **B474**, 355 (2000) [hep-ph/9911395]; G. Altarelli and F. Feruglio, Springer Tracts Mod. Phys. **190**, 169 (2003) [hep-ph/0206077]; G. Altarelli and F. Feruglio, New J. Phys. **6**, 106 (2004) [hep-ph/0405048]; S. Bertolini, M. Frigerio and M. Malinsky, Phys. Rev. **D70**, 095002 (2004) [hep-ph/0406117]; S.F. King, Rept. Prog. Phys. **67**, 107 (2004) [hep-ph/0310204].

[17] J. Schechter and J.W.F. Valle, Phys. Rev. **D22**, 2227 (1980); J. Schechter and J.W.F. Valle, Phys. Rev. **D25**, 774 (1982); A. Mendez and F.I. Olness, Int. J.

Mod. Phys. **A2**, 1085 (1987); J.F. Gunion, J. Grifols, A. Mendez, B. Kayser and F.I. Olness, Phys. Rev. **D40**, 1546 (1989); N.G. Deshpande, J.F. Gunion, B. Kayser and F.I. Olness, Phys. Rev. **D44**, 837 (1991); E. Ma, Phys. Rev. Lett. **81**, 1171 (1998); P.Q. Hung, Phys. Lett. **B649**, 275 (2007) [arXiv:0612004 [hep-ph]]; A. Hektor, M. Kadastik, M. Muntel, M. Raidal and L. Rebane, Nucl. Phys. **B787**, 198 (2007) [arXiv:0705.1495 [hep-ph]]; T. Han, B. Mukhopadhyaya, Z. Si and K. Wang, Phys. Rev. **D76**, 075013 (2007) [arXiv:0706.0441 [hep-ph]].

[18] S. P. Martin and P. Ramond, Phys. Rev. D **48** 5365 (1993), [arXiv:hep-ph/9306314].

[19] N. Arkani-Hamed, L. J. Hall, H. Murayama, D. Tucker-Smith and N. Weiner, Phys. Rev. D **64**, 115011 (2001), [arXiv:hep-ph/0006312].

[20] E. Komatsu *et al.* [WMAP Collaboration], Astrophys. J. Suppl. **192**, 18 (2011), [arXiv:1001.4538 [astro-ph.CO]].

[21] D. N. Spergel *et al.*, astro-ph/0603449.

[22] S. Gopalakrishna, A. de Gouvea and W. Porod, JCAP **0605**, 005 (2006) [arXiv:hep-ph/0602027].

[23] K. Hamaguchi, M. M. Nojiri and A. de Roeck, JHEP **0703**, 046 (2007), [arXiv:hep-ph/0612060].

[24] D. Choudhury, S. K. Gupta and B. Mukhopadhyaya, Phys. Rev. D **78**, 015023 (2008), [arXiv:0804.3560 [hep-ph]].

[25] R. Kitano and M. Nakamura, Phys. Rev. D **82**, 035007 (2010) [arXiv:1006.2904 [hep-ph]].

Part II

Collider study

Chapter 4

Neutralino mass reconstruction

4.1 Introduction

Measurement of mass of the superparticle, if SUSY at all exists at the TeV scale, will be a crucial objective of physicists at the LHC. In general, mass measurement at the LHC is one of the most challenging task when large $\not{E}_T$ is the only signature of SUSY. However, as we have mentioned earlier when the NLSP is a charged particle and stable at the length scale of the detector, it is possible to reconstruct the masses of the superparticles by studying the details kinematics of the final state.

We have considered the mass reconstruction of the neutralinos [1] in the scenario where $\tilde{\nu}_R$ is the LSP and $\tilde{\tau}$ is the NLSP. Measurement of neutralino masses can give some hints about the gaugino mass ratio at the low scale, which in turn may points towards some high-scale relation between the gaugino masses.

Neutralinos are produced in SUSY cascade via the cascade decay of squarks and gluinos. The neutralino further decays into a $\tilde{\tau}\tau$ pair. It is to be noted that, although we have worked under an mSUGRA framework for economy of param-

eters, the cascades that lead to our desired final state are quite generic in SUSY models.

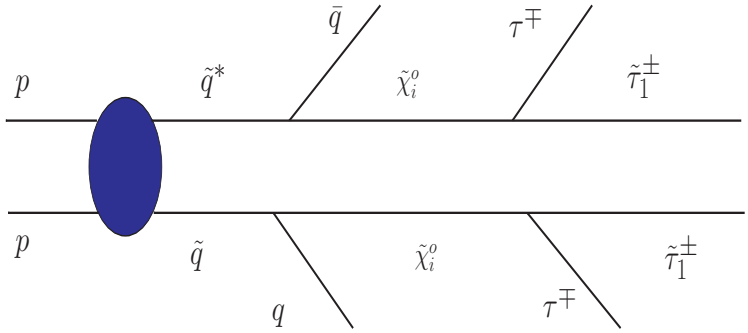

Figure 4.1: Schematic diagram of a typical SUSY cascade for reconstruction of the neutralinos.

We use the technique of tau reconstruction for this purpose. Often on-shell intermediate states are helpful here (and in the subsequent two chapters as well) in reconstructing various masses. Also, we depend neither on ionisation energy-loss nor on time delay for extracting the mass of the stable stau, but rather obtain it using an algorithm that depends on event-by-event information on two taus and two stable tracks in the final state.

In section 4.2, we discuss the choice of benchmark points used for demonstrating our claims, in the context of a supergravity scenario. The signal looked for, the corresponding standard model backgrounds and the event selection criteria chosen by us are discussed in section 4.3. Section 4.4 contains discussions on the various steps in reconstructing neutralinos. The regions in the $m_0 - m_{1/2}$ plane in a SUGRA scenario, where neutralino reconstruction is possible in our method, are also pointed out in this section. We summarise and conclude in section 4.5.

4.2 Choice of benchmark points

We try to identify regions of the parameter space, where neutralinos decaying into a tau and a stau can be reconstructed, through the reconstruction of the tau and the detection of the stau in the muon chamber. The rates for electroweak production of neutralinos are generally rather low for this process. Therefore, the

procedure works better when neutralinos are produced from the cascade decays of squarks and gluinos. This is in spite of the additional number of jets in such processes, which may fake the tau in certain cases and complicate the analysis of the signals. We are thus limited to those regions of the parameter space, where the gluino and squark production rates are appreciable, and therefore the value of $m_{1/2}$ is not too high.

With all the above considerations in mind, we concentrate on the lighter stau ($\tilde{\tau}_1$) to be the NLSP with lifetime large enough to penetrate collider detectors like the muons themselves. Using the spectrum generator of ISAJET 7.78 [2], we find that a large mSUGRA parameter space can realise this scenario of a right-sneutrino LSP and stau NLSP, provided that $m_0 < m_{1/2}$ and one has $tan\beta$ in the range $\gtrsim 25$, the latter condition being responsible for a larger left-right off-diagonal term in the stau mass matrix (and thus one smaller eigenvalue). In Table 4.1 we identify a few benchmark points, all within a SUGRA scenario with universal scalar and gaugino masses, characterised by long-lived staus at the LHC.

In the next section we use these benchmark points to discuss the signatures of the stau NLSP at the LHC and look for the final states in which it is possible to reconstruct the neutralinos.

4.3 Signal and backgrounds

The signal which we have studied as a signature of stau NLSP and motivated by the possible reconstruction of the neutralinos from the final state, is given by

- $2\tau_j + 2\tilde{\tau}(charged - track) + \not{E}_T + X$

where τ_j denotes a jet out of a one-prong decay of the tau, $\not{E}_T$ stands for missing transverse energy and all accompanying hard jets arising from cascades are included in X. The $\not{E}_T$, of course, consists of two neutrinos out of tau decays in the final state.

We have simulated pp collisions with a centre-of-mass energy $E_{CM} = 14TeV$. The prediction of events assumes an integrated luminosity of 300 fb^{-1}. The signal and various backgrounds are calculated using PYTHIA (version-6.4.16) [3]. Numerical values of various parameters, used in our calculation, are as follows [4]:

$$M_Z = 91.2\ \text{GeV}\ M_W = 80.4\ \text{GeV}\ M_t = 171.4\ \text{GeV}\ M_H = 120\ \text{GeV}$$
$$\alpha_{em}^{-1}(M_Z) = 127.9 \quad \alpha_s(M_Z) = 0.118$$

We have worked with the **CTEQ5L** parton distribution function [5]. The factorisation and renormalisation scales are set at $\mu_F = \mu_R = m_{average}^{final}$, average mass of the final state particles produced in the initial hard scattering. In order to make our estimate conservative, the signal rates have not been multiplied by any K-factor [6], while the main background, namely, that from $t\bar{t}$ production, has been multiplied by a K-factor of 1.8 [7]. The effects of initial state radiation (ISR) and final state radiation (FSR) have been considered in our study.

4.3.1 Signal subprocesses:

We have studied all SUSY subprocesses leading to the desired final states. Neutralinos are mostly produced in cascade decays of strongly interacting sparticles. The dominant contributions thus come from

- **gluino pair production:** $pp \to \tilde{g}\tilde{g}$
- **squark pair production:** $pp \to \tilde{q}_i\tilde{q}_j, \tilde{q}_i\tilde{q}_i^*$
- **associated squark-gluino production:** $pp \to \tilde{q}\tilde{g}$

In addition, electroweak pair-production of neutralinos can also contribute to the signal we are looking for. The rates are, however, much smaller [see Table 4.2]. Moreover, the relatively small masses of the lightest and the second lightest neutralinos (as compared to the squarks and the gluino) cause the signal from such subprocesses to be drastically reduced by the cut employed by us on the scalar sum of all visible p_T's. For example, for benchmark point 1 (BP1), one has less than 5% of the total contribution from electroweak processes.

The production of squarks and gluinos have potentially large cross sections at the LHC. For all our benchmark points listed in Table 4.1, the gluino is heavier than the squarks. Thus its dominant decay is into a squark and a quark. χ_1^0 being mostly $\tilde{B}$ dominated the main contribution to χ_1^0 production comes from the decay of right handed squarks ($\tilde{q}_R$) and its decay branching ratio into the $\tilde{\tau}$-τ pair is almost 100% when it is just above the lighter stau in the spectrum. On the other hand, the χ_2^0 is mostly $\widetilde{W}_3$-dominated, and therefore the main source of its production is cascade decay of left-chiral squarks ($\tilde{q}_L$). Such a χ_2^0 can also decay

into a $\tilde{\tau}$-τ pair.

If one can obtain complete information on the four-momentum of the $\tilde{\tau}$ and the τ, then it is possible to reconstruct both χ_1^0 and χ_2^0 using the final state mentioned above. The other two heavier neutralinos (χ_3^0 and χ_4^0), due to their low production rate and small decay branching ratios into the $\tilde{\tau}$-τ pair, are relatively difficult to reconstruct.

4.3.2 Background subprocesses:

The standard model background to $2\tau_j + 2\tilde{\tau} + \not{E}_T$ comes mainly from the following subprocesses :

- $t\bar{t}$ **production,** $\mathbf{t\bar{t} \rightarrow bWbW}$:
  Where two of the resulting jets can be faked as a tau-jet, and muons can come from the W's. One can also have a situation in which any (or both) of the b-quark decays semileptonically ($b \rightarrow c\mu\nu_\mu$) and any (or both) of the W decays to a $\tau - \nu_\tau$ pair. Though the efficiency of a non-tau jet being identified as a narrow tau-like jet is small (as will be discussed in a later section), and it is very unlikely to have isolated muons from semileptonic decays of the b, the overwhelmingly large number of $t\bar{t}$ events produced at the LHC makes this subprocess quite a serious source of backgrounds.

- Z^0**-pair production,** $ZZ \rightarrow 2\tau + 2\mu$:
  This subprocess also gives an additional contribution to the background, when one Z decays into a $\tau\tau$ pair and the other one into a pair of muons.

- **Associated ZH-production,** $ZH \rightarrow 2\tau + 2\mu$:
  This subprocess, though have a small cross-section, can contribute to the background through the decay of $H \rightarrow \tau\tau$ and $Z \rightarrow \mu\mu$, which can fake our signal as well.

The additional backgrounds from $t\bar{t}W$, $t\bar{t}Z$ and Z+jets can be suppressed by the same cuts as those described below. Also a higher non-tau-jet rejection factor and Z invariant mass cut can reduce the $t\bar{t}Z$ and Z+jets backgrounds considerably.

4.3.3 Event selection criteria :

In selecting the candidate events selected for neutralino reconstruction, we choose the two highest-p_T isolated charged tracks showing up in the muon chamber, both with $p_T > 100\ GeV$, as stable staus (see the detailed discussion later in this section.). The isolation criteria for the tracks are shown in Table 4.3. In addition to the p_T cut, the scalar sum of all jets and lepton in each event is required to be greater than 1 TeV. It is clear from Figures 4.2 and 4.3 that the standard model backgrounds are effectively eliminated through the above criteria. In addition, we require two τ-jets with $p_T > 50\ GeV$, and $\not{E}_T > 40\ GeV$ for each event. The justification for both of these cuts is provided when we discuss τ-tagging and reconstruction.

The isolation and 3-momentum reconstruction of the charged track at the muon chamber is done following the same criteria and procedure as those for muons.

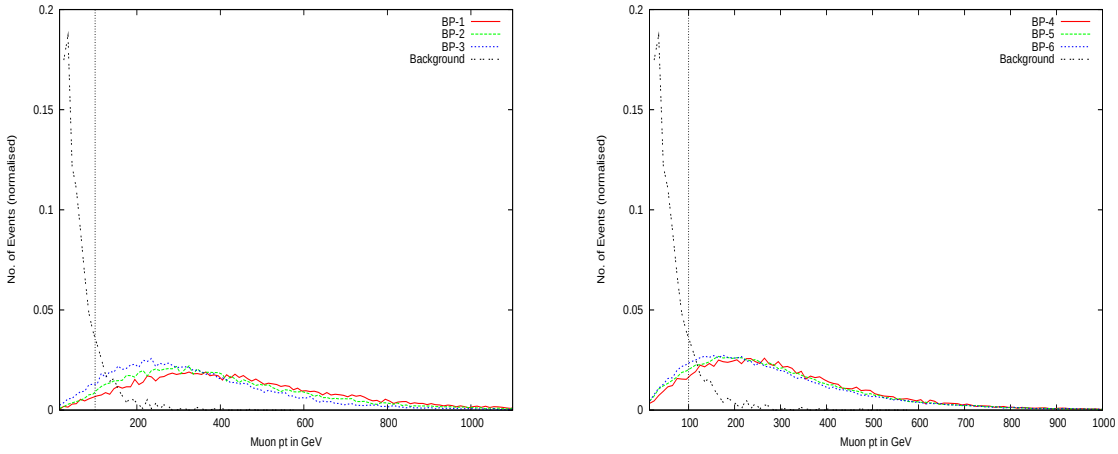

Figure 4.2: p_T distribution (normalised to unity) of the muon like track for the signal and the background, for all benchmark points. The vertical lines indicate the effects of a p_T cut at 100 GeV.

In order to obtain the invariant mass of a tau-stau pair, one needs to extract information on the mass of the stable charged particle (the stau in our context). While standard techniques such as time delay measurement or the degree of ionisation produced has been suggested in a number of earlier works [8], we extract mass information from an event-by-event analysis which is reported in the next

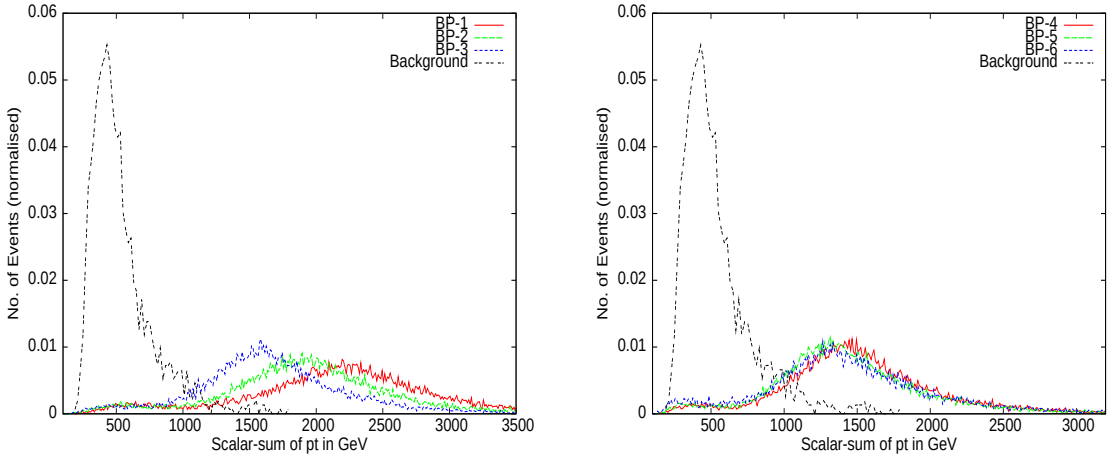

Figure 4.3: $\Sigma|\vec{p_T}|$ distribution (normalised to unity) for the signal and the background, for all benchmark points.

section. The efficiency for the reconstruction of staus has been taken to be the same as that of muons with $p_T > 10\ GeV$ in the pseudorapidity range $|\eta| < 2.5$, and is set at 90% following [9].

τ-jet tagging and τ-reconstruction:

τ-jet identification and τ-reconstruction are necessary for both background reduction and mass reconstruction of the neutralinos. We have concentrated on hadronic decays of the τ in the one-prong channel [1]. These are jet-like clusters in the calorimeter containing a relatively small number of charged and neutral hadrons. A τ decays hadronically about 65% of the time, producing a τ-jet. The momentum of such a jet in the plane transverse to the parent τ is small compared to the τ-energy, so long as the p_T of the τ-jet is large compared to the *tau* mass. In this limit, hadronic τ decays produce narrow jets collinear with the parent τ. The neutrinos that carry missing E_T also have the same direction in this limit. This gives one a handle in reconstructing the τ's, if one selects events where no other invisible particle is likely to be produced.

Given the masses of the SUSY particles in our benchmark scenarios, the τ's produced out of neutralino decay are hard enough, so that one can simulate τ-decays in the collinear approximation described above. A detailed discussion

[1] We have not considered the leptonic decay of tau, as it is difficult to identify lepton coming from tau decay to that coming from cascade decay of other objects like heavy quarks or W's

on the procedure followed for complete reconstruction of a pair of τ's is found in [10]. We have selected hadronic jets with $E_T > 50$ GeV as candidate products of τ-decay. A rather conservative non-tau jet rejection factor of 20 has been assumed, while the identification efficiency of a true tau-jet has been assumed to be 50% following [11, 12].

To describe the procedure in brief, one can fully reconstruct the τ by knowing $x_{\tau_{hi}}$ $(i = 1, 2)$, the fractions of the parent τ-energy carried by each product jet. Here $i = 1, 2$ represent the two branches of cascades that lead to the two τ's. The two unknowns can be solved from the two components of the missing transverse momentum ($\not{p}_T$) of a particular event.

If $p^{\mu}_{\tau_i}$, p^{μ}_{hi} are, respectively the components of four-momentum of the parent τ and the collinear jet produced from it (i = 1,2), then

$$p^{\mu}_{hi} = x_{\tau_{hi}}\, p^{\mu}_{\tau_i} \qquad (\mu = 0, 1, .., 4) \tag{4.1}$$

(as $E_\tau \approx |\vec{p_\tau}|$, in the limit $m_\tau \to 0$)

and one can write

$$\not{\vec{p}}_T = (\frac{1}{x_{\tau_{h1}}} - 1)\ \vec{p}_{h1} + (\frac{1}{x_{\tau_{h2}}} - 1)\ \vec{p}_{h2}$$

This yields two conditions for $x_{\tau_{hi}}$. Solving them, one obtains the τ four-momenta as $p_{hi}/x_{\tau_{hi}}$, from the knowledge of the energy and momenta of the resulting jets. In practice, as will be discussed below, the recorded missing momentum, $\not{\vec{p}}^{rec}_T$, is different from the true one, namely, $\not{\vec{p}}^{true}_T$. This error can lead to unphysical solutions for the reconstructed τ-momenta in some cases. Such a situation often arises when the two taus are produced back-to-back. This in turn means that the τ-neutrino's are also produced back-to-back in the collinear approximation. This reduces the magnitude of $\not{\vec{p}}_T$, when errors due to mismeasurements can lead to unphysical solutions. This is sometimes avoided by leaving out back-to-back orientation of the two τ-jet candidates, with some tolerance. In our analysis, a minimum value for $\not{E}_T$ ($\approx 40\ GeV$) and positivity of $x_{\tau_{hi}}$'s have been imposed as necessary conditions, in order to minimise the number of unphysical solutions. Besides, $p_T > 50$ GeV for each τ-jets ensures the validity of the collinear approximation in τ-decays. The τ-identification efficiency and the jet rejection factor are also better optimized with this p_T-cut [11, 12].

Of course, with a jet rejection factor of 1/20, one cannot rule out the possibility of QCD jets masquerading as τ's, in view of the huge number of QCD events at the LHC. Such fakes constitute irreducible backgrounds to the τ-reconstruction procedure. However, as we shall see in the numerical results presented in the next section, triggering on the rather strikingly spectacular properties of the quasi-stable stau-pair enables one to filter out the genuine events in the majority of cases.

Reconstruction of $\not{p}_T$:

It is evident from the above observations that the reconstruction of $\not{p}_T$ is very crucial for our study. The reconstructed $\not{p}_T$ differs considerably from true $\not{p}_T$, due to several reasons. The true $\not{p}_T^{true}$ is related to the experimentally reconstructed $\not{p}_T^{rec}$ by the following relation

$$\not{p}_T^{rec} = \not{p}_T^{true} + \not{p}_T^{Forw} + \not{p}_T^{<0.5}$$

where $\not{p}_T^{Forw}$ corresponds to the total transverse momentum carried by the particles escaping detection in the range $|\eta| > 5$ and $\not{p}_T^{<0.5}$ corresponds to the total transverse momentum carried by the particles in the range $|\eta| < 5$ with $p_T < 0.5$ GeV[2], which contributes to the true $\not{p}_T$. In addition to this, mismeasurement of the transverse momenta for jets, leptons etc. alters the true $\not{p}_T$ by an sizable amount. This is due to the finite resolution of detectors, and is handled in theoretical predictions by smearing the energy/momentum of a particle through a Gaussian function.

In our study, we have tried to reconstruct $\not{p}_T$, taking into account all the above issues. The missing transverse momentum in any event is defined as

$$\not{p}_T = -\Sigma \vec{p}_T^{visible}$$

where the $\Sigma \vec{p}_T^{visible}$ consists of isolated leptons/photons/jets and also those objects which do not belong to any of these components but are detected at the detector, constituting the so called 'soft part' or the 'unclustered component' of the visible momentum. We describe below the various components of the visible $\not{p}_T$, and their respective resolution functions.

Resolution effects:

Among the finite resolution effects of the detector, taken into account in our analysis, most important are the finite resolutions of the'electromagnetic and

[2]The threshold is 0.5 GeV for CMS and 1 GeV for ATLAS.

hadron calorimeters, and the muon track resolution. Since the kind of final state we are dealing with does not require any isolated electrons/photons, we have not considered electron or photon resolution. The electrons/photons which are not isolated but have $E_T \geq 10$ GeV and $|\eta| < 5$ have been considered as jets and their resolution has been parametrised according to that of jets. Jets have been defined within a cone of $\Delta R = 0.4$ and $E_T \geq 20GeV$ using the PYCELL fixed cone jet formation algorithm in PYTHIA. Since the staus are long-lived and leave charged tracks in the muon chamber, their smearing criteria have been taken to be the same as those of isolated muons. Though one can describe the resolution of the track of staus and muons by different resolution functions (as $m_{\tilde{\tau}} >> m_{\mu}$), one does not envision any significant deviation in the prediction of events via such difference. Therefore, in the absence of any clear guidelines, we have treated them on equal footing, as far as the Gaussian smearing function is concerned. The tracks which show up in the muon chamber, but are not isolated, having $E_T > 10$GeV and $|\eta| < 2.5$, have been considered as jets and smeared accordingly. All the particles (electron, photon, muon, and stau) with $0.5 < E_T < 10$GeV and $|\eta| < 5$ (for muon or muon-like tracks, $|\eta| < 2.5$), or hadrons with $0.5 < E_T < 20$GeV and $|\eta| < 5$, which constitute 'hits' in the detector, are considered as *soft or unclustered components*. Their resolution functions have been considered separately. We present below the different parametrisation of the different component of the final state, assuming the smearing to be Gaussian in nature.

- **Jet energy resolution :**

$$\sigma(E)/E = a/\sqrt{E} \oplus b \oplus c/E \tag{4.2}$$

where

a= 0.7 [GeV$^{1/2}$], b= 0.08 & c= 0.009 [GeV] for $|\eta| < 1.5$

= 1 = 0.1 = 0.009 $1.5 < |\eta| < 5$

- **Muon/Stau p_T resolution :**

$$\sigma(p_T)/p_T = a \quad \text{if } p_T < \xi \tag{4.3}$$

$$= a + b\log(p_T/\xi) \quad \text{if } p_T > \xi \tag{4.4}$$

where

a= 0.008, b= 0.037 & $\xi = 100$ [GeV] for $|\eta| < 1.5$

= 0.02 = 0.05 $\xi = 100$ $1.5 < |\eta| < 2.5$

- **Soft component resolution :**

$$\sigma(E_T) = \alpha\sqrt{\Sigma_i E_T^{(soft)i}} \tag{4.5}$$

with $\alpha \approx 0.55$. One should keep in mind that the x and y component of E_T^{soft} need to be smeared independently.

It is of great importance to ensure that the stable $\tilde{\tau}$ leaving a track in the muon chamber is not faked by an actual muon arising from a standard model process. As has been mentioned in section 4.3.3, we have found certain kinematic prescriptions to be effective as well as reliable in this respect. In order to see this clearly, we present the p_T-distributions of the harder muon and the $\tilde{\tau}$-track in Figure 4.2. The $\tilde{\tau}$-p_T clearly shows a harder distribution, owing to the fact that the stau takes away the lion's share of the p_T possessed by the parent neutralino. Another useful discriminator is the scalar sum of transverse momenta of all detected particles (jets, leptons and unclustered components). The distribution in $\Sigma|\vec{p_T}|$, defined in the above manner, displays a marked distinction for the signal events, as shown in Figure 4.3. The cuts chosen in Table 4.3 have been guided by both of the above considerations. They have been applied for all the benchmark points, as also for the background calculation.

4.4 Numerical results and neutralino reconstruction:

4.4.1 The reconstruction strategy

Having obtained the τ four-momenta, the neutralinos can be reconstructed, once we obtain the energy of the $\tilde{\tau}$'s whose three-momenta are already known from the curvature of the tracks in the muon chamber. For this, one needs to know the $\tilde{\tau}$-mass. In addition, the requirements are, of course, sufficient statistics, minimisation of errors due to QCD jets faking the τ's, and the suppression of combinatorial backgrounds. For the first of these, we have presented our numerical results uniformly for an integrated luminosity of 300 fb^{-1}, although some of our benchmark points requires much less luminosity for effective reconstruction. We have already remarked on the possibility of reducing the faking of τ's. As we shall

show below, a systematic procedure can also be adopted for minimising combinatorial backgrounds to the reconstruction of neutralinos. The primary step in this is to combine each such τ with one of the two hardest tracks in the muon chamber, which satisfy the cuts listed in Table 4.3. A particular τ is combined with a heavy track of opposite charge. However, since neutralinos are Majorana fermions, producing pairs of $\tau^+\tilde{\tau}^-$ and $\tau^-\tilde{\tau}^+$ with equal probability, this is not enough to avoid the combinatorial backgrounds. Therefore, out of the two τ's and two heavy tracks, we select those pairs which give the closer spaced invariant masses, with $|M^{pair1}_{\tilde{\tau}\tau} - M^{pair2}_{\tilde{\tau}\tau}| < 50\ GeV$. The number of signal and background events, after the successive application of cuts are listed in Table 4.4.

This finally brings us to the all-important issue of knowing the stau-mass. The $\tilde{\tau}$-mass can be reconstructed from the information on time delay (Δt) between the inner tracker and the outer muon system and the measured three-momentum of the charged track [8]. The accuracy of this method depends on the accurate determination of Δt, which can be limited when the particles are highly boosted. We have followed a somewhat different approach to find the actual mass of the particle associated with the charged track. We have found this method effective when both pairs of $\tau\tilde{\tau}$ come from $\chi^0_1\chi^0_1$ or $\chi^0_2\chi^0_2$.

Solving for the $\tilde{\tau}$-mass: The actual $\tilde{\tau}$-mass can be extracted by demanding that the invariant mass of the two correct $\tilde{\tau}\tau$-pairs are equal, which yields an equation involving one unknown, namely, $m_{\tilde{\tau}}$:

$$\sqrt{m^2_{\tilde{\tau}} + |\vec{p}_{\tilde{\tau}_1}|^2}.E_{\tau_1} - \sqrt{m^2_{\tilde{\tau}} + |\vec{p}_{\tilde{\tau}_2}|^2}.E_{\tau_2} = \vec{p}_{\tilde{\tau}_1}.\vec{p_{\tau_1}} - \vec{p}_{\tilde{\tau}_2}.\vec{p_{\tau_2}} \tag{4.6}$$

where the variables have their usual meanings and are experimentally measurable event-by-event. ($\tilde{\tau}_{1,2}$ here denote the lighter $\tilde{\tau}$s on two sides of the cascade, and not the two $\tilde{\tau}$ mass eigenstates.)

The right combination is assumed to be selected whenever the difference between $|M^{pair1}_{\tilde{\tau}\tau} - M^{pair2}_{\tilde{\tau}\tau}|$ is minimum and differ by not more than 50 GeV, as mentioned earlier. It should be noted that the unambiguous identification of the right $\tau\tilde{\tau}$-pairs which come from decays of two neutralinos ($\chi^0_1\chi^0_1$ or $\chi^0_2\chi^0_2$) does not depend on the actual stau mass. Thus we can use a 'seed value' of the stau mass as input to the above equation, in identifying the right $\tau\tilde{\tau}$ combinations. We have used a seed value of $m_{\tilde{\tau}} \approx 100\ GeV$ (motivated by the LEP limit on $m_{\tilde{\tau}}$). The SM background has already been suppressed by demanding the p_T of each charged track to be greater than 100 GeV, together with $\Sigma|\vec{p_T}| > 1\ TeV$.

Once the right pairs are chosen using the seed value of the $\tilde{\tau}$-mass, we need

not use that value any more, and instead solve equation 4.6 which is quadratic in $m_{\tilde{\tau}}^2$. We have kept only those events in which at least one positive solution for $m_{\tilde{\tau}}^2$ exists. When both roots of the equation are positive, the higher value is always found to be beyond the reach of the maximum centre-of-mass energy available for the process. Hence we have considered the solution corresponding to the lower value of the root. The distribution of the solutions thus obtained has a peak around the actual $\tilde{\tau}$-mass. The $\tilde{\tau}$-track four-momenta are completely constructed, using this peak value as the actual mass of the $\tilde{\tau}$-NLSP (see Figure 4.4).

This sets the stage fully for the reconstruction of neutralinos, the results of which are shown in Figure 4.5. For BP1, BP2 and BP3 one can see that there is only one peak which corresponds to the χ_1^0. This is because the χ_2^0 production rate in cascade is relatively small for these points. For BP4 and BP5, on the other hand, we have distinct peaks for both χ_1^0 and χ_2^0. At BP6, however, we only have the χ_2^0 peak. This is due to the small mass splitting between χ_1^0 ($m_{\chi_1^0} = 129\ GeV$) and $\tilde{\tau}$ ($m_{\tilde{\tau}} = 124\ GeV$), which softens the tau (jet) arising from its decay, preventing it from passing the requisite hardness cuts. On the whole, it is clear from Figure 4.5 (comparing the peaks with the input values of the neutralino masses) that, in spite of adulteration by QCD jets that fake the τ's, our event selection criteria can lead to faithful reconstruction of neutralino masses.

One may still like to know whether a neutralino reconstructed in this manner is the χ_1^0 or the χ_2^0, when only one peak is visible. This requires further information on the SUSY spectrum. For example, the information on the gluino mass, extracted from the effective mass (defined as $(\Sigma|\vec{p}_T| + \not{E}_T)$) distribution, may enable one to distinguish between the χ_1^0 and the χ_2^0, once gaugino mass unification at high scale is assumed.

4.4.2 LHC reach in the $m_0 - m_{1/2}$ -plane:

We have also identified the region in the $m_0 - m_{1/2}$ plane, where at least one of the two lightest neutralinos can be reconstructed. For this, we have scanned over the region of the $m_0 - m_{1/2}$ plane using the spectrum generator SuSpect (v 2.34) [13] which leads to a $\tilde{\tau}$ LSP in a usual mSUGRA scenario without the right handed sneutrino [14]. Results of this scan are shown in Figure 4.6. The coloured (shaded) areas are consistent with all the low energy constraints like $b \rightarrow s\gamma$, $B_s \rightarrow \mu^+\mu^-$, $\Delta(g_\mu - 2)$ and the LEP limits on the low energy spectrum. The value of $tan\beta$ has been fixed at 30, and A_0 = 100 has been chosen.

The regions where reconstruction is possible have been determined using the following criteria:

- In the parameter space, we have not gone into regions where the gluino mass exceeds $\approx 2\ TeV$.

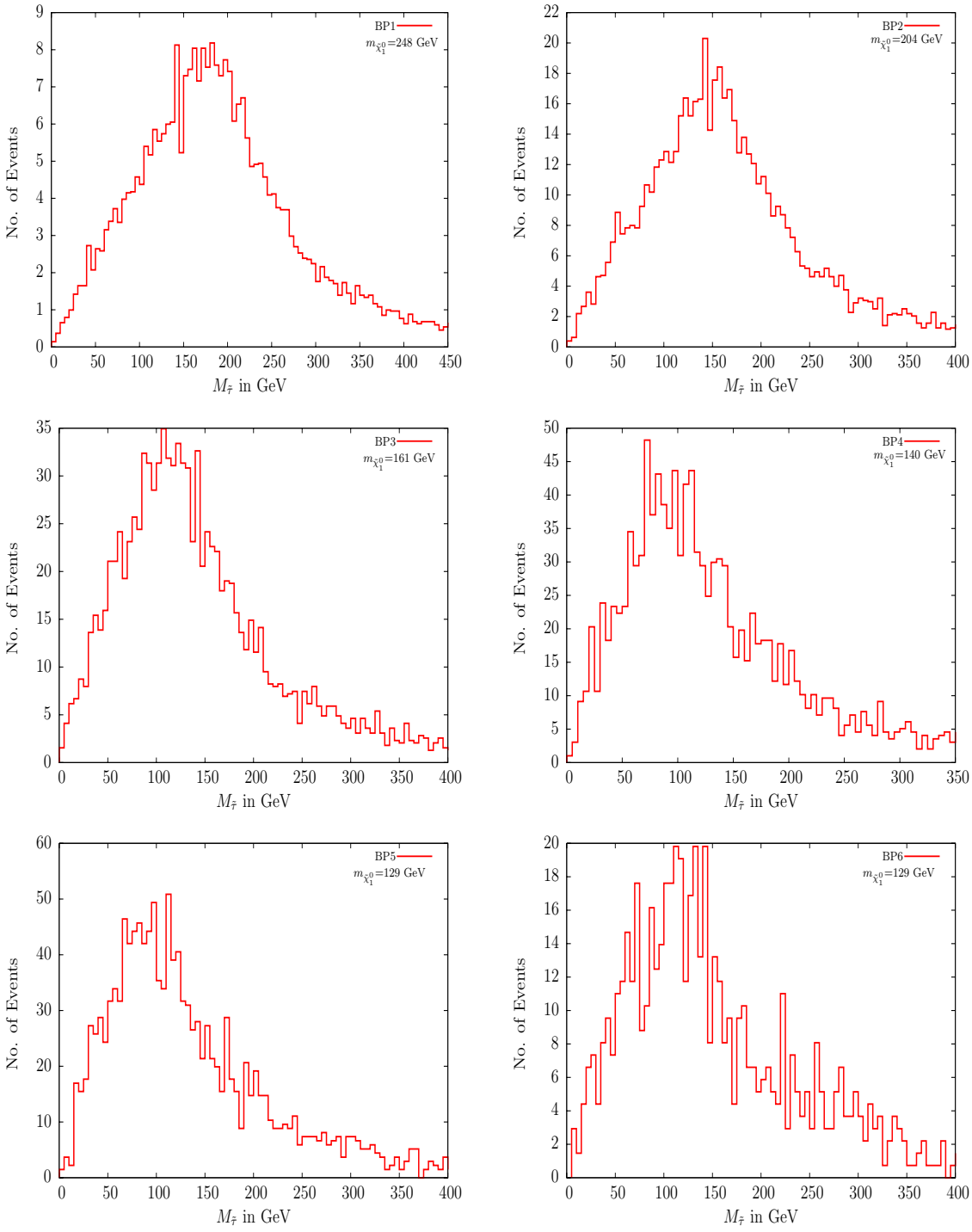

Figure 4.4: The $\tilde{\tau}$ mass peak as obtained from eventwise reconstruction as described in the text, for all the benchmark points at luminosity 300 fb^{-1}.

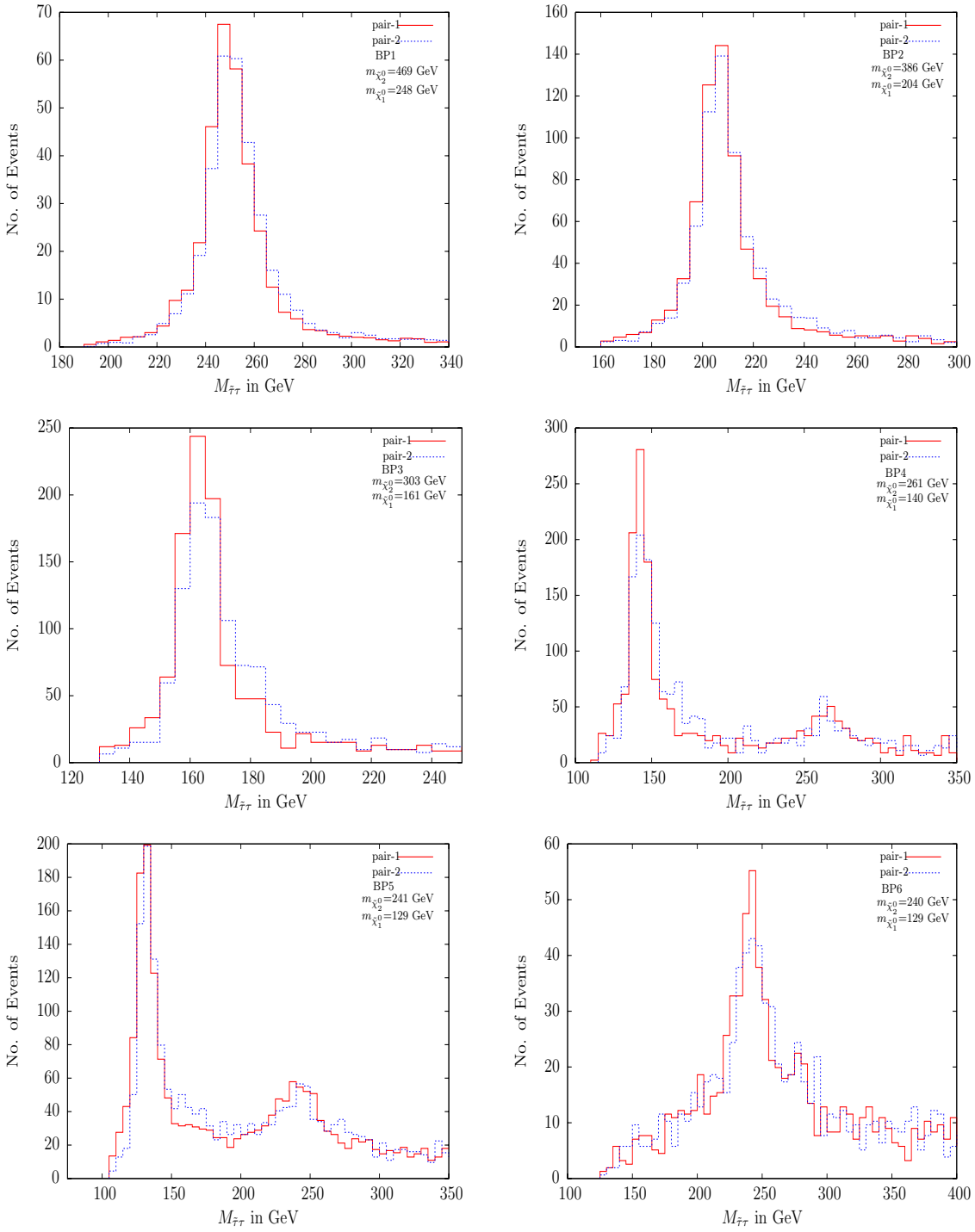

Figure 4.5: $M_{\tilde{\tau}\tau}$ distribution for all the benchmark points at luminosity 300 fb^{-1}. BP1, BP2 and BP3 show only the χ_1^0 peak. Both the χ_1^0 and χ_2^0 peaks are visible for BP4 and BP5, while BP6 displays only the χ_2^0 peak.

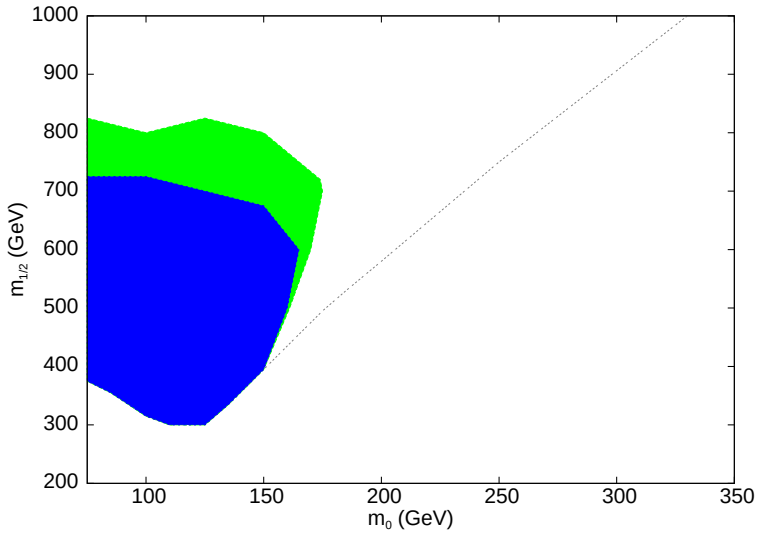

Figure 4.6: The region in the $m_0 - m_{1/2}$ plane, where it is possible to reconstruct at least one of the neutralinos at the LHC, with $tan\beta = 30$ and $A_0 = 100$ GeV. In the blue (dark shade) region, at least 100 events are predicted in the vicinity of the peak. The additional available region where 50 events in the vicinity of the peak are assumed to suffice for reconstruction, is marked in green (light shade). The entire region above the dashed line indicates the scenario where one has a $\tilde{\nu}_R$-LSP and a $\tilde{\tau}$-NLSP.

- The number of events satisfying $|M_{\tilde{\tau}\tau} - M_{peak}| < 0.1.M_{peak}$ at an integrated luminosity of 300 fb^{-1} must be greater than a specific number in order that the peak is said to be reconstructed. One obtains the blue (dark shade) region if this number is set at 100. If the peak can be constructed from more than 50 events, the additional region, marked in green (light shade), becomes allowed.

4.5 Summary and conclusions

We have considered a SUGRA scenario, with universal scalar and gaugino masses, where a right-chiral neutrino superfield exists for each family. We have identified several benchmark points in the parameter space of such a theory, where a right-sneutrino is the LSP, and a $\tilde{\tau}$ mass eigenstate is the NLSP. The $\tilde{\tau}$, stable on the distance scale of the detectors, leaves a charged track in the muon chamber, which is the characteristic feature of SUSY signals in this scenario. We use this feature to reconstruct neutralinos in the $\tau\tilde{\tau}$ channel. For this, we use the collinear approximation to obtain the four-momentum of the τ, and suggest a number of

event selection criteria to reduce backgrounds, including combinatorial ones. We also suggest that the $\tilde{\tau}$ mass may be extracted by solving the equation encapsulating the equality of invariant masses of two $\tau\tilde{\tau}$ pairs in each event. We find that at least one of the two lightest neutralinos can be thus reconstructed clearly over a rather large region in the $m_0 - m_{1/2}$ plane, following our specified criteria.

Input	BP-1	BP-2	BP-3	BP-4	BP-5	BP-6
mSUGRA	$m_0 = 100$ $m_{1/2} = 600$ $\tan\beta = 30$	$m_0 = 100$ $m_{1/2} = 500$ $\tan\beta = 30$	$m_0 = 100$ $m_{1/2} = 400$ $\tan\beta = 30$	$m_0 = 100$ $m_{1/2} = 350$ $\tan\beta = 30$	$m_0 = 100$ $m_{1/2} = 325$ $\tan\beta = 30$	$m_0 = 100$ $m_{1/2} = 325$ $\tan\beta = 25$
$m_{\tilde{e_L}}, m_{\tilde{\mu}_L}$	418	355	292	262	247	247
$m_{\tilde{e_R}}, m_{\tilde{\mu}_R}$	246	214	183	169	162	162
$m_{\tilde{\nu}_{eL}}, m_{\tilde{\nu}_{\mu L}}$	408	343	279	247	232	232
$m_{\tilde{\nu}_{\tau L}}$	395	333	270	239	224	226
$m_{\tilde{\nu}_{iR}}$	100	100	100	100	100	100
$m_{\tilde{\tau}_1}$	189	158	127	112	106	124
$m_{\tilde{\tau}_2}$	419	359	301	273	259	255
$m_{\chi_1^0}$	248	204	161	140	129	129
$m_{\chi_2^0}$	469	386	303	261	241	240
$m_{\chi_1^\pm}$	470	387	303	262	241	241
$m_{\tilde{g}}$	1362	1151	937	829	774	774
$m_{\tilde{t}_1}$	969	816	772	582	634	543
$m_{\tilde{t}_2}$	1179	1008	818	750	683	709
m_{h^0}	115	114	112	111	111	111

Table 4.1: *Proposed benchmark points (BP) for the study of the stau-NLSP scenario in the SUGRA with right-sneutrino LSP. The value of m_0 and $m_{1/2}$ are given in GeV. We have also set $A_0 = 100$ GeV and $sgn(\mu) = +$ for benchmark points under study.*

Subprocesses	**BP-1**	**BP-2**	**BP-3**	**BP-4**	**BP-5**	**BP-6**
All SUSY	1765	4143	11726	20889	28864	15439
$\tilde{q}\tilde{q}^*, \tilde{g}\tilde{g}, \tilde{q}\tilde{g}$	1616	3897	11061	19765	27785	14426

Table 4.2: *The number of* $2\tau_j + 2\tilde{\tau}$ *(charged-track)+*$\not{E}_T$*+ X events, satisfying our basic cuts, for* $\int Ldt = 300\ GeV$*, from various channel.*

Cuts	
Basic Cuts	$p_T^{lep,stau} > 10$ GeV $p_T^{hardest-jet} > 75$ GeV $p_T^{other-jets} > 50$ GeV $40\ GeV < \not{E}_T < 150\ GeV$ $\|\eta\| < 2.5$ for Leptons, Jets & Stau $\Delta R_{ll} > 0.2,\ \Delta R_{lj} > 0.4$ $\Delta R_{\tilde{\tau}l} > 0.2,\ \Delta R_{\tilde{\tau}j} > 0.4$ $\Delta R_{jj} > 0.7$
Cuts for Background Elimination	$p_T^{iso\ charg\ track} > 100\ GeV$ $\Sigma\|\vec{p_T}\| > 1\ TeV$
Invariant mass difference of two nearby pairs	$\|M_{\tilde{\tau}\tau}^{pair1} - M_{\tilde{\tau}\tau}^{pair2}\| < 50\ GeV$

Table 4.3: *Cuts applied for event selection, background elimination and neutralino reconstruction.*

CUTS	SIGNAL						BACKGROUND			
	BP1	BP2	BP3	BP4	BP5	BP6	$t\bar{t}$	ZZ	ZH	total
Basic Cuts	1765	4143	11726	20889	28864	15439	4129	45	6	4180
$+P_T$ Cut	1588	3631	9471	15526	20282	9920	210	3	1	214
$+\Sigma\lvert P_T\rvert$ Cut	1442	3076	6777	9538	11266	5724	63	0	0	63
$+\lvert M^{pair1}_{\tilde{\tau}\tau} - M^{pair2}_{\tilde{\tau}\tau}\rvert$ Cut	408	887	1622	2004	2244	858	6	0	0	6

Table 4.4: *Number of signal and background events for $2\tau_j + 2\tilde{\tau}$ (charged-track)+$\not{E}_T$+ X final state with an integrated luminosity of 300 fb^{-1}, considering all SUSY processes. The standard model Higgs mass is taken to be 120 GeV in background calculation.*

Bibliography

[1] S. Biswas and B. Mukhopadhyaya, Phys. Rev. D **79**, 115009 (2009) [arXiv:0902.4349 [hep-ph]].

[2] F. E. Paige, S. D. Protopopescu, H. Baer and X. Tata, arXiv:hep-ph/0312045.

[3] T. Sjostrand, S. Mrenna and P. Skands, JHEP **0605**, 026 (2006) [arXiv:hep-ph/0603175].

[4] C. Amsler *et al.* [Particle Data Group], Phys. Lett. B **667**, 1 (2008).

[5] H. L. Lai *et al.* [CTEQ Collaboration], Eur. Phys. J. C **12**, 375 (2000) [arXiv:hep-ph/9903282].

[6] W. Beenakker, R. Hopker, M. Spira and P. M. Zerwas, Nucl. Phys. B **492**, 51 (1997) [arXiv:hep-ph/9610490].

[7] W. Beenakker, S. Dittmaier, M. Kramer, B. Plumper, M. Spira and P. M. Zerwas, Nucl. Phys. B **653**, 151 (2003) [arXiv:hep-ph/0211352].

[8] I. Hinchliffe and F. E. Paige, Phys. Rev. D **60**, 095002 (1999) [arXiv:hep-ph/9812233].

[9] G. Aad *et al.* [The ATLAS Collaboration], [arXiv:0901.0512].

[10] D. L. Rainwater, D. Zeppenfeld and K. Hagiwara, Phys. Rev. D **59**, 014037 (1998) [arXiv:hep-ph/9808468].

[11] Y. Coadou *et al.* ATLAS Internal Note ATL-PHYS-98-126

[12] The CMS Collaboration, CMS-TDR-8.1, CERN/LHCC 2006-001

[13] A. Djouadi, J. L. Kneur and G. Moultaka, Comput. Phys. Commun. **176**, 426 (2007) [arXiv:hep-ph/0211331].

[14] A. V. Gladyshev and D. I. Kazakov, Phys. Atom. Nucl. **70**, 1553 (2007) [arXiv:hep-ph/0606288].

Chapter 5

Chargino mass reconstruction

5.1 Introduction

In this chapter, we discuss the reconstruction of the chargino mass [1] in the scenario under consideration (referred to chapter 3). Measurement of the chargino mass, in addition to the neutralino masses, would confirm one important prediction of the MSSM, i.e. the correlation between the masses of the charginos and neutralinos. In the MSSM, the masses of the charginos are correlated with some of the neutralino masses. As has been already mentioned in the previous chapter, in models with universal gaugino masses at high-scale, one would have

$$M_1 \approx \frac{5}{3}\tan^2\theta_W M_2 \approx 0.5 M_2 \tag{5.1}$$

at the electroweak scale. Any deviation from this will give some hints about high-scale non-universality. However, the measurement of the neutralino masses alone can not confirm the gaugino mass universality when say, the lightest neutralino mass turns out to be nearly half to that of the second lightest neutralino. One need some information about the chargino mass as well to pin down this universality.

With stau NLSP and $\tilde{\nu}_R$ LSP, the chargino can, among other things, decay into a $\tilde{\tau}\nu_\tau$-pair. Due to the presence of the invisible neutrino, the information about the chargino mass can be obtained from the transverse mass distribution of the $\tilde{\tau}\nu_\tau$-pair, rather than from the invariant mass distribution [2]. We have prescribed a method to extract the transverse component of the four-momentum

of the neutrino out of a chargino decay from the total $\not{E}_T$ of a particular event, in order to reconstruct the transverse mass variable. For this purpose, we consider chargino production in association with the neutralinos in SUSY cascade.

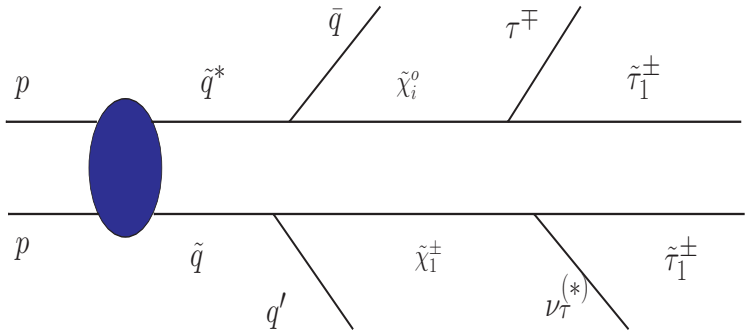

Figure 5.1: Schematic diagram of a typical SUSY cascade for the reconstruction of the lighter chargino.

In the next section, we motivate the signal under study and the reconstruction strategy for determining the chargino mass. In section 5.3 the possible sources of background, both from the SM and within the model itself, and their possible discrimination, are discussed. We present the numerical results in section 5.4. We summarise and conclude in section 5.5.

5.2 Reconstruction of the lighter chargino

The final state of use for the reconstruction of the lighter chargino is

- $\tau_j + 2\tilde{\tau}(\text{opposite} - \text{sign charged tracks}) + \not{E}_T + X$

where, τ_j represents a jet which has been identified as a tau jet, the missing transverse energy is denoted by $\not{E}_T$ and all other jets coming from cascade decays are included in X.

The benchmark points under consideration are presented in Table **??**, section 4.2. Simulation for the LHC has been done for the signal as well as backgrounds using **PYTHIA** (v6.4.16) [3]. The pp events have been studied with a centre-of-mass energy ($E_{c.m.}$)=14 TeV at an integrated luminosity of 300 fb^{-1}. The numerical values of the electromagnetic and the strong coupling constant have been set at $\alpha_{em}^{-1}(M_Z) = 127.9$ and $\alpha_s(M_Z) = 0.118$ respectively [4]. The hard scattering process has been folded with CTEQ5L parton distribution function [5]. We have set the factorisation and renormalisation scales at the average mass of the particles produced in the parton level hard scattering process. In order to make our estimate conservative, the signal rates have not been multiplied by any

K-factor [6]. The effects of initial and final state radiation as well as the finite detector resolution of the energies/momenta of the final state particles have been taken into account.

5.2.1 Chargino reconstruction from transverse mass distribution

Now we are all set to describe the main principle adopted by us for chargino ($\chi_1^\pm$) reconstruction. For this purpose, we have looked for the processes in which $\chi_1^\pm - \chi_1^0/\chi_2^0$ is being produced in association with hard jets in cascade decays of squarks and gluinos. The $\chi_1^\pm$ subsequently decays into a $\tilde{\tau}$-ν_τ pair, while the χ_1^0 (or χ_2^0) decays into a $\tilde{\tau}$-τ pair. Since the decay of $\chi_1^\pm$ involves an invisible particle (ν_τ), for which it is not possible to know all the four components of momenta, a transverse mass distribution, rather than invariant mass distribution, of $\tilde{\tau}$-ν_τ pair will give us mass information of $\chi_1^\pm$. In spite of the recent progress in measuring the masses of particles in semi-invisible decay mode (for example the m_{T_2} variable introduced by [7] and its further implications [8]), we have focused on transverse mass variable (m_T) because of the fact that the only invisible particle present in the final state is the neutrino, which is massless.

The procedure, however, still remains problematic, because the τ on the other side (arising from neutralino decay) also produces a neutrino in the final state, which contributes to $\not{E}_T$. In order to correctly reconstruct the transverse mass of the $\tilde{\tau} - \nu_\tau$ pair from chargino decay, the contribution to $\not{E}_T$ from the aforementioned neutrino must be subtracted.

Keeping this in mind, we have prescribed a method for reconstruction of the transverse component of the neutrino 4-momenta ($\vec{P}^T_{\nu_1}$) produced from the decay of $\chi_1^\pm$, in association with $\tilde{\tau}$. To describe it in short:

We label the transverse momentum of the neutrino coming from a chargino decay by $\vec{P}^T_{\nu_1}$. Attention is focused on cases where the tau, produced from a neutralino, decays hadronically and the τ-jet, out of a one-prong decay of tau, is identified. We have assumed a true tau-jet identification efficiency to be 50%, while a non-tau jet rejection factor of 100 has been used [9–11] (The results for higher identification efficiency are also shown in section 5.4.). Though we have used a non-taujet rejection factor of 20 earlier, we have used a better fake jet rejection factor here in view of some more optimistic recent estimates. We have also assumed that there is no invisible particle other than the two neutrinos mentioned above. We have attempted to ensure this by vetoing any event with isolated charged leptons. This only leaves out neutrinos from Z-decay and W-decays into a $\tau\nu_\tau$ pair. The contamination of our signal from these are found to be rather modest.

The transverse momenta of the neutrino ($\vec{P}^T_{\nu_2}$), out of a tau decay, is first reconstructed in the collinear approximation, where the product neutrino and the jet are both assumed to move collinearly with the parent tau. In this approxima-

tion, one can write

$$P_{\tau_j} = xP_\tau \tag{5.2}$$

Following the decay χ_1^0 (or, χ_2^0)$\rightarrow$ $\tilde{\tau}^\pm\tau^\mp$ we have then combined the identified tau-jet with the oppositely charged stau (track), thus forming the invariant mass

$$m^2_{\chi_i^0} = (P_{\tilde{\tau}} + P_\tau)^2 = (P_{\tilde{\tau}} + P_{\tau_j}/x)^2 \quad (i = 1, 2) \tag{5.3}$$

This pairing requires the charge information of the tau-induced jet. We have assumed that, for a true tau-jet, the charge identification efficiency is 100%, while to a non-tau jet we have randomly assigned positive and negative charge, each with 50% weight. One can solve this equation for x (neglecting the tau-jet invariant mass[1]), to obtain

$$x \approx \frac{2P_{\tilde{\tau}}.P_{\tau_j}}{m^0_{\chi_i^0} - m^0_{\tilde{\tau}}} \tag{5.4}$$

This requires the information of $m_{\chi_1^0}$ (or, $m_{\chi_2^0}$) and $m_{\tilde{\tau}}$ as well, which we have used from our earlier work for the respective benchmark points. Once x is known we have,

$$\vec{P}^T_{\nu_2} = \vec{P}^T_\tau - \vec{P}^T_{\tau_j} = \frac{1-x}{x}.\vec{P}^T_{\tau_j} \tag{5.5}$$

Hence, the transverse component of the neutrino, out of $\chi_1^\pm$-decay can be extracted from the knowledge of $\vec{\not{E}}_T$ of that particular event[2]. This is given by,

$$\vec{P}^T_{\nu_1} = \vec{\not{E}}_T - \vec{P}^T_{\nu_2} \tag{5.6}$$

Finally, from the end point of the transverse mass distribution of the $\tilde{\tau}$-ν_τ pair the value of $m_{\chi_1^\pm}$ can be obtained. However, one should keep in mind that, both χ_1^0 or χ_2^0 can decay into a $\tilde{\tau}\tau$ pair. Therefore, it is necessary to specify some criterion to separate whether a given $\tilde{\tau}\tau$ pair has originated from a χ_1^0 or χ_2^0 which we have discussed in the next subsection.

5.2.2 Distinguishing between decay products of χ_1^0 and χ_2^0

In order to identify the origin of a given opposite sign $\tilde{\tau}$-τ pair, the first information that is to be extracted from data is which benchmark region one is in. We have assumed of gaugino mass universality for this process, for the sake of simplicity.

If one looks at the effective mass (defined by $M_{eff} = \sum |\vec{p}_T| + \vec{\not{E}}_T$) distribution of the final state, then the peak of the distribution gives one an idea of the

[1]This approximation is not valid for small x, say $x < 0.1$. However, the jet out of a tau decay almost always carries a larger fraction of τ-energy, thus justifying the approximation.

[2]For details on the reconstruction of $\vec{\not{E}}_T$ see section 4.3.3.

masses of the strongly interacting superparticles which are the dominant products of the initial hard scattering process. This is seen from Figure 5.2. Once the order of magnitude of the gluino mass is inferred from this distribution, one can use the universality of gaugino masses, which, in turn, indicates where $m_{\chi_1^0}$ and $m_{\chi_2^0}$, masses of the two lightest neutralinos, are expected to lie.

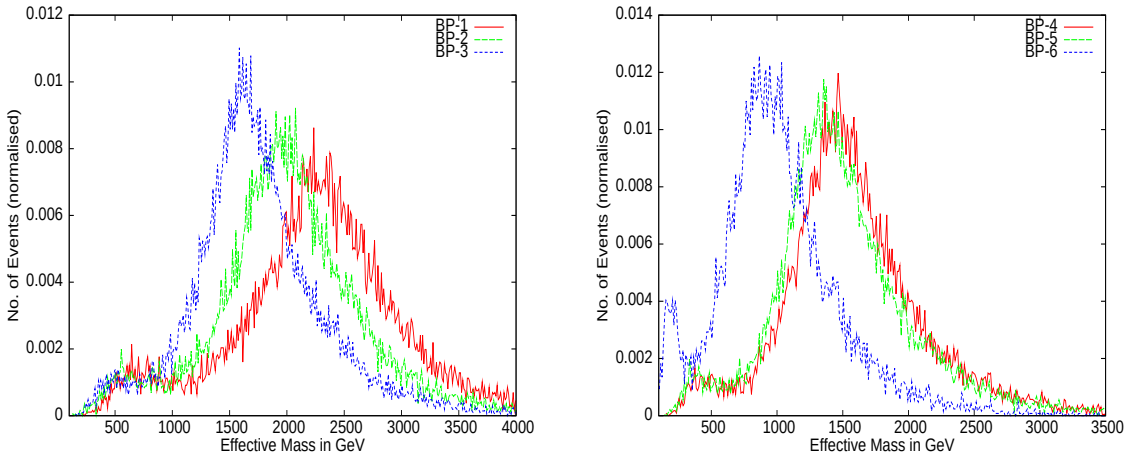

Figure 5.2: *M_{eff} distribution (normalized to unity) of the final state under consideration, for all benchmark points.*

Next, for each event that we record, we look at a $\tilde{\tau}$ and a τ-jet of opposite signs. The invariant mass distribution of this $\tilde{\tau}\tau_j$ pair displays a peak whose location, although not precisely telling us about the parent neutralino, is still in the vicinity of the mass values. Thus, by observing these distributions (Figure 5.3) one often is able to tell whether it is a χ_1^0 or a χ_2^0, once one simultaneously uses information obtained from the M_{eff} distribution.

As has already been noted in the previous chapter, the mass of either χ_1^0 or χ_2^0 or both can be reconstructed in this scenario, depending on one's location in the parameter space. Once a peak in the $\tau\tilde{\tau}$ invariant mass is located, the next step is to check whether $|M_{\tilde{\tau}\tau_j} - m_{\chi_i^0}| < 0.1.m_{\chi_i^0}$, where $m_{\chi_i^0}$ is either one (*or the only one*) of the two lightest neutralinos deemed reconstructible in the corresponding region. The mass of that neutralino is used in equation 5.3. If this equality is not satisfied for either neutralino or the only one reconstructed, then the event is not included in the analysis.

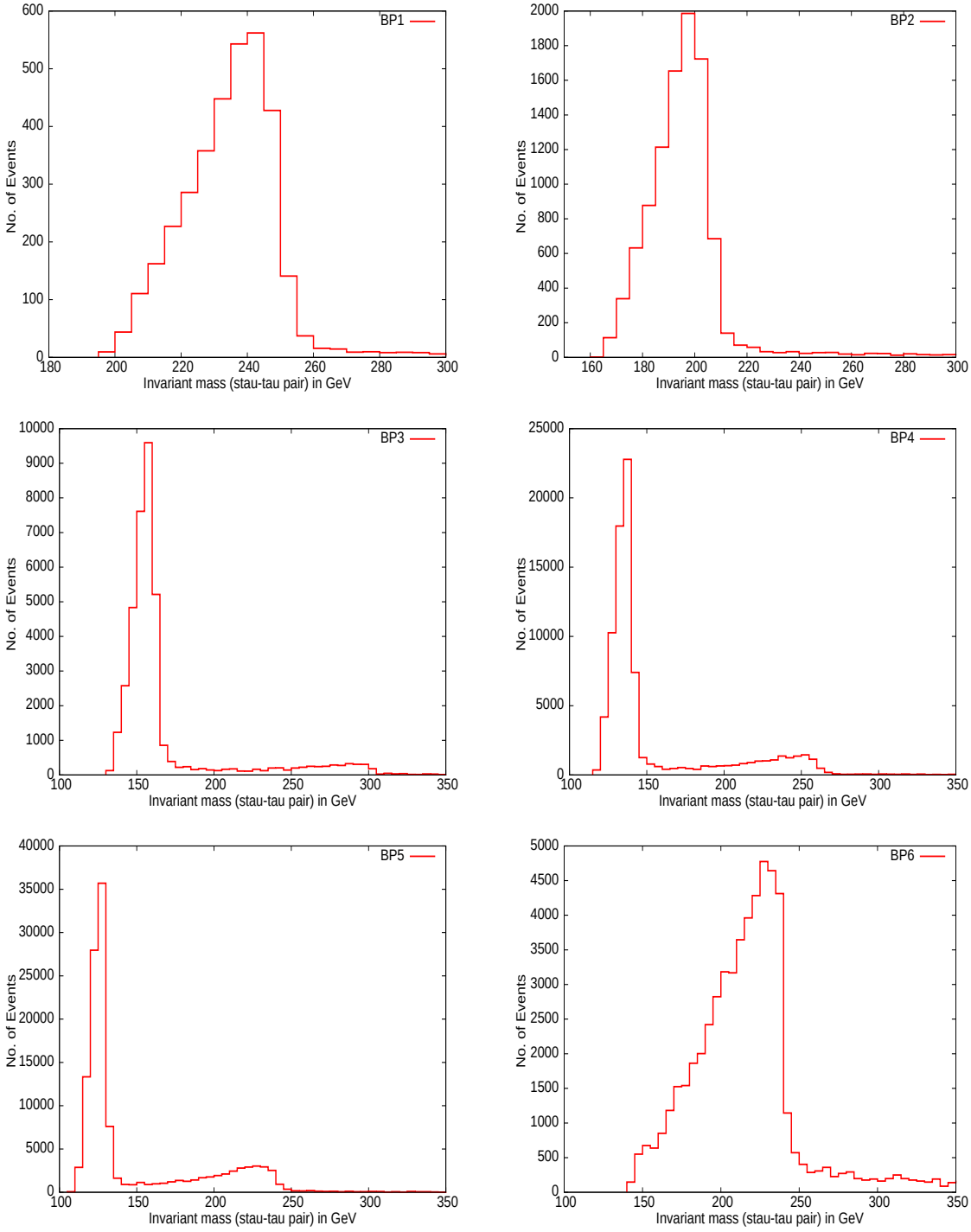

Figure 5.3: *$M_{\tilde{\tau}\tau_j}$ distribution for all the benchmark points. BP1, BP2 and BP3 show only the χ_1^0 peak. Both the χ_1^0 and χ_2^0 peaks are visible for BP4 and BP5, while BP6 displays only the χ_2^0 peak.*

5.3 Backgrounds and cuts

5.3.1 SM backgrounds

The final state we have considered, namely, $\tau_j + 2\tilde{\tau}(\text{opposite} - \text{sign charged track}) + \not{E}_T + X$, suffers from several SM background processes. This is because charged tracks in the muon chamber due to the presence of quasistable charged particle can be faked by muons. Such faking is particularly likely for ultra-relativistic particles, for which neither the time-delay measurement nor the degree of ionisation in the inner tracking chamber is a reliable discriminator. The dominant contributions come from the following subprocesses:

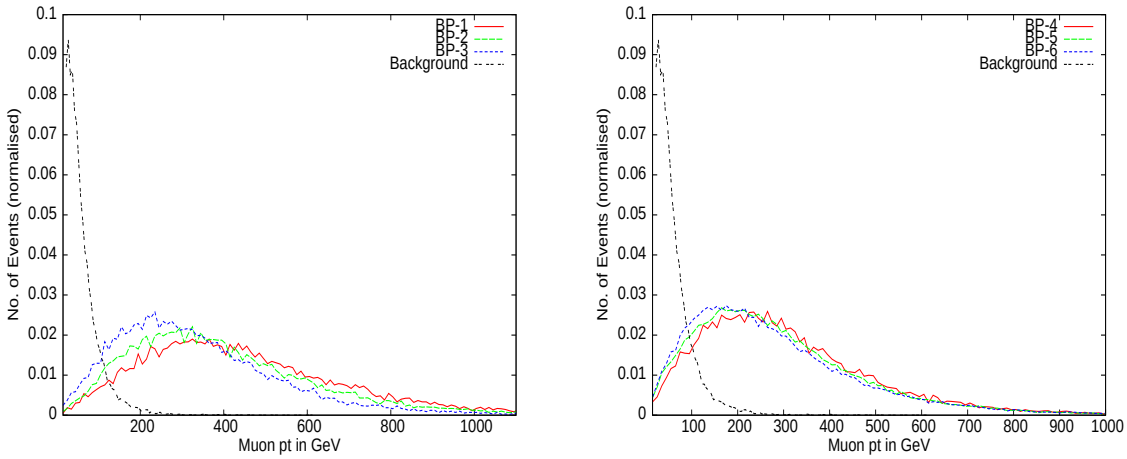

Figure 5.4: *p_T distribution (normalised to unity) of the harder muonlike track for the signal and the background, for all benchmark points. The vertical lines indicate the effects of a p_T-cut at 100 GeV.*

1. $\underline{t\bar{t}}$: This is a potential background for any final state in the context of LHC, due to its large production cross-section. In this case $t\bar{t} \to bW^+\bar{b}W^-$, followed by various combinations of leptonic as well as hadronic decays of the b and the W, can produce opposite sign dimuons and jets. The jets may emanate from actual taus, but may as well be fake. One has an efficiency of 50% in the former case, and a mistagging probability of 1% in the latter. The $t\bar{t}$ cross-section has been multiplied by a K-factor of 1.8 [12].

2. $\underline{b\bar{b}}$: This, too, has an overwhelmingly large event rate at the LHC. The semileptonic decay of both the b's ($b \to c\mu\nu_\mu$) can give rise to a dimuon final state and any of the associated jets can be faked as tau-jet. Though the mistagging probability of a non-tau jet being identified as a tau-jet is small, the large cross-section of $b\bar{b}$ production warrants serious attention to this background.

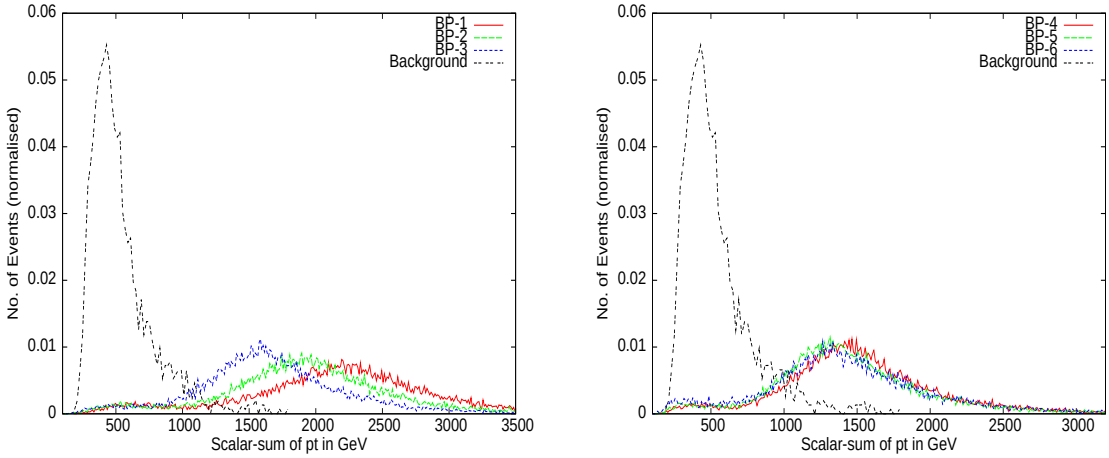

Figure 5.5: $\Sigma|p_T|$ *distribution (normalized to unity) for the signal and the background, for all benchmark points.*

3. $\underline{ZZ}$: In this case any one of the Z's can decays into a dimuon pair ($Z \rightarrow \mu\mu$) while the other one can decays into $\tau\tau$ pair where only one of the tau can be identified. The hadronic decay of Z and the subsequent misidentification of any of them as tau-jet is also possible.
4. $\underline{ZW}$: This SM process also contributes to the final state under consideration with $Z \rightarrow \mu\mu$ and $W \rightarrow \tau\bar{\nu}_\tau$.
5. $\underline{ZH}$: This subprocess can also contribute to the final state $\tau_j + 2\mu(charged - track) + \not{E}_T$where the Higgs decaying into a pair of τ's, with only one of the τ being identified has been considered.

Our chosen event selection criteria have been prompted by all the above backgrounds. First of all, we have subjected the events to the following basic cuts:

- $p_T^{lep,track} > 10$ GeV
- $p_T^{hardest-jet} > 75$ GeV
- $p_T^{other-jets} > 30$ GeV
- $40\ GeV < \not{E}_T < 180\ GeV$
- $|\eta| < 2.5$ for Leptons, Jets & Stau
- $\Delta R_{ll} > 0.2,\ \Delta R_{lj} > 0.4$, where $\Delta R^2 = \Delta\eta^2 + \Delta\phi^2$
- $\Delta R_{\tilde{\tau}l} > 0.2,\ \Delta R_{\tilde{\tau}j} > 0.4$
- $\Delta R_{jj} > 0.7$

Though the above cuts largely establish the *bona fide* of a signal event, the background events are too numerous to be effectively suppressed by them. One there-

fore has to use the fact that the jets and stau-tracks are all arising from the decays of substantially heavy sparticles. This endows them with added degrees of hardness, as compound to jets and muons produced in SM process. Thus we can impose a p_T cut on each track on the muon chamber, and also demand a large value of the scalar sum of transverse momenta of all the visible final state particles:

- $p_T^{muonlike\ track} > 100\ GeV$
- $\Sigma|\vec{p_T}| > 1\ TeV$

The justification of these cuts can also be seen from Figures 5.4 and 5.5. It may be noted that no invariant mass cut on the pair of charged tracks has been imposed. While such a cut, too, can suppress the dimuon background, we find it more rewarding to use the scalar sum of p_T cut.

5.3.2 SUSY backgrounds

Apart from the SM backgrounds, SUSY processes in this scenario itself contribute to the final state $\tau_j + 2\tilde{\tau} + \not{E}_T + X$, which are often more serious than the SM backgrounds. These events will survive the kinematic cuts listed in the previous subsection, since they, too, originate in heavy sparticles produced in the initial hard scattering. The dominant contributions of this kind come from:

1. $\underline{\chi_i^0\chi_j^0 \text{ production in cascade decay of squarks/gluinos}}$: This is one of the potentially dangerous background where both the χ_i^0's $(i,j = 1,2)$ decay into $\tilde{\tau}\tau$-pairs, with only one tau being identified. This then mimics our final state in all details with a much higher event rate.
2. $\underline{\tilde{\nu}_{\tau_L}\chi_i^0 \text{ production in cascade decay of squarks/gluinos}}$: The decay of $\tilde{\nu}_{\tau_L}$ as part of the cascade produces a $W\tilde{\tau}_1$-pair, while the χ_i^0 decays into a $\tilde{\tau}\tau$-pair to give rise to same final state with an additional W which then can decay hadronically. The $\tilde{\nu}_{\tau L}$ is produced in association with a tau in large number of events (e.g., $\chi_1^{\pm} \rightarrow \tilde{\nu}_{\tau L}\tau$). The $\tilde{\nu}_{\tau_L}$ can also be produced from, say, a χ_2^0. In both of the above situations, a tau-stau pair can be seen together with another stau track, thus leading to a background event.

The first background can be reduced partially by looking at the invariant mass distribution of the $\tilde{\tau}$ (having same sign as that of the *identified* τ in the final state) with each jet in the final state. If this distribution for any particular combinations falls within $m_{\chi_i} - 20 < M_{\tilde{\tau}j} < m_{\chi_i} + 20$ (where $m_{\chi_i} = m_{\chi_1^0}$ *or* $\frac{m_{\chi_2^0}}{2}$, depending on whether χ_1^0 or χ_2^0 is better constructed), we have thrown away that event. The reason for this lies in the observations depicted in Figure 5.3; the invariant mass of a τ-induced jet and the $\tilde{\tau}$ which shows a peak close to the mass of the neutralino from which the $\tilde{\tau}$-τ pair is produced. This has been denoted by Cut X in Tables 5.1 and 5.2. In addition, if the available information on the effec-

tive mass tells us that the χ_2^0 is better reconstructed in the region, and is produced along with a χ_1^0 with substantial rate, then a similar invariant mass cut around the χ_2^0 mass will also be useful. A further cut on the transverse mass distribution $M_{\tilde{\tau}\nu_\tau}^T$ ($> 1.5m_{\chi_1^0}$ or $0.75m_{\chi_2^0}$) substantially decreases this background without seriously effecting the signal.

The background of the second kind can in principle be reduced by vetoing events with additional W's. To identify events with W we have considered only the hadronic decays of W's. We first observe the ΔR separation between the stau (produced in decay of $\tilde{\nu}_{\tau L}$) and the direction formed out of the vector sum of the momenta of the two jets produced in W decay. If this separation lies within $\Delta R = 0.8$ and the invariant mass of the two jets lies within $M_W - 20 < M_{jj} < M_W + 20$ we discard that particular event. In addition, for a sufficiently boosted W, one can have a situation where the two jets merge to form a single jet. For such a case, we again look at the stau and each jet within $\Delta R < 0.8$ around it. The invariant mass of the resultant jet is taken to be 20% of the jet energy. The event is rejected if a jet with the mass lies within ± 20 GeV of the W-mass. We have denoted this by Cut Y in Tables 5.1 and 5.2. Of course, while it is useful in reducing the background, a fraction of the signal events also gets discarded in the process.

5.4 Numerical results

We finally present the numerical results of our study, after imposing the various cuts for all the benchmark points. From Tables 5.1 and 5.2 one can see that, after demanding a minimum hardness of the charged track ($p_T^{track} > 100$ GeV), together with the cut on the scalar sum of p_T ($\Sigma|p_T| > 1TeV$), the contribution from the SM processes get reduced substantially. The cuts X and Y, defined in the previous subsection, are relatively inconsequential for SM processes. However, in the process of solving for neutrino momentum in tau decay, most of the SM background events gets eliminated on demanding the invariant mass of the tau, paired with a oppositely charged track, to be around the neutralino mass ($m_{\chi_1^0}$ *or* $m_{\chi_2^0}$). This is due to the demand that the solution be physical, i.e. the fraction x lies between 0 and 1. It is very unlikely to have admissible solutions for x in SM processes, with the τ-muon track pair invariant mass peaking at $m_{\chi_1^0}/m_{\chi_2^0}$. Thus, although the demand $0 < x < 1$ is not meant specifically for background elimination, it is nonetheless helpful in reducing backgrounds. We have verified that the SM contributions within a bin of $\pm$20GeV around the reconstructed peak is very small.

As has been already mentioned, SUSY backgrounds within the model itself is hard to get rid of completely. The peak in the transverse mass distribution of the $\tilde{\tau}$-ν_τ pair get smeared due to such background events. We have already mentioned two suggested cuts, namely, X and Y, which partially reduce these

backgrounds. Of these, cut Y suppresses (by about 15%) some of the $\tilde{\nu}_{\tau_L}$-$\chi^0_{1/2}$ events, as can be seen from Tables 5.1 and 5.2. The effects of this cut on the other SUSY backgrounds as well as the signal are very similar.

Cut X is meant to eliminate mainly the χ^0_i-χ^0_j background. Our analysis shows that this cut is rather effective in this respect; the event rate is reduced by almost 50%. Surprisingly, it also reduces the $\tilde{\nu}_{\tau_L}$-$\chi^0_{1/2}$ background by a considerable amount. The reason for this is the following: $\tilde{\nu}_{\tau_L}$-$\chi^0_{1/2}$ is produced in cascade decays of squarks and gluinos and the $\tilde{\nu}_{\tau_L}$ is often produced from a $\chi^\pm_1$ (the branching fraction being 30% or more in some BP's). In that case the decay process is $\chi^\pm_1 \to \tau^\pm \tilde{\nu}_{\tau_L}$. The tau out of such a $\chi^\pm_1$ is sometimes identified, whereas the tau out of a $\chi^0_{1/2}$ ($\chi^0_{1/2} \to \tau^\pm \tilde{\tau}^\mp$) from the other decay chain goes untagged. The invariant mass distribution of a track and the jet coming from an unidentified τ is clustered around $m_{\chi^0_i}$ (i = 1,2). Thus cut X turns out to be effective in eliminating this type of background.

After all this effort, however, one still left with background events which smear the sharp fall in the transverse mass distribution of the $\tilde{\tau}\nu_\tau$-pair. We have to impose an additional cut on the transverse mass distribution to separate it from the background. This is in the form of the demand $M^T_{\tilde{\tau}\nu_\tau} > \frac{3}{4} m_{\chi^0_2}$, whereby it is possible to reduce these backgrounds further, as can be seen from Tables 5.1 and 5.2. It is then possible to determine the chargino mass ($m_{\chi^\pm_1}$) by looking at the peak, followed by a sharp descent, in the transverse mass distribution for several benchmark points.

The transverse mass distributions for different benchmark points are shown in Figures 5.6 and 5.7. The tau-identification efficiency is assumed to be 50% in Figure 5.6; Figure 5.7 reflects the improvement achieved in a relatively optimistic situation when this efficiency is 70%.

At BP1 the statistics is very poor and we have relatively few events within a bin of 40 GeV around $m_{\chi^\pm_1}$. One has about 50% of the events coming from other SUSY processes (Table 5.1). Also the sharp edge is not clearly visible due to the presence of a large number of $\chi^0_1\chi^0_1$ events, even after imposing the $M^T_{\tilde{\tau}\nu_\tau} > \frac{3}{4} m_{\chi^0_2}$ cut.

The situation is similar for BP2 as well. In BP3 and BP4 a peak-like behaviour, followed by a sharp fall, is considerably more distinct, from which one can extract the value of $m_{\chi^\pm_1}$.

For BP5 and BP6 the contamination due to the SUSY background is found to be small compared to the other benchmark points. The $\chi^\pm_1$ production rate in cascade decays of squarks/gluinos is also higher there. Hence the transverse mass distribution shows a distinctly sharp fall, from which a faithful reconstruction of chargino mass is possible.

A comparison between Figures 5.6 and 5.7 shows, the prospect can be im-

proved noticeably if one has a better tau identification efficiency ($\epsilon_\tau = 70\%$). In such a case, the background from χ_1^0-χ_1^0/χ_1^0-χ_2^0/χ_2^0-χ_2^0 is less severe compared to the case where the tau identification efficiency is 50%.

From Figures 5.6 and 5.7, one can also see some small peaks in the $M^T_{\tilde{\tau}\nu_\tau}$ distribution with very few event rate, in the region where $M^T_{\tilde{\tau}\nu_\tau} > m_{\chi_2^0}$. This can be attributed to those events where a χ_3^0 or a χ_4^0 decays into a $\tilde{\tau}\tau$ pair, and also to the production of the heavier chargino.

5.5 Summary and conclusions

We have extended our earlier study on the mass reconstruction of non-strongly interacting superparticles in such cases, by considering final states resulting from the decays of a $\chi_1^\pm \chi_{1(2)}^0$ pair in SUSY cascades. The final state under consideration is $\tau_j + 2\tilde{\tau}(\text{opposite} - \text{sign charged tracks}) + \not{E}_T + X$. We have systematically developed a procedure for identifying the contribution to $\vec{\not{p}}_T$ from the neutrino produced in $\chi_1^\pm$-decay, together with a quasi-stable stau. Once this is possible, the transverse mass distribution of the corresponding $\tilde{\tau} - \nu_\tau$ pair can be extracted from data at the LHC, and a sharp edge in that distribution yields information on the chargino mass. While eliminating the SM backgrounds in this process is straightforward, we have suggested ways of minimising the contamination of the relevant final state from competing processes in the same SUSY scenario. Selecting a number of benchmark points in the parameter space, we show regions where the above procedure works. In cases where it does not, the main causes of failure are identified as the overwhelmingly large contribution from χ_1^0-pairs, and, for example, in the first two benchmark points, somewhat poor statistics. The other important issue is the differentiation between the χ_1^0 and the χ_2^0 produced in association with the $\chi_1^\pm$. For this, we make use of the assumption of gaugino universality as well as the information extracted from the effective mass distribution in SUSY processes.

To conclude, we reiterate that the existence of quasi-stable charged particles, a possibility not too far-fetched, opens a new vista in the reconstruction of superparticle masses. While the utilisation of this possibility has already been discussed in the previous chapter, the present work underscores a relatively arduous task in this respect, in obtaining transverse mass edges in chargino decays. In spite of rather challenging obstacles from underlying SUSY processes, we demonstrate the feasibility of our procedure, which is likely to be enhanced by improvement in, for example, the W-and tau-identification efficiencies.

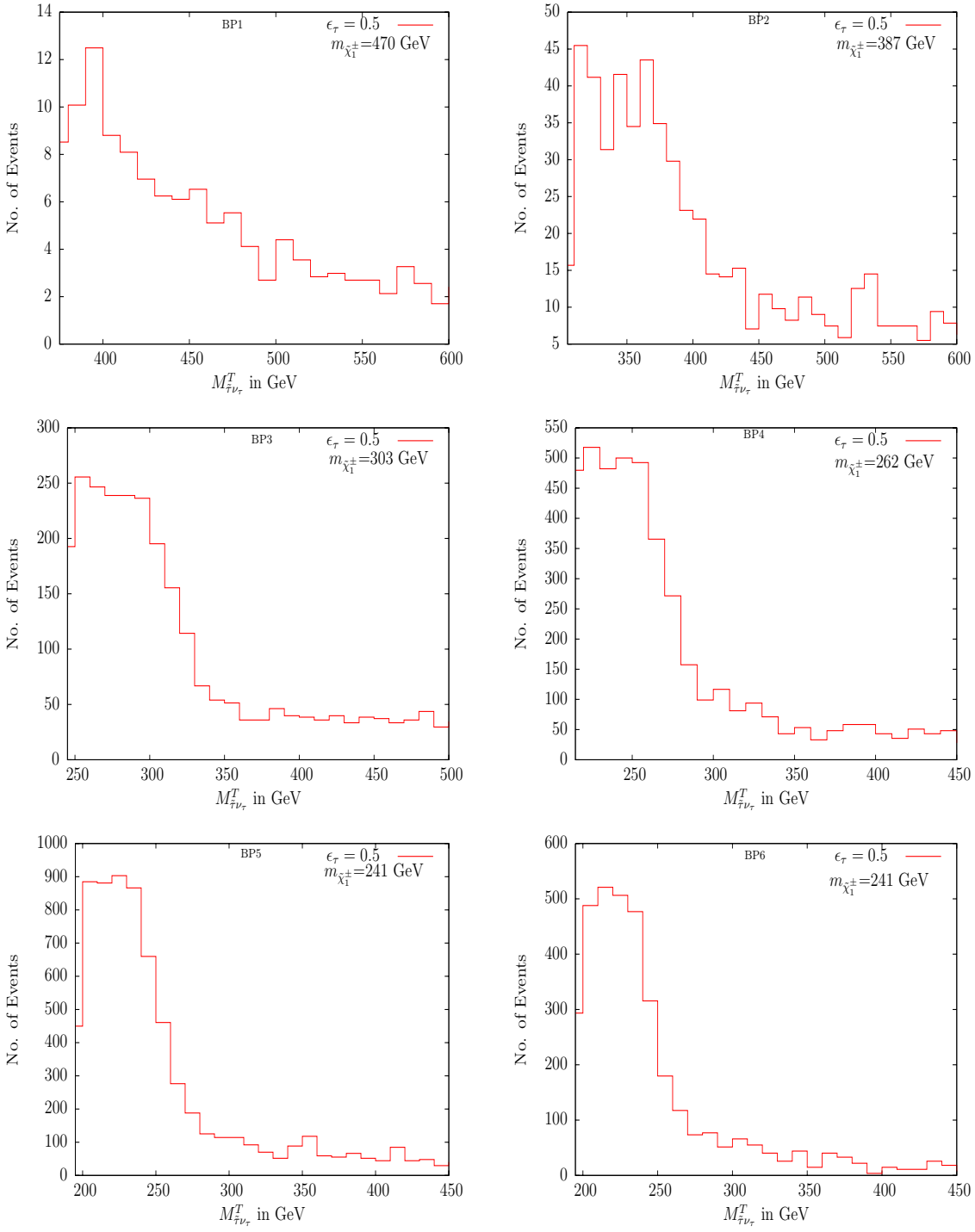

Figure 5.6: *The transverse mass $\tilde{\tau}\nu_\tau$-pair from chargino decay described in the text, for all the benchmark points with tau identification efficiency (ϵ_τ) = 50%.*

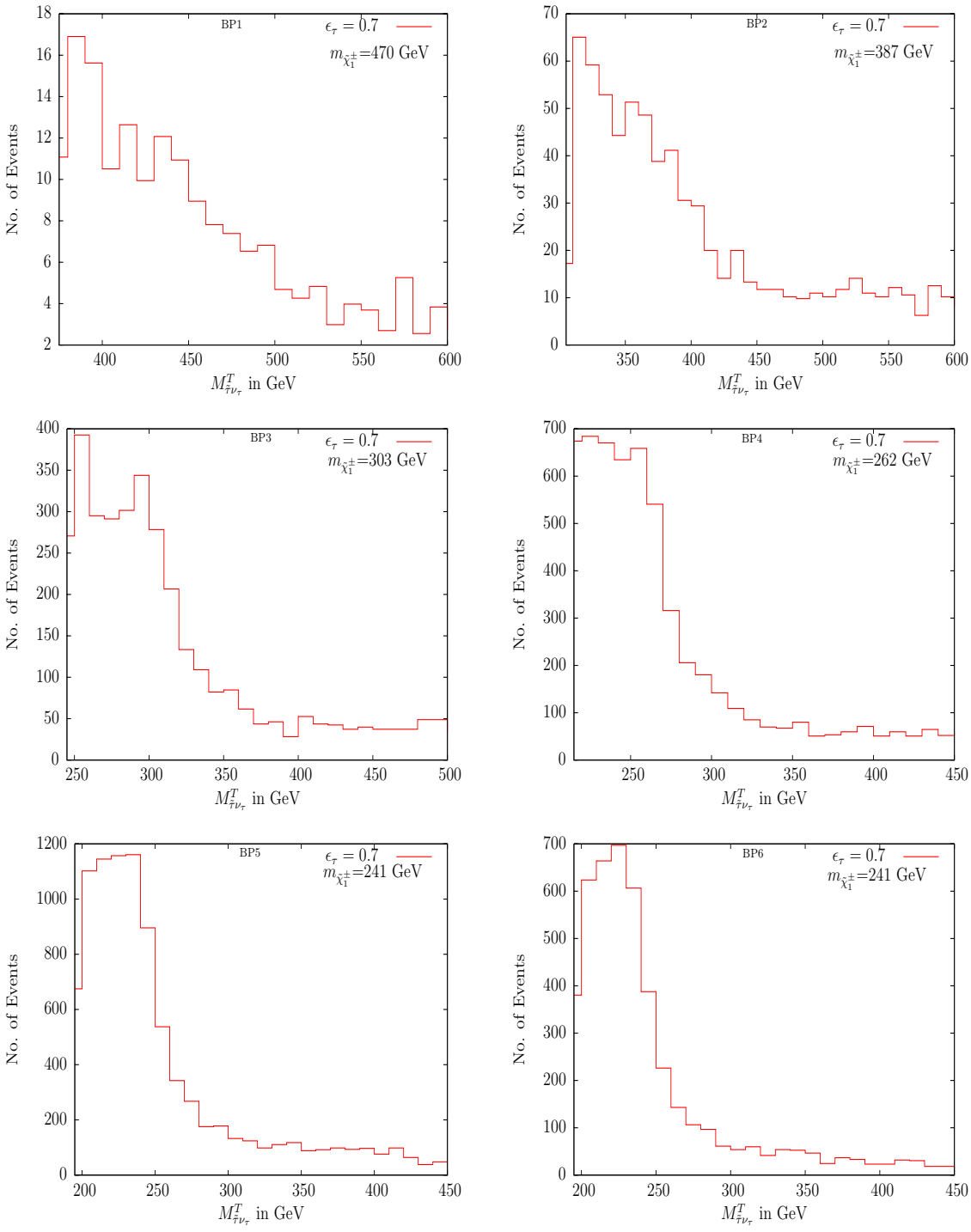

Figure 5.7: *Same as in Figure 5.6, but with tau identification efficiency* $(\epsilon_\tau) = 70\%$.

BP1	Signal	SM	SUSY backgrounds			
	$(\chi^0_{1/2}-\chi^\pm_1)$	backgrounds	$\chi^0_1-\chi^0_1$	$\chi^0_1-\chi^0_2$	$\chi^0_2-\chi^0_2$	$\chi^0_{1/2}-\tilde{\nu}_{\tau L}$
Basic cuts	121	65588	2557	62	1	786
With p_T+$\Sigma\lvert p_T\rvert$ Cut	92	202	2236	49	1	551
Cut Y	83	202	1969	42	1	433
Cut X	58	202	1130	26	1	244
$M^T_{\tilde{\tau}\nu_\tau} > \frac{3}{4}m_{\chi^0_2}$	28	0	83	2	0	25
$\lvert M_{peak}-M^T_{\tilde{\tau}\nu_\tau}\rvert \leq 20$	9	0	7	0	0	2
BP2	Signal	SM	SUSY backgrounds			
	$(\chi^0_{1/2}-\chi^\pm_1)$	backgrounds	$\chi^0_1-\chi^0_1$	$\chi^0_1-\chi^0_2$	$\chi^0_2-\chi^0_2$	$\chi^0_{1/2}-\tilde{\nu}_{\tau L}$
Basic cuts	677	65588	6600	390	9	2157
With p_T+$\Sigma\lvert p_T\rvert$ Cut	492	202	5552	301	7	1418
Cut Y	444	202	4885	262	6	1106
Cut X	336	202	2675	170	5	605
$M^T_{\tilde{\tau}\nu_\tau} > \frac{3}{4}m_{\chi^0_2}$	173	0	278	26	1	76
$\lvert M_{peak}-M^T_{\tilde{\tau}\nu_\tau}\rvert \leq 20$	62	0	33	5	0	11
BP3	Signal	SM	SUSY backgrounds			
	$(\chi^0_{1/2}-\chi^\pm_1)$	backgrounds	$\chi^0_1-\chi^0_1$	$\chi^0_1-\chi^0_2$	$\chi^0_2-\chi^0_2$	$\chi^0_{1/2}-\tilde{\nu}_{\tau L}$
Basic cuts	5519	65588	19400	3361	170	6959
With p_T+$\Sigma\lvert p_T\rvert$ Cut	3571	202	15181	2240	98	4186
Cut Y	3131	202	13091	1924	91	3231
Cut X	2372	202	6974	1192	71	1679
$M^T_{\tilde{\tau}\nu_\tau} > \frac{3}{4}m_{\chi^0_2}$	1189	0	985	205	14	208
$\lvert M_{peak}-M^T_{\tilde{\tau}\nu_\tau}\rvert \leq 20$	523	0	154	46	1	27

Table 5.1: *Number of signal and background events for the $\tau_j + 2\tilde{\tau}$ (charged-track)+$\not{E}_T + X$ final state, considering all SUSY processes, for BP1, BP2 and BP3 at an integrated luminosity 300 fb^{-1} assuming tau identification efficiency $\epsilon_\tau = 50\%$.*

BP4	Signal	SM	SUSY backgrounds			
	$(\chi^0_{1/2}-\chi^\pm_1)$	backgrounds	$\chi^0_1-\chi^0_1$	$\chi^0_1-\chi^0_2$	$\chi^0_2-\chi^0_2$	$\chi^0_{1/2}-\tilde{\nu}_{\tau L}$
Basic cuts	18194	65588	33076	10618	886	10613
With p_T+$\Sigma\lvert p_T\rvert$ Cut	10697	202	24475	6342	439	5713
Cut Y	9431	202	21100	5431	368	4436
Cut X	4875	202	7583	2132	157	1480
$M^T_{\tilde{\tau}\nu_\tau} > \frac{3}{4}m_{\chi^0_2}$	2345	0	1274	439	41	231
$\lvert M_{peak}-M^T_{\tilde{\tau}\nu_\tau}\rvert \leq 20$	1076	0	254	114	13	58
BP5	Signal	SM	SUSY backgrounds			
	$(\chi^0_{1/2}-\chi^\pm_1)$	backgrounds	$\chi^0_1-\chi^0_1$	$\chi^0_1-\chi^0_2$	$\chi^0_2-\chi^0_2$	$\chi^0_{1/2}-\tilde{\nu}_{\tau L}$
Basic cuts	34489	65588	39521	19574	1976	12039
With p_T+$\Sigma\lvert p_T\rvert$ Cut	18748	202	28329	10827	958	5953
Cut Y	16419	202	24348	9326	815	4586
Cut X	8508	186	8869	3764	376	1626
$M^T_{\tilde{\tau}\nu_\tau} > \frac{3}{4}m_{\chi^0_2}$	4099	0	1574	866	144	258
$\lvert M_{peak}-M^T_{\tilde{\tau}\nu_\tau}\rvert \leq 20$	2145	0	339	221	52	37
BP6	Signal	SM	SUSY backgrounds			
	$(\chi^0_{1/2}-\chi^\pm_1)$	backgrounds	$\chi^0_1-\chi^0_1$	$\chi^0_1-\chi^0_2$	$\chi^0_2-\chi^0_2$	$\chi^0_{1/2}-\tilde{\nu}_{\tau L}$
Basic cuts	17146	65588	14519	20756	1970	4644
With p_T+$\Sigma\lvert p_T\rvert$ Cut	8379	202	9593	11405	968	2524
Cut Y	7326	202	8004	9776	778	2025
Cut X	4204	186	3837	5697	374	1038
$M^T_{\tilde{\tau}\nu_\tau} > \frac{3}{4}m_{\chi^0_2}$	1475	0	231	1783	128	15
$\lvert M_{peak}-M^T_{\tilde{\tau}\nu_\tau}\rvert \leq 20$	774	0	62	569	44	0

Table 5.2: *Same as in Table 5.1, but for BP4, BP5 and BP6.*

Bibliography

[1] S. Biswas and B. Mukhopadhyaya, Phys. Rev. D **81**, 015003 (2010) [arXiv:0910.3446 [hep-ph]].

[2] J. Smith, W. L. van Neerven and J. A. M. Vermaseren, Phys. Rev. Lett. **50**, 1738 (1983).

[3] T. Sjostrand, S. Mrenna and P. Skands, JHEP **0605**, 026 (2006) [arXiv:hep-ph/0603175].

[4] C. Amsler *et al.* [Particle Data Group], Phys. Lett. B **667**, 1 (2008).

[5] H. L. Lai *et al.* [CTEQ Collaboration], Eur. Phys. J. C **12**, 375 (2000) [arXiv:hep-ph/9903282].

[6] W. Beenakker, R. Hopker, M. Spira and P. M. Zerwas, Nucl. Phys. B **492**, 51 (1997) [arXiv:hep-ph/9610490].

[7] C. G. Lester and D. J. Summers, Phys. Lett. B **463**, 99 (1999) [arXiv:hep-ph/9906349].

[8] B. Gripaios, JHEP **0802**, 053 (2008) [arXiv:0709.2740 [hep-ph]]; H. C. Cheng and Z. Han, JHEP **0812**, 063 (2008) [arXiv:0810.5178 [hep-ph]]; A. J. Barr, B. Gripaios and C. G. Lester, arXiv:0908.3779 [hep-ph].

[9] Y. Coadou *et al.* ATLAS Internal Note ATL-PHYS-98-126

[10] The CMS Collaboration, CMS-TDR-8.1, CERN/LHCC 2006-001

[11] S. Asai *et al.*, Eur. Phys. J. C **32S2**, 19 (2004) [arXiv:hep-ph/0402254].

[12] W. Beenakker, S. Dittmaier, M. Kramer, B. Plumper, M. Spira and P. M. Zerwas, Nucl. Phys. B **653**, 151 (2003) [arXiv:hep-ph/0211352].

Chapter 6

Left-chiral tau-sneutrino reconstruction

6.1 Introduction

Next, we will describe the possibility of mass reconstruction of the heavier tau-sneutrino whose dominant constituent is the left-chiral state at the LHC [1]. It is produced in cascade decay of squarks and/or gluinos, mainly via the decay of the second lightest neutralino or the lighter chargino. The $\tilde{\nu}_{\tau_L}$ thus produced has a substantial branching fraction of decaying into a $W\tilde{\tau}$-pair. Hence, reconstructing the four-momenta of the W's in its hadronic decay mode, it is possible to reconstruct the heavier mass eigenstate of the tau-sneutrino. We have considered two different ways of reconstructing the $\tilde{\nu}_{\tau_L}$ mass. In one case, we use the mass information of the lighter chargino and the neutralino and the other one is more model independent, which does not use any mass information.

Though one can have a W in the final state in association with two charged tracks in this long-lived stau scenario, our emphasis nonetheless is on the fact that the W, paired with a particular track giving an invariant mass peak offers a definite signature of $\tilde{\nu}_{\tau_L}$ production in the SUSY cascade.

In the following section we have discussed the signal under study and the reconstruction strategy. Backgrounds and the event selection criteria have also been discussed there. The numerical results which comprise a scan over the region of m_0-$m_{1/2}$ plane are presented in section 6.3. We conclude in section 6.4.

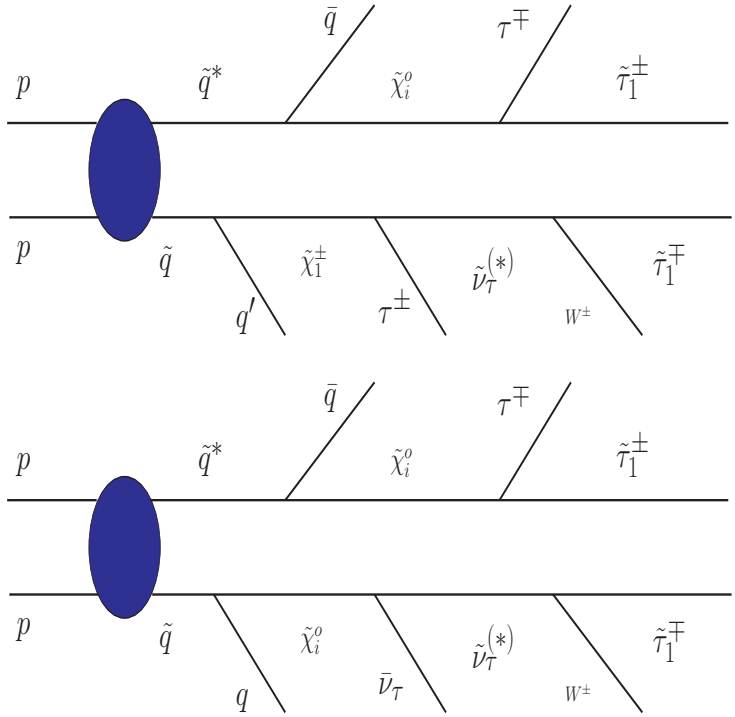

Figure 6.1: Schematic diagrams of typical SUSY cascades for reconstruction of the left-chiral tau-sneutrino.

6.2 Signal and reconstruction

We have worked with the benchmark points listed in Table 4.1, section 4.2. In order to illustrate that it is possible to reconstruct the left-chiral τ-sneutrino in this scenario we have considered the following final state:

- $\tau_j + W + 2\tilde{\tau} + \not{E}_T + X$

where, τ_j represents a tau jet, the missing transverse energy is denoted by $\not{E}_T$, W symbolizes a W-boson that has been identified in its hadronic decay mode[1] and all other jets coming from cascade decays are included in X. The collider simulation has been done with a centre of mass energy E_{cm}=14 TeV, at two different integrated luminosities of $30fb^{-1}$ and $100fb^{-1}$ using the event generator **PYTHIA 6.4.16** [2]. A simulation for the early LHC run at E_{cm}=10 TeV and integrated luminosity of $3fb^{-1}$ has also been predicted. We have used the parton distribution function CTEQ5L [3] with the factorisation (μ_F) and renormalisation (μ_R) scale set at $\mu_F = \mu_R = m^{final}_{average}$, average mass of the final state particles produced in the initial hard scattering. Following are the numerical values of various parameters,

[1]We have not considered the leptonic decay of W since it is difficult to reconstruct the four momenta of the W in its leptonic decay mode due to the presence of the invisible neutrino .

used in our calculation [4]:

$$M_Z = 91.187 \text{ GeV}, M_W = 80.398 \text{ GeV}, M_t = 171.4 \text{ GeV}$$
$$\alpha_{em}^{-1}(M_Z) = 127.9, \quad \alpha_s(M_Z) = 0.118$$

where, M_Z, M_W and M_t are the masses of the Z, W boson and top-quark respectively; $\alpha_{em}(M_Z)$ and $\alpha_s(M_Z)$ are the electromagnetic and strong coupling constants respectively at the scale of M_Z.

6.2.1 Basic idea

The $\tilde{\nu}_{\tau_L}$ is produced in SUSY cascade predominantly via the decay of lightest chargino ($\chi_1^+ \to \tilde{\nu}_{\tau_L}\tau^+$) or second lightest neutralino ($\chi_2^0 \to \tilde{\nu}_{\tau_L}\bar{\nu}_\tau$). The corresponding decay branching fractions are given in Table 6.1. The momentum information of the charged track enables us to reconstruct the $\tilde{\nu}_{\tau_L}$ mass in this scenario. This closely follows our earlier studies on neutralino and chargino reconstruction. A procedure for reconstructing the mass of a left-chiral tau-sneutrino, making occasional use of the earlier results, is outlined here.

BP-1		**BP-2**		**BP-3**	
$\chi_2^0 \to \tilde{\nu}_{\tau_L}\bar{\nu}_\tau$(+cc)	$\chi_1^+ \to \tilde{\nu}_{\tau_L}\tau^+$	$\chi_2^0 \to \tilde{\nu}_{\tau_L}\bar{\nu}_\tau$(+cc)	$\chi_1^+ \to \tilde{\nu}_{\tau_L}\tau^+$	$\chi_2^0 \to \tilde{\nu}_{\tau_L}\bar{\nu}_\tau$(+cc)	$\chi_1^+ \to \tilde{\nu}_{\tau_L}\tau^+$
23%	24.7%	25%	27.6%	26.6%	32.5%
BP-4		**BP-5**		**BP-6**	
$\chi_2^0 \to \tilde{\nu}_{\tau_L}\bar{\nu}_\tau$(+cc)	$\chi_1^+ \to \tilde{\nu}_{\tau_L}\tau^+$	$\chi_2^0 \to \tilde{\nu}_{\tau_L}\bar{\nu}_\tau$(+cc)	$\chi_1^+ \to \tilde{\nu}_{\tau_L}\tau^+$	$\chi_2^0 \to \tilde{\nu}_{\tau_L}\bar{\nu}_\tau$(+cc)	$\chi_1^+ \to \tilde{\nu}_{\tau_L}\tau^+$
22%	31.7%	17.8%	28.2%	17.8%	26.4%

Table 6.1: *The branching fractions for $\chi_2^0 \to \tilde{\nu}_{\tau_L}\bar{\nu}_\tau$, including the charge-conjugated (cc) mode and $\chi_1^+ \to \tilde{\nu}_{\tau_L}\tau^+$ for respective benchmark points.*

The $\tilde{\nu}_{\tau_L}$ has a sizeable decay branching fraction into a $W^+\tilde{\tau}_1^-$-pair (ranging from $\approx$ 34% to 84%). Since the W will always be produced in association with two staus, it is crucial to identify the correct $W^\pm\tilde{\tau}_1^\mp$ -pair and thus avoid the combinatorial background. Since charge identification of a W in its hadronic decay mode is difficult, we have adopted the following methods for finding the correct pair:

1. Using opposite sign charged tracks (OSCT): To determine the correct $W^\pm\tilde{\tau}_1^\mp$-pair we have make use of two opposite sign charged tracks. For the signal, one has $\tau_j + W + 2\tilde{\tau} + \not{E}_T + X$ with one tau in the final state, where the $\tilde{\tau}_1^\pm\tau^\mp$ pair has originated in the decay of a neutralino χ_1^0 (or χ_2^0) and $\tilde{\nu}_{\tau_L}$ has

decayed into a $W^+\tilde{\tau}_1^-$ pair. The stau-track produced in a $\tilde{\nu}_{\tau_L}$ decay always has the same charge as that of the tau if one has two opposite sign charged track in the final state. Hence combining the four momenta of this track with that of W one can obtain a $W^+\tilde{\tau}_1^-$ invariant mass distribution peaking at the $\tilde{\nu}_{\tau_L}$ mass ($m_{\tilde{\nu}_{\tau_L}}$).This requires identification of the charge of a jet out of a tau decay, the efficiency of which has been assumed to be 100%. The events in which the tau has originated from the decay of a chargino ($\chi_1^+ \rightarrow \tilde{\nu}_{\tau_L}\tau^+$), and the tau out of a neutralino decay goes unidentified, will contribute to the background events in this method, which we will discuss in the next subsection. Nevertheless, this method works very well in determining the correct $W^\pm\tilde{\tau}_1^\mp$ pair and one obtains the invariant mass peak at the correct value of the corresponding mass of the left-chiral sneutrino ($m_{\tilde{\nu}_{\tau_L}}$). Furthermore, this method can be used irrespective of the possibility of reconstruction of the neutralino and chargino mass[2].

2. Using chargino-neutralino mass information (CNMI): Though the method based on OSCT does not depend on the reconstructability of other superparticle masses, its main disadvantage is that it not only reduces half of the signal event but also includes many background events. The correct $W^\pm\tilde{\tau}_1^\mp$ pair can also be determined if one uses the information of the chargino or/and neutralino mass, by looking at the end point in the invariant mass distribution of the track and tau-jet pair. The right combination will have the end point at the corresponding neutralino mass ($m_{\chi_i^0}$, $i = 1, 2$). In cases where the tau out of a neutralino decay goes undetected and the tau out of a chargino decay gets identified, then the $\tilde{\tau} - W - \tau_j$ pair invariant mass distribution will have an end point at the corresponding chargino mass ($m_{\chi_1^\pm}$). We have combined the $W^\pm$ with the corresponding track ($\tilde{\tau}_1^\mp$) when either of the $|m_{\chi_i^0} - M_{\tilde{\tau}\tau_j}| \leq 20\ GeV$ or $|m_{\chi_i^\pm} - M_{\tilde{\tau}W\tau_j}| \leq 20\ GeV$ criterion is satisfied.

6.2.2 Backgrounds and event selection criteria

In this subsection we discuss the possible SM backgrounds that can fake our signal, namely, $W + \tau_j + 2\tilde{\tau} + \not{E}_T + X$ and prescribe the requisite cuts to minimise them. First of all, we have advocated the following basic cuts for each event to validate our desired final state:

- $p_T^{lep},\ p_T^{track} > 10$ GeV
- $p_T^{hardest-jet} > 75$ GeV
- $p_T^{other-jets} > 30$ GeV

[2]It should be mentioned here, that the mass associated with the charge track, which can be found following our discussion in section 4.4.1, is an inevitable input for both the methods.

- $\not{E}_T > 40$ GeV
- $|\eta| < 2.5$ for leptons, jets and stau
- $\Delta R_{ll} > 0.2,\ \Delta R_{lj} > 0.4$, where $\Delta R^2 = \Delta\eta^2 + \Delta\phi^2$
- $\Delta R_{\tilde{\tau}l} > 0.2,\ \Delta R_{\tilde{\tau}j} > 0.4$
- $\Delta R_{jj} > 0.7$

A jet has been formed using the simple cone algorithm of PYCELL in **PYTHIA 6.4.16** [2] with the following specifications:

- A cone of $\Delta R = 0.4$ has been taken around the jet initiator.
- A minimum E_T ($\geq 20GeV$) has been demanded for the each cluster of energy to be considered as a jet.

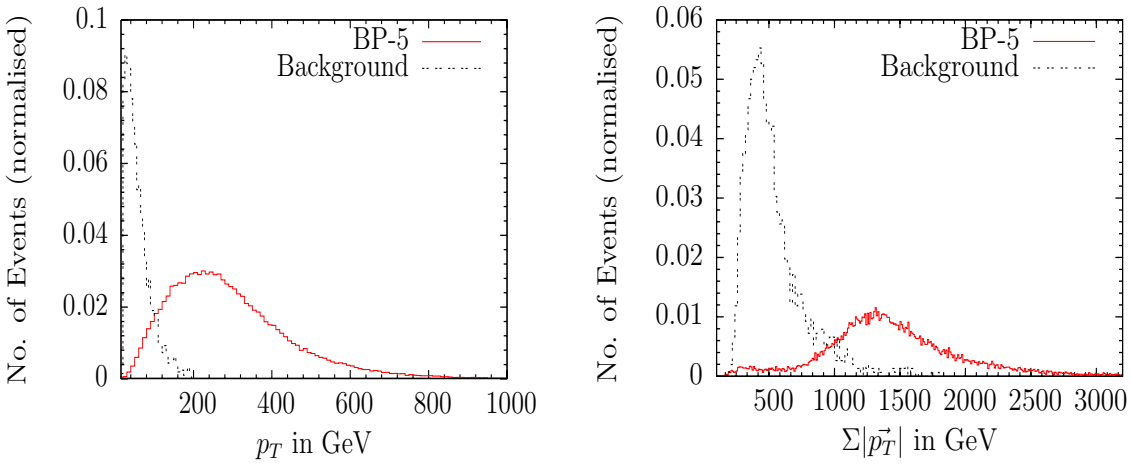

Figure 6.2: *p_T of the harder muonlike track (left) and $\Sigma|\vec{p_T}|$ (right) distribution (normalised to unity) for the signal (BP5) and the background, with E_{cm}=10 TeV.*

The above cuts are applied for simulation with both the center-of-mass energies of 10 and 14 TeV. Keeping detector resolutions of the momenta of each particle in mind, different Gaussian resolution functions have been used for electrons, muons/staus and jets. These exactly follow the path prescribed in section 4.3.3. We have assumed a tau identification efficiency of 50% for one prong decay of a tau lepton, whereas a rejection factor of 100 has been used for the non-taujets [5–7]. To identify the W in its hadronic decay mode, we have used the following criteria:

- the invariant mass of any two jets should lie within $M_W - 20GeV < M_{jj} < M_W + 20GeV$
- the separation between the stau and the direction formed out of the vector sum of the momenta of the two jets (produced in W decay) should lie within

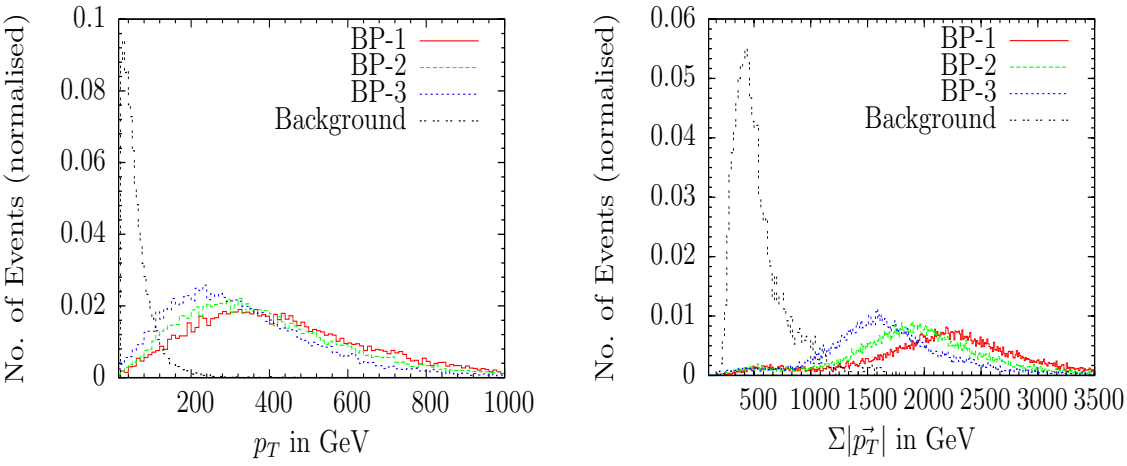

Figure 6.3: *p_T of the harder muonlike track (left) and $\Sigma|\vec{p_T}|$ (right) distribution (normalised to unity) for the signal (BP1, BP2 and BP3) and the background, with E_{cm}=14 TeV.*

$\Delta R = 0.8$

The charged track of a massive particle in the muon chamber can be faked by the muon itself. In our earlier study, we have shown that the SM backgrounds like $t\bar{t}$, ZZ, ZW, ZH can contribute to the $\tau_j + 2\tilde{\tau} + \not{E}_T + X$ final state. In the present study we have an additional W in the final state. This requirement further reduces the contribution from SM processes. Above all, demanding an added degree of hardness of the charged tracks and a minimum value of the scalar sum of transverse momenta ($\Sigma|\vec{p_T}|$) of all the visible particle in the final state, the contribution from above SM processes to the $W + \tau_j + 2\tilde{\tau} + \not{E}_T + X$ final state can be suppressed considerably as can be seen from Table 6.2. We have considered $t\bar{t}$ and ZW subprocesses, as the contribution from the ZZ and ZH background are negligible even after the basic cuts, due to the requirement of additional W. For the model dependent case (CNMI), which uses the mass information of the neutralino and chargino for pairing W with a charged track, we have used the values of $m_{\chi_1^0}$ and $m_{\chi_1^\pm}$ as given in BP5. Because this gives a conservative estimate of the background, as the event rates are even smaller if one uses different values of $m_{\chi_1^0}$ and $m_{\chi_1^\pm}$ for different benchmark points (*e.g.* BP1, BP2, etc.).

For the simulation at $E_{cm} = 10\ TeV$, we have adopted the following cuts on the $p_T^{\tilde{\tau}}$ and $\Sigma|\vec{p_T}|$ variables (See Figure 6.2):

- $p_T^{track} > 75$ GeV
- $\Sigma|\vec{p_T}| > 700$ GeV

where as, for the simulation at a higher center of mass energy $E_{cm} = 14\ TeV$ the degree of hardness raised to (See Figure 6.3 and 6.4):

- $p_T^{track} > 100$ GeV

- $\Sigma|\vec{p_T}| > 1$ TeV

Background	**10 TeV**		**14 TeV**	
$(t\bar{t} + ZW)$	CNMI	OSCT	CNMI	OSCT
basic cuts	21	19	1440	715
p_T+$\Sigma|p_T|$ cut	1	1	6	5
$\lvert M_{peak} - M_{\tilde{\tau}W}\rvert \leq 20GeV$	0	0	1	1

Table 6.2: *Number of background events for the $W + \tau_j + 2\tilde{\tau}$ (charged-track)+$\not{E}_T$+ X final state for two cases, with E_{cm}=10 TeV and 14 TeV at an integrated luminosity of 3 fb^{-1} and 100 fb^{-1} respectively. In Table CNMI and OSCT stand for reconstruction of $m_{\tilde{\nu}_{\tau_L}}$ using Chargino-Neutralino Mass Information whereas OSCT implies reconstruction of the same using Opposite Sign Charged Tracks.*

6.3 Results and discussions

We present the numerical results of our study in this section. At the early phase of LHC run, *i.e.*, $E_{cm} = 7\ TeV$ and integrated luminosity of 1 fb^{-1}, we have very few number of signal events (~ 2 events). Therefore, it is hard to obtain a distinct peak in the $W^{\pm}\tilde{\tau}_1^{\mp}$ invariant mass distribution. In Table 6.3 we have presented the results of simulation at $E_{cm} = 10\ TeV$ for BP5, to illustrate that it is possible to reconstruct the left-chiral tau-sneutrino even at an integrated luminosity of 3 fb^{-1} (Figure 6.5). Though for other benchmark points, it is very difficult to obtain the mass of the $\tilde{\nu}_{\tau_L}$, as the event rate is even smaller than BP5 and the peak is hardly visible. The results of simulation at $E_{cm} = 14\ TeV$ have also been shown in Tables 6.4 and 6.5. Depending on the luminosity and available center of mass energy, it is possible to probe some or all of the benchmark points we have studied, at the LHC.

The numerical results enable us to assess the relative merits of the OSCT and CNMI methods. It is obvious from Tables 6.3-6.5 that we have larger number of events when the chargino-neutrlino mass information (CNMI) rather than the opposite sign charged tracks (OSCT) has been used to reconstruct the mass of the $\tilde{\nu}_{\tau_L}$, as one would expect the number of events to be less if one is restricted to opposite sign charged tracks. Also, the chance of including the wrong $W^{\pm}\tilde{\tau}_1^{\mp}$-pair is more in the OSCT method. For example, as has already been mentioned, $\chi_1^{\pm}\chi_1^0$ produced in cascades can give rise to $W + \tau_j + 2\tilde{\tau} + \not{E}_T + X$ final state, where the tau out of a chargino decay ($\chi_1^+ \rightarrow \tilde{\nu}_{\tau_L}\tau^+$) has been identified and not the one originated from a neutralino decay. In this situation one ends up with

a wrong combination of $W^{\pm}\tilde{\tau}_1^{\mp}$ pair if one is using OSCT. The contribution of such background, however, is not counted when CNMI is used. In spite of this, the fact that no information on chargino and neutralino masses is used in OSCT, is of advantage in independently confirming the nature of the spectrum. Both the methods discussed above are prone to background contamination within the model itself, such as misidentification of W and the decay like $\chi^{\pm}_{1/2} \rightarrow \chi^0_{1/2}W^{\pm} \rightarrow \tilde{\tau}_1 W^{\pm}\tau$, which smear the peak, as is visible from Figure 6.6 and 6.7.

From the numerical results, it is seen that the number of events start getting increased as one moves from BP1 to BP5, due to the fact that the production cross section of $\tilde{\nu}_{\tau_L}$ in cascade decay of squarks and/or gluinos get enhanced. However, at BP6 one has less number of events. The reason is twofold: First, the decay branching fraction of $\tilde{\nu}_{\tau_L} \rightarrow \tilde{\tau}_1^- W^+$ reduces from 84% for BP1 to 60% for BP5. The enhanced production cross-section thus has dominant effect. However, for BP6 the branching ratio falls to 34.5%, thus affecting the event rates adversely. Secondly, the mass difference $m_{\tilde{\nu}_{\tau_L}} - (m_{\tilde{\tau}_1} + m_W)$ is of the order of 20 GeV, which restricts the stau track from passing the requisite hardness cut for a sizeable number of events. Also, the $\tilde{\tau}_1 W$ invariant mass peak is badly affected at BP6, as the contribution from the decay $\chi^{\pm}_{1/2} \rightarrow \chi^0_{1/2}W^{\pm}$ is maximum due to the increase in the branching ratio. The number of events within a bin of $\pm 20\ GeV$ around the peak obtained using CNMI is comparable to that obtained using OSCT at this benchmark point. This is due to the fact that in case of mass reconstruction using CNMI, the information about the lightest neutralino mass is not available at BP6 (see section 4.4.1).

We have also explored the mSUGRA parameter space to study the feasibility of sneutrino reconstruction. A thorough scan over the $m_0 - m_{1/2}$ plane has been done using the spectrum generator **SuSpect v2.34** [8], which leads to a $\tilde{\tau}$ LSP in a usual mSUGRA scenario without the right handed sneutrino and identified the region where it is possible to reconstruct the left-chiral stau neutrino with more than 25 events within the vicinity of the $\tilde{\nu}_{\tau_L}$ mass peak at an integrated luminosity of 30 fb^{-1}. The corresponding plots are depicted in Figure 6.8.

The regions where reconstruction is possible have been determined using the following criteria:

- In the parameter space, we have not gone into regions where the gluino mass exceeds $\approx 2\ TeV$.
- The number of events within a bin of $\pm 20\ GeV$ around the peak must be greater than a specific number for the corresponding luminosity.
- When the mass information is used, as a criterion for finding the correct $W^{\pm}\tilde{\tau}_1^{\mp}$ pair, we demand that at least one of the neutralinos can be reconstructed in that region of $m_0 - m_{1/2}$ plane under consideration.

  We should mention here that, to find the LHC reach in the $m_0 - m_{1/2}$ plane

we have used neutralino mass information alone and not the information on chargino mass.

	basic cuts		p_T+$\Sigma\|p_T\|$		$\|M_{peak} - M_{\tilde{\tau}W}\| \leq 20GeV$	
BP5	CNMI	OSCT	CNMI	OSCT	CNMI	OSCT
	132	84	107	66	23	15

Table 6.3: *Number of signal events for the $W + \tau_j + 2\tilde{\tau}$ (charged-track)+$\not{E}_T + X$ final state, considering all SUSY processes for BP5 with E_{cm}=10 TeV at an integrated luminosity of 3 fb^{-1} assuming tau identification efficiency $\epsilon_\tau = 50\%$. In Table CNMI stands for the same as in Table 6.2.*

	BP1		**BP2**		**BP3**	
	CNMI	OSCT	CNMI	OSCT	CNMI	OSCT
basic cuts	318	248	984	715	4060	2550
p_T+$\Sigma\|p_T\|$ cut	250	205	775	574	3030	1904
$\|M_{peak} - M_{\tilde{\tau}W}\| \leq 20GeV$	62	38	187	119	634	364

Table 6.4: *Number of signal events for the $W + \tau_j + 2\tilde{\tau}$ (charged-track)+$\not{E}_T + X$ final state, considering all SUSY processes, for BP1, BP2 and BP3 with E_{cm}=14 TeV at an integrated luminosity of 100 fb^{-1} assuming tau identification efficiency $\epsilon_\tau = 50\%$. In Table CNMI and OSCT stand for the same as in Table 6.2.*

6.4 Summary and conclusions

We have investigated the possibility of reconstruction of the left-chiral tau-sneutrino in a scenario with a $\tilde{\nu}_R$-LSP and the lighter stau being long-lived. For that we have studied the final state consisting of $W + \tau_j + 2\tilde{\tau} + \not{E}_T + X$. We have also prescribed two different strategies for the reconstruction of the mass of the $\tilde{\nu}_{\tau_L}$. One is independent of the reconstructability of other particles as it does not use the mass information and the other one does depend on the reconstructability of the chargino and neutralino masses. The cuts imposed on the kinematic variables to eliminate the SM backgrounds are motivated by our studies on chargino and neutralino reconstruction under similar circumstances. We have demonstrated the feasibility of reconstructing the mass of the $\tilde{\nu}_{\tau_L}$ even at the early phase of LHC run with $E_{cm} = 10\ TeV$ and at an integrated luminosity of 3 fb^{-1} for a particular benchmark point (BP5) for illustration. The results for simulation with higher

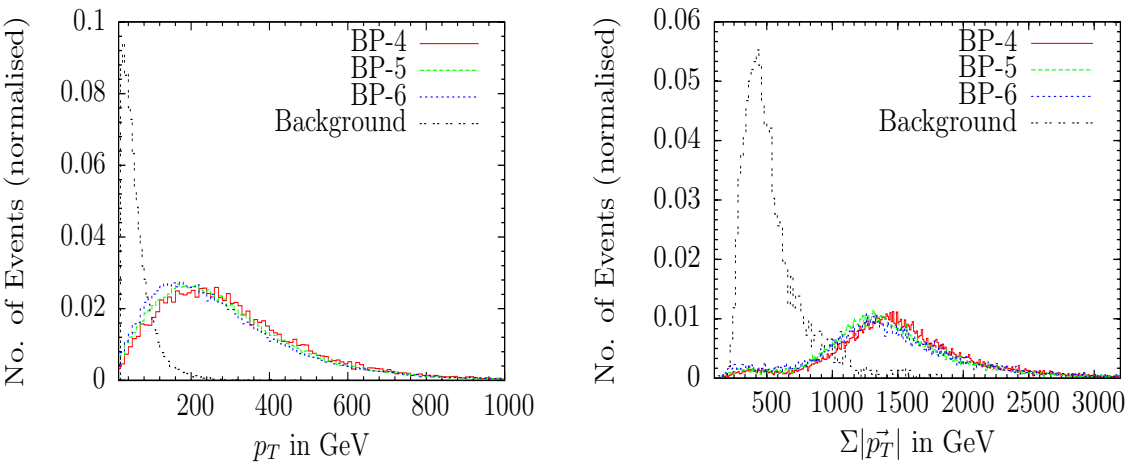

Figure 6.4: *p_T of the harder muonlike track (left)and $\Sigma|\vec{p_T}|$ (right) distribution (normalised to unity) for the signal (BP4, BP5 and BP6) and the background, with E_{cm}=14 TeV.*

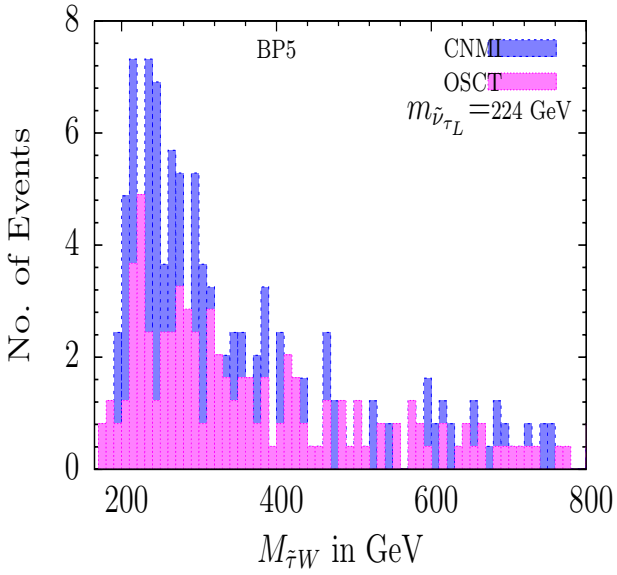

Figure 6.5: *The invariant mass ($M_{\tilde{\tau}W}$) distribution in $W + \tau_j + 2\tilde{\tau}$ (charged-track)+$\not{E}_T$+ X final state for BP5 assuming tau identification efficiency (ϵ_τ) = 50% at an integrated luminosity of 3 fb^{-1} and with E_{cm}=10 TeV. In Figure CNMI stands for reconstruction of $m_{\tilde{\nu}_{\tau_L}}$ using Chargino- Neutralino Mass Information whereas OSCT implies reconstruction of the same using Opposite Sign Charged Tracks.*

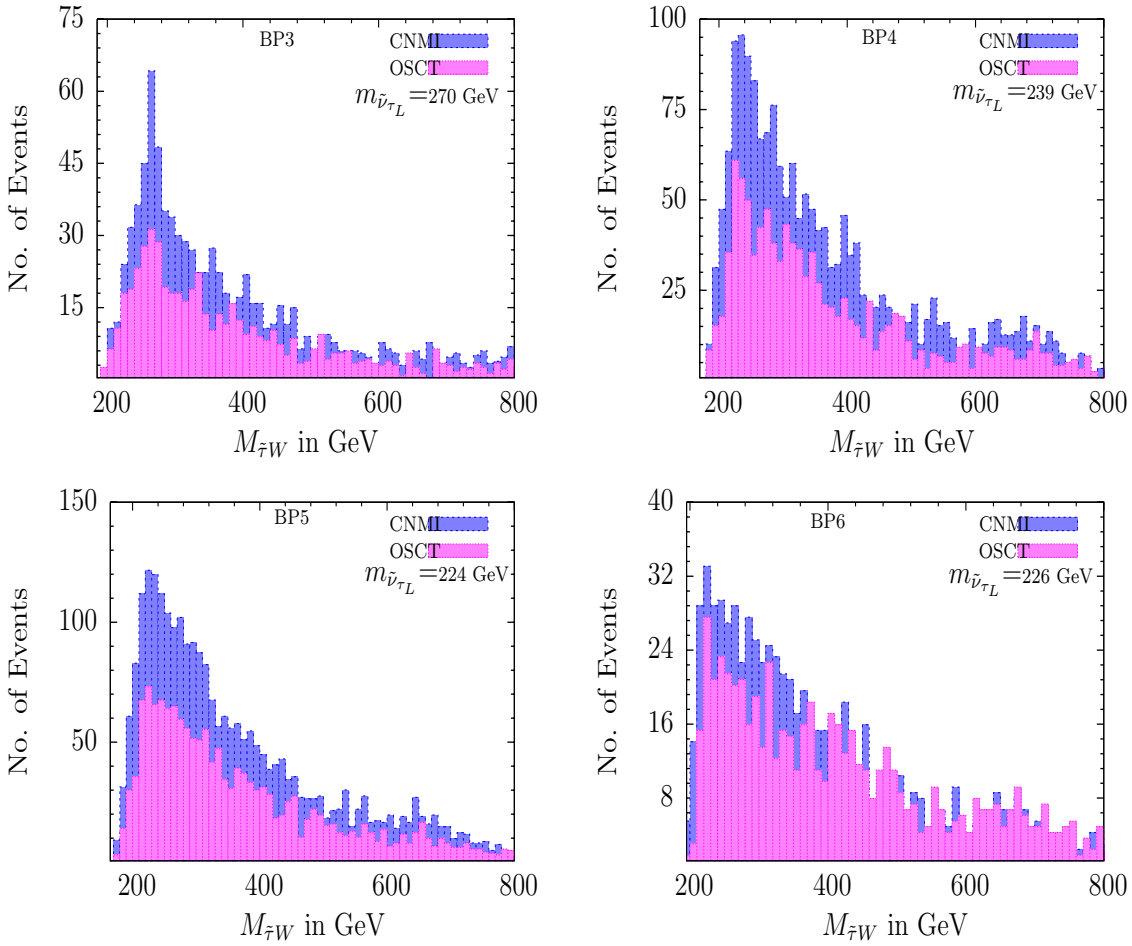

Figure 6.6: *The invariant mass ($M_{\tilde{\tau}W}$) distribution in $W + \tau_j + 2\tilde{\tau}$ (charged-track)+$\not{E}_T + X$ final state for four of our proposed benchmark points assuming tau identification efficiency (ϵ_τ) = 50% at an integrated luminosity of 30 fb^{-1} and centre of mass energy 14 TeV. In Figure CNMI and OSCT stand for the same as in Figure 6.5.*

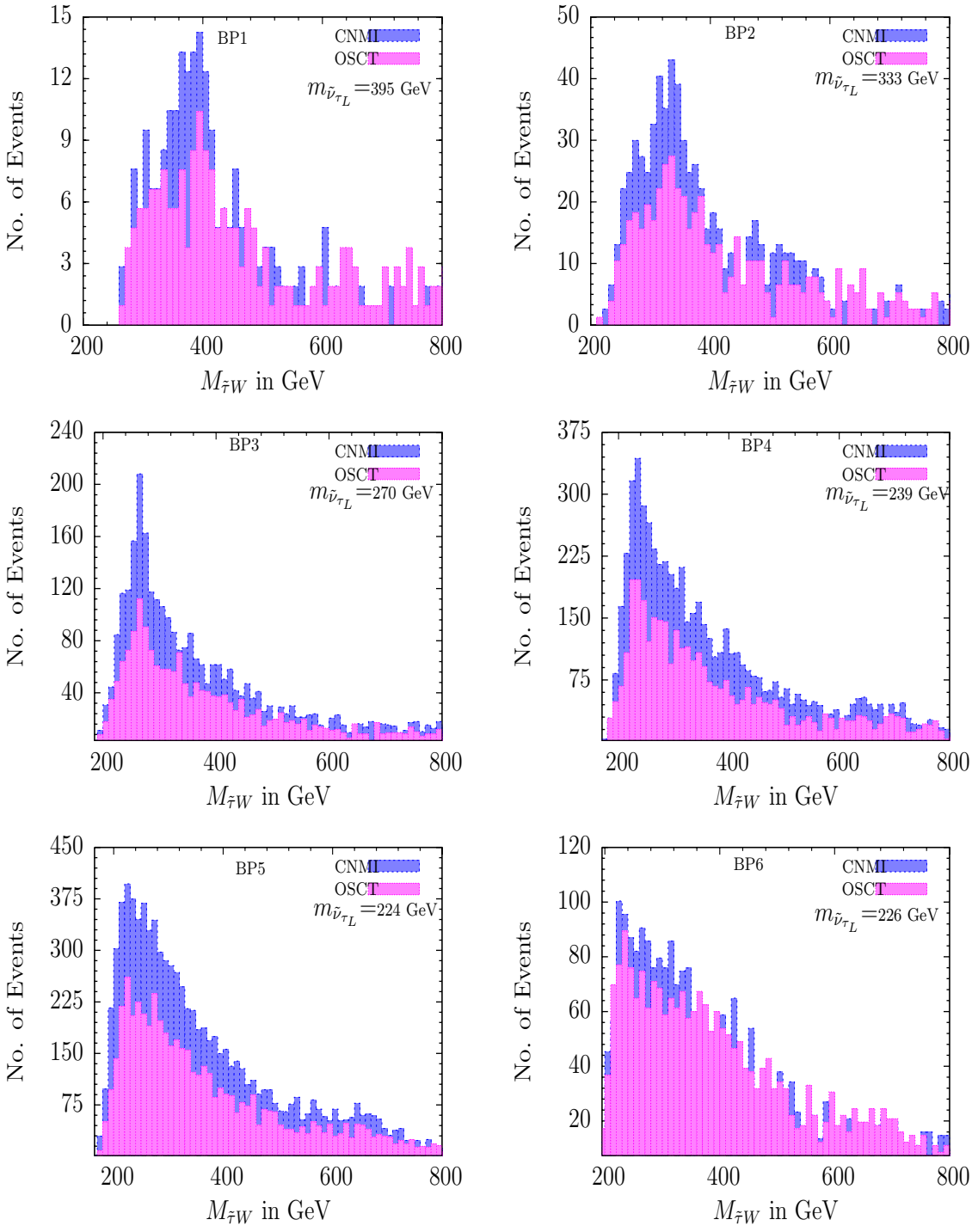

Figure 6.7: *The invariant mass ($M_{\tilde{\tau}W}$) distribution in $W + \tau_j + 2\tilde{\tau}$ (charged-track)+$\not{E}_T$+ X final state for all the benchmark points assuming tau identification efficiency (ϵ_τ) = 50% at an integrated luminosity of 100 fb^{-1} and centre of mass energy 14 TeV. In Figure CNMI and OSCT stand for the same as in Figure 6.5.*

	BP4		BP5		BP6	
	CNMI	OSCT	CNMI	OSCT	CNMI	OSCT
basic cuts	8634	5450	12519	8014	4013	3995
p_T+$\Sigma\|p_T\|$ cut	6145	3709	8654	5363	2560	2537
$\|M_{peak} - M_{\tilde{\tau}W}\| \leq 20GeV$	1218	689	1471	866	385	349

Table 6.5: *Number of signal events for the $W + \tau_j + 2\tilde{\tau}$ (charged-track)+$\not{E}_T + X$ final state, considering all SUSY processes, for BP4, BP5 and BP6 with E_{cm}=14 TeV at an integrated luminosity of 100 fb^{-1} assuming tau identification efficiency $\epsilon_\tau = 50\%$. In Table CNMI and OSCT stand for the same as in Table 6.2.*

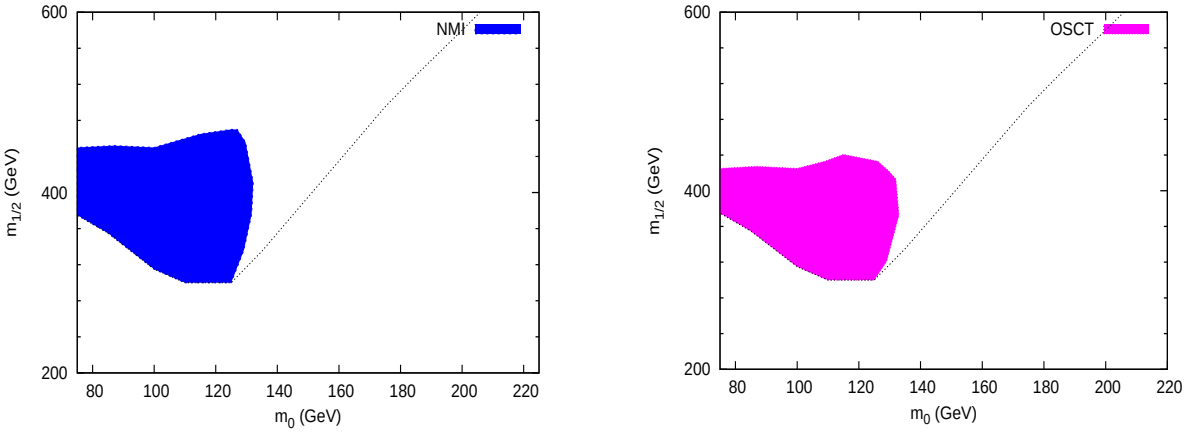

Figure 6.8: The region in the $m_0 - m_{1/2}$ plane (with $tan\beta = 30$ and $A_0 = 100$ GeV), where it is possible to reconstruct the left-chiral sneutrino at an integrated luminosity of 30 fb^{-1} and center-of-mass energy 14 TeV with more than 25 events in the vicinity of the peak. In the Figure blue (dark shade) region represents reconstruction of $m_{\tilde{\nu}_{\tau_L}}$ using only Neutralino Mass Information (NMI), while the pink region (light shade) stands for reconstruction of the same using Opposite Sign Charged Tracks (OSCT) for the $W + \tau_j + 2\tilde{\tau}$ (charged-track)+$\not{E}_T + X$ final state. The entire region above the dashed line indicates the scenario where one has a $\tilde{\nu}_R$-LSP and a $\tilde{\tau}$-NLSP.

LHC center-of-mass energy $E_{cm} = 14\ TeV$ at two different luminosities have also been shown.

A thorough scan over the $m_0 - m_{1/2}$ plane has been performed in this study, which shows that a significant region of the mSUGRA parameter space can be probed at the LHC with sufficient number of events at an integrated luminosity of 30 fb^{-1} with $E_{cm} = 14\ TeV$ using our prescribed methods.

To conclude, the MSSM with a right-chiral sneutrino superfield for each generation is a worthful possibility to look for at the LHC. It not only offers a distinct SUSY signal in the form of a pair of charged tracks of massive particles but also opens a new vista in the reconstruction of the superparticle masses.

Bibliography

[1] S. Biswas, Phys. Rev. D **82**, 075020 (2010) [arXiv:1002.4395 [hep-ph]].

[2] T. Sjostrand, S. Mrenna and P. Skands, JHEP **0605**, 026 (2006) [arXiv:hep-ph/0603175].

[3] H. L. Lai *et al.* [CTEQ Collaboration], Eur. Phys. J. C **12**, 375 (2000) [arXiv:hep-ph/9903282].

[4] C. Amsler *et al.* [Particle Data Group], Phys. Lett. B **667**, 1 (2008).

[5] D. L. Rainwater, D. Zeppenfeld and K. Hagiwara, Phys. Rev. D **59**, 014037 (1998) [arXiv:hep-ph/9808468].

[6] S. Asai *et al.*, Eur. Phys. J. C **32S2**, 19 (2004) [arXiv:hep-ph/0402254].

[7] The CMS Collaboration, CMS-TDR-8.1, CERN/LHCC 2006-001

[8] A. Djouadi, J. L. Kneur and G. Moultaka, Comput. Phys. Commun. **176**, 426 (2007) [arXiv:hep-ph/0211331].

Chapter 7

Signatures of supersymmetry with non-universal Higgs mass at the Large Hadron Collider

7.1 Introduction

In the foregoing chapters, we have made use of the tau lepton for studying features of a particular SUSY scenario, i.e., SUSY with a long-lived stau. We now use the tau to extract signatures of another kind of model, namely, one where the Higgs boson masses have their origins in SUSY breaking parameters at high scale, which are different from those for the other scalars. The simplistic logic behind this is that the assumption of universality of high scale parameters (which is the case in an mSUGRA scenario) doesn't follow from any known symmetry principle. For example, gaugino mass non-universality can occur in supersymmetric Grand Unified Theories (SUSY-GUT) [1] with non-trivial gauge kinetic functions [2, 3]. Non-universality in the scalar sector can also be motivated from the $SO(10)$ D-terms [4], apart from the phenomenological requirement to keep CP-violation and flavour changing neutral currents (FCNC) under control [5]. Moreover, in SUSY-GUT theories based on the $SO(10)$ group, sfermions and Higgs fields belong to different representations and can therefore arise from independent high-scale mass parameters.

In view of this, one can, within the SUGRA scenario itself, expect the Higgs

mass parameters to arise from high scale value(s) different from m_0. Thus models with non-universal Higgs mass (NUHM) are of considerable interest, and their viability in respect of both collider signals and issues such as the dark matter content of the universe has been recently investigated [6–8].

One can incorporate the non-universality in the Higgs sector in two different ways. In the first kind, one can have both of the soft Higgs mass parameters originating in a high-scale value $m_0^{'}$ which is different from m_0, the universal high-scale mass for squarks and sleptons. In other words, one can postulate $m_{H_u}^2 = m_{H_d}^2 = {m_0^{'}}^2 \neq m_0^2$ [7]. On the other hand, it is also possible to have H_u and H_d evolve down from *two different high-scale inputs*. In the later case, the high-scale SUSY parameters are given by:

$$m_{1/2}, m_0, m_{H_u}^2, m_{H_d}^2, A_0, \tan\beta \text{ and } sgn(\mu)$$

The split between the two Higgs squared masses at high scale introduces additional features in the running of various mass parameters down to the electroweak scale. In its most drastic manifestation, such a situation can give rise to the sneutrino ($\tilde{\nu}$) as the lightest superpartner of standard model particles. Since a sneutrino dark matter candidate is disfavoured from available results on direct search, one then has to postulate the sneutrino(s) to be the next-to-lightest supersymmetric particle(s) (NLSP), and, for example, gravitino as the lightest supersymmetric particle (LSP). With this achieved, most of the allowed region of the NUHM parameter space leads to the right amount of relic density [9].

In this work, we propose using the LHC data to distinguish those cases where the superparticle spectrum in NUHM is most strikingly different from the usual mSUGRA scenario [10]. As we shall see in the next section, this happens for a large negative high-scale value of ${m_{H_u}}^2 - {m_{H_d}}^2$. It not only leads to a large splitting between the left and right chiral sleptons, but also leads to the lighter slepton mass eigenstate of any flavour being dominated by the left chiral component.

This feature, marking a drastic departure from the expectations in mSUGRA, can be reflected in the signals of staus through the polarisation of the taus that are produced either in their decay or in association with them [11–13]. In addition, the above hierarchy between left-and right-chiral sleptons can be probed by studying the spin correlation of jets and leptons produced in cascade decays of squarks. This correlation, as we shall see, affects the angular distribution of the lepton in $\chi_2^0 \to l^{\pm}\tilde{l}^{\mp}$, manifested through certain measurable kinematical variables [14–16].

To explain further, the large splitting between the left-and right-chiral sleptons sometimes yields a hierarchy where the right-chiral ones become much heavier than not only the left-chiral ones but also the low-lying chargino/ second lightest neutralinos over a large region of the NUHM parameter space. Thus they are hardly produced in collider experiments. At the same time, the (dominantly) left-

chiral stau and the corresponding sneutrino being considerably lighter — even lighter than the lightest neutralino— the taus produced in their association are dominantly left-handed. This is due to the fact that the gauge couplings involved in the decay are chirality conserving, so long as one has large gaugino components in the lighter neutralinos and charginos.

The consequences that we focus on are two-fold. First, one notices the practically ubiquitous τ in SUSY signals. Secondly, the signals often bear the stamp of left-polarized τ^-'s, in the products of their one-prong decay. With this in view, we analyse the polarisation of the taus produced in the SUSY cascades in the same-sign di-tau ($SSD\tau$) final states associated with hard jets and missing transverse energy ($\not{E}_T$). We show how this leads to noticeable differences between the NUHM and mSUGRA spectra in the LHC environment.

Furthermore, we study the polarisation dependence of the angular distribution of the lepton produced in χ_2^0 decay, which shows up in the charge asymmetry of the jet-lepton invariant mass (m_{jl}) distribution discussed in detail later. Though the effect tends to wash out due to the presence of antisquark decay, nevertheless it can be observed at the LHC as more squarks are produced than antisquarks.

This chapter is organized as follows. We discuss various aspects of the model under consideration in the following section and identify the region of the $m_0 - m_{1/2}$ parameter space where the lighter stau is dominantly left-chiral. As we shall see below, this is achieved for large negative values of S. We choose a few benchmark points for our collider simulation. Tau-polarisation and its implications are discussed in section 7.3, while the analysis revealing the chirality information on sleptons of the first two families is outlined in section 7.4. The numerical results for each of the two analyses mentioned above, based on a simulation for the 14 TeV run of the LHC, is presented in section 7.5. We summarise and conclude in section 7.6.

7.2 Features of the NUHM scenario and our choice of benchmark points

7.2.1 Salient features of the scenario

We consider the general case of NUHM, having a two parameter extension of the mSUGRA scenario, in which the soft SUSY breaking masses $m_{H_u}^2$ and $m_{H_d}^2$ are inputs at high scale. The most important thing to remember here is that the renormalisation group evolution (RGE) of soft scalar masses is in general modified by the presence of a non-zero boundary value of the quantity S, defined as [17]

$$S = m_{H_u}^2 - m_{H_d}^2 + Tr\left[\mathbf{m}_Q^2 - \mathbf{m}_L^2 - 2\mathbf{m}_U^2 + \mathbf{m}_D^2 + \mathbf{m}_E^2\right] \tag{7.1}$$

We assume universality in the sfermion masses, so that $S = m_{H_u}^2 - m_{H_d}^2$ is high scale boundary condition. The running of soft scalar masses of the third family squarks and sleptons are given at the one-loop level by [17]

$$\begin{aligned}
\frac{dm_{Q_3}^2}{dt} &= \frac{2}{16\pi^2}(-\frac{1}{15}g_1^2M_1^2 - 3g_2^2M_2^2 - \frac{16}{3}g_3^2M_3^2 + \frac{1}{10}g_1^2S \\
&\qquad + y_t^2X_t + y_b^2X_b) \qquad (7.2)\\
\frac{dm_{\tilde{t}_R}^2}{dt} &= \frac{2}{16\pi^2}(-\frac{16}{15}g_1^2M_1^2 - \frac{16}{3}g_3^2M_3^2 - \frac{2}{5}g_1^2S + 2y_t^2X_t) \qquad (7.3)\\
\frac{dm_{\tilde{b}_R}^2}{dt} &= \frac{2}{16\pi^2}(-\frac{4}{15}g_1^2M_1^2 - \frac{16}{3}g_3^2M_3^2 + \frac{1}{5}g_1^2S + 2y_b^2X_b) \qquad (7.4)\\
\frac{dm_{L_3}^2}{dt} &= \frac{2}{16\pi^2}(-\frac{3}{5}g_1^2M_1^2 - 3g_2^2M_2^2 - \frac{3}{10}g_1^2S + y_\tau^2X_\tau) \qquad (7.5)\\
\frac{dm_{\tilde{\tau}_R}^2}{dt} &= \frac{2}{16\pi^2}(-\frac{12}{5}g_1^2M_1^2 + \frac{3}{5}g_1^2S + 2y_\tau^2X_\tau) \qquad (7.6)
\end{aligned}$$

where the notations for squark, slepton and gaugino masses have their usual meaning, and $t = \log(Q)$, $y_{t,b,\tau}$ are the t, b and τ Yukawa couplings, and

$$\begin{aligned}
X_t &= m_{Q_3}^2 + m_{\tilde{t}_R}^2 + m_{H_u}^2 + A_t^2 \qquad (7.7)\\
X_b &= m_{Q_3}^2 + m_{\tilde{b}_R}^2 + m_{H_d}^2 + A_b^2 \qquad (7.8)\\
X_\tau &= m_{L_3}^2 + m_{\tilde{\tau}_R}^2 + m_{H_d}^2 + A_\tau^2 \qquad (7.9)
\end{aligned}$$

Mass parameters of the first two family scalars run in a similar manner, excepting that the Yukawa contributions are vanishingly small. The main difference in the SUSY particle spectrum with respect to an mSUGRA scenario is the non-vanishing boundary value of S. If this boundary value is large in magnitude, the effect on the spectrum at low scale is naturally a rather pronounced departure from mSUGRA. Since the contribution of the term containing S comes with different factors in the running of left-handed squarks (sleptons) and right-handed squarks (sleptons), due to different $U(1)$ hypercharge assignments, one can have large splitting in the left-right sector within each generation when $|S|$ is substantially large.

One can see from equation 7.5 and 7.6 that the effect of non-universal Higgs mass is rather pronounced in the slepton sector. The primary reason being that the running masses are not controlled by the strong sector. The most important difference it makes to the spectrum is that, for large negative values of S ($\mathcal{O}(\text{TeV})^2$)) [6,7], the left-chiral sleptons tend to become considerably lighter than their right-chiral counterparts. This is in striking contrast to both mSUGRA and gauge mediated SUSY breaking (GMSB). An immediate temptation that the phenomenologist faces, therefore, is to extract some signature of this 'chirality swap'

in the lightest sleptons at the LHC, which may put a distinctive stamp of NUHM on them. This, of course, has to be done with the help of leptons that are produced either in association with the low-lying sleptons or in their decays. Since the helicity of leptons of the first two families is difficult to measure in the collider environment, we feel that it is our best bet to latch on to the copious number of taus arising from SUSY cascades, and concentrate on those features of their decay products that tell us about their helicities.

As has been noted already, the above effect is seen for large negative S. Such values of S therefore become the benchmarks for testing the special features of NUHM, and it is likely that in such condition only its footprints are noticeable at the LHC. Thus we examine next the kinds of spectra ensuing from large negative S, and look for their observable signature.

A large negative S at high scale affects the running of the third family SU(2) doublet slepton (both the stau and the tau-sneutrino) masses in the same way as is done by their Yukawa couplings, thus bringing them down substantially at low energy. As a consequence, one can have both of them of the same order as, or lighter than, the lightest neutralino (χ_1^0). In the latter situation, the left-chiral tau-sneutrino is lighter than the corresponding stau due to the SU(2) breaking D-terms (for $\tan\beta > 1$) :

$$m^2_{\tilde{\tau}_L} = m^2_L - \cos(2\beta) m^2_Z (\frac{1}{2} - \sin^2\theta_W) \tag{7.10}$$

$$m^2_{\tilde{\nu}_\tau} = m^2_L + \cos(2\beta) m^2_Z \frac{1}{2} \tag{7.11}$$

In such cases, the tau-sneutrino has to be the NLSP, due to its unsuitability as a dark matter candidate as laid down by direct search results. A gravitino, for example, can be envisioned as the LSP and dark matter candidate in such cases. The lighter stau mass eigenstate can in principle also become the NLSP through mixing of the left and right chiral fields. However, this happens only in very restricted regions of the parameter space, as large mixing requires $\tan\beta$ to be on the higher side, a feature that is highly restricted in NUHM by the requirements of absence of tachyonic states as well as of electroweak symmetry breaking.

The role of S in the running of $m^2_{H_u}$ and $m^2_{H_d}$ is described by

$$\frac{dm^2_{H_u}}{dt} = \frac{2}{16\pi^2}(-\frac{3}{5}g_1^2 M_1^2 - 3g_2^2 M_2^2 + \frac{3}{10}g_1^2 S + 3f_t^2 X_t) \tag{7.12}$$

$$\frac{dm^2_{H_d}}{dt} = \frac{2}{16\pi^2}(-\frac{3}{5}g_1^2 M_1^2 - 3g_2^2 M_2^2 - \frac{3}{10}g_1^2 S + 3f_b^2 X_b + f_\tau^2 X_\tau) \tag{7.13}$$

One can see above that a negative S tends to partially cancel the effects of top quark Yukawa coupling in the running of $m^2_{H_u}$ and make it positive at low

energy. $m^2_{H_d}$, on the other hand, is routinely rendered positive at low scale due to the gauge interactions, and the effects of the term proportional to S often fails to make it negative as one comes down to the electroweak scale. Consequently, radiative electroweak symmetry breaking at the right energy requires a negative value of $m^2_{H_u}$ at high scale. Of course, one is led to have a sufficiently large magnitude of μ to ensure that $m^2_{H_u} + \mu^2$ remains positive at high energy.

7.2.2 The choice of benchmark points

As has been already explained, our purpose is to suggest some observations at the LHC, which will bring out the distinctive characteristics of the NUHM spectrum. Such distinction is most pronounced when the chiralities of the low-lying sleptons are reversed with respect to the corresponding cases in mSUGRA. This, we have found, is best achieved (and one is indeed optimistic about clear distinction) when S is large and negative ($\sim 10^6$ GeV^2). For smaller magnitudes of S ($\leq 10^5$ GeV^2), the $\tilde{\tau}_L$ component of $\tilde{\tau}_1$ decreases, and the collider signature of this scenario is relatively less distinct. With this in view, the region in the parameter space with more than 90% of $\tilde{\tau}_L$ in $\tilde{\tau}_1$ has been shown in Figure 7.1. This region offers the best hope for recognising NUHM if SUSY is detected at the LHC. We have accordingly chosen some benchmark points for the study reported in the subsequent sections. Out of the regions answering to our chosen criterion, we have selected points with three possible mass hierarchies:

$$m_{\tilde{\nu}_{\tau_L}} < m_{\chi_1^0} < m_{\tilde{\tau}_1}$$
$$m_{\tilde{\nu}_{\tau_L}} < m_{\tilde{\tau}_1} < m_{\chi_1^0}$$
$$m_{\chi_1^0} < m_{\tilde{\nu}_{\tau_L}} < m_{\tilde{\tau}_1}$$

Our benchmark points (BP) NUHM-1 - NUHM-3 (shown in Table 7.1) are taken from three regions of the parameter space, corresponding to each of the above hierarchies. The code SuSpect (version 2.41) [18] has been used for this purpose. Two-loop renormalisation group equations have been used for running the mass parameters down to low energy, with the default option (namely, $\sqrt{\tilde{t}_1 \tilde{t}_2}$) for the electroweak symmetry breaking scale. The spectra are consistent with low energy constraints [19, 20] such as those coming from $b \longrightarrow s\gamma$ and the muon anomalous magnetic moment, and also with those from LEP-2 limits, such as $m_{\chi_1^\pm} > 103.5$ GeV, $m_{\tilde{l}^\pm} > 98.8$ GeV and $m_h > 111$ GeV. Electroweak symmetry breaking in a consistent fashion has been taken as a necessary condition in the allowed parameter space. For the case with χ_1^0 LSP, the requirement of relic density consistent with the recent data has also been taken into account in choosing the benchmark point(s) [21].

We have obtained the mSUGRA BP's (see Table 7.2) for comparison with the NUHM points using the criterion based on similar event rates (within $\pm 30\%$

tolerance) in two different channels. For the case where the distinction between these two scenarios is done using tau-polarisation, we have compared the event rates in the same-sign ditau ($SSD\tau$) channel for choosing our mSUGRA points. For the analysis based upon lepton-charge asymmetry, the event rates in the opposite-sign same-flavour dilepton ($OSSFD\ell$) channel have been compared as a benchmarking criterion. All the three NUHM BP's have been used for the first case and for the second case, only NUHM-1 and NUHM-3 have been considered, as the hierarchies mentioned above are not relevant for analysis based on lepton-charge asymmetry. Thus, we have obtained mSUGRA-1 which corresponds to both NUHM-1 and NUHM-3 following the criterion mentioned above in the $SSD\tau$ channel and mSUGRA-3 corresponds to NUHM-3 in the $OSSFD\ell$ channel[1]. The benchmark point mSUGRA-2 corresponds to NUHM-2 having similar rates in the $SSD\tau$ channel. Two of the chosen mSUGRA points (mSUGRA-1 and mSUGRA-2) are approximately compatible with the observed relic density. One has to further assume in the case of $\tilde{\nu}_\tau$ -NLSP and gravitino ($\tilde{G}$) LSP that the $\tilde{\nu}_\tau \rightarrow \nu_\tau \tilde{G}$ decay lifetime is less than the age of the Universe. The gravitino mass has to have accordingly allowed values, as dictated by the hidden sector of the overseeing theory [22].

7.3 Tau polarisation

The signal of left-polarised tau is expected to be a very good discriminator between scenarios with NUHM and its universal counter part. Tau lepton plays a crucial role in the search for new physics. In particular, information on the chirality of a tau can be extracted following some standard procedures. The fact that the tau decays within the detector, in contrast to the electron or the muon, enables us to know about its chirality from the kinematic distribution of the decay products. In the massless limit where the tau is boosted in the laboratory frame, tau decay products are nearly collinear with the parent tau. In this limit, hadronic tau decays produce narrow jets of low multiplicity, to be identified as tau-jets. From the angle of polarisation studies, it is most cost-effective to work with the one-prong hadronic decay modes of the tau, which comprise 80% of its hadronic decay width and about 50% of its total decay width. The main channels here are:

$$\begin{aligned} \tau^- &\rightarrow \pi^- \nu_\tau \\ \tau^- &\rightarrow (\rho^- \nu_\tau) \quad \rightarrow \pi^- \pi^0 \nu_\tau \\ \tau^- &\rightarrow (a_1^- \nu_\tau) \quad \rightarrow \pi^- \pi^0 \pi^0 \nu_\tau \end{aligned}$$

From here on we shall often denote both the ρ^- and the a_1^- by v.

[1]However, we have compared NUHM-1 with mSUGRA-1 for the study of lepton-charge asymmetry as well.

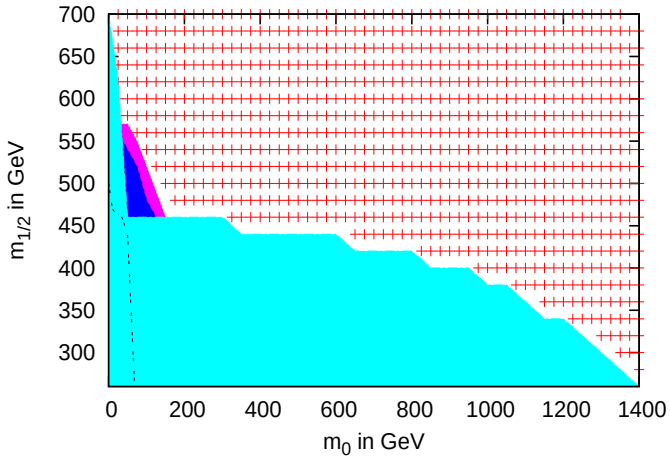

Figure 7.1: *The allowed region for NUHM in the $m_0 - m_{1/2}$ plane for $tan\beta = 10$, $m^2_{H_u} = -1.0 \times 10^6\ \mathrm{GeV}^2$, $m^2_{H_d} = 2.0 \times 10^6\ \mathrm{GeV}^2$ and $A_0 = 0$. The light blue region is disallowed due to tachyonic stau and/or non-compliance of electroweak symmetry breaking conditions. The region on the left of the dashed line is also disallowed by constraints from $b \to s\gamma$. In the region marked by +, one has $m_{\chi^0_1} < m_{\tilde{\nu}_{\tau_L}} < m_{\tilde{\tau}_1}$, whereas the pink region corresponds to $m_{\tilde{\nu}_{\tau_L}} < m_{\chi^0_1} < m_{\tilde{\tau}_1}$. The dark blue region has the hierarchy $m_{\tilde{\nu}_{\tau_L}} < m_{\tilde{\tau}_1} < m_{\chi^0_1}$. The lighter stau has 90% or more of $\tilde{\tau}_L$ over the entire allowed region.*

Benchmark points	**NUHM-1**	**NUHM-2**	**NUHM-3**
Input parameters	$m_0 = 300$ $m_{1/2} = 300$ $\tan\beta = 10$	$m_0 = 80$ $m_{1/2} = 460$ $\tan\beta = 10$	$m_0 = 300$ $m_{1/2} = 280$ $\tan\beta = 7$
$m_{\tilde{e_L}}, m_{\tilde{\mu}_L}$	170	154	154
$m_{\tilde{e_R}}, m_{\tilde{\mu}_R}$	552	437	551
$m_{\tilde{\nu}_{e_L}}, m_{\tilde{\nu}_{\mu_L}}$	151	132	133
$m_{\tilde{\nu}_{\tau_L}}$	119	106	116
$m_{\tilde{\tau}_1}$	139	124	137
$m_{\tilde{\tau}_2}$	537	424	543
$m_{\chi_1^0}$	120	187	112
$m_{\chi_2^0}$	234	361	216
$m_{\chi_3^0}$	939	982	950
$m_{\chi_4^0}$	944	987	954
$m_{\chi_1^\pm}$	234	361	217
$m_{\chi_2^\pm}$	944	987	955
$m_{\tilde{g}}$	734	1066	691
$m_{\tilde{t}_1}$	645	826	618
$m_{\tilde{t}_2}$	814	1018	791
$m_{\tilde{d}_L}$	741	986	706
$m_{\tilde{d}_R}$	742	962	710
$m_{\tilde{u}_L}$	737	984	701
$m_{\tilde{u}_R}$	591	879	549
m_{h^0}	111	114	112

Table 7.1: *Proposed benchmark points for the study of the NUHM scenario with* $m^2_{H_u} = -1.10 \times 10^6$ GeV^2 *and* $m^2_{H_d} = 2.78 \times 10^6$ GeV^2. *All the mass parameters are given in units of GeV. The value of* A_0 *is taken to be zero and sign of* μ *to be positive for all of the benchmark points.*

Benchmark points	**mSUGRA-1**	**mSUGRA-2**	**mSUGRA-3**
Input parameters	$m_0 = 80$ $m_{1/2} = 250$ $\tan\beta = 40$	$m_0 = 350$ $m_{1/2} = 300$ $\tan\beta = 40$	$m_0 = 300$ $m_{1/2} = 350$ $\tan\beta = 10$
$m_{\tilde{e_L}}, m_{\tilde{\mu}_L}$	389	362	284
$m_{\tilde{e_R}}, m_{\tilde{\mu}_R}$	363	322	202
$m_{\tilde{\nu}_{e_L}}, m_{\tilde{\nu}_{\mu_L}}$	381	354	271
$m_{\tilde{\nu}_{\tau_L}}$	353	329	269
$m_{\tilde{\tau}_1}$	283	238	197
$m_{\tilde{\tau}_2}$	377	358	285
$m_{\chi_1^0}$	99	120	140
$m_{\chi_2^0}$	183	224	261
$m_{\chi_3^0}$	333	392	455
$m_{\chi_4^0}$	352	409	473
$m_{\chi_1^\pm}$	182	224	262
$m_{\chi_2^\pm}$	353	410	473
$m_{\tilde{g}}$	623	726	831
$m_{\tilde{t}_1}$	464	525	573
$m_{\tilde{t}_2}$	615	683	764
$m_{\tilde{d}_L}$	654	720	776
$m_{\tilde{d}_R}$	636	697	745
$m_{\tilde{u}_L}$	649	716	771
$m_{\tilde{u}_R}$	636	698	747
m_{h^0}	111	112	111

Table 7.2: *mSUGRA benchmark points obtained based on similar cross-section in the same-sign ditau channel (mSUGRA-1 and mSUGRA-2) and in the opposite-sign same-flavour dilepton channel (mSUGRA-3). All the mass parameters are given in units of GeV. The value of A_0 is taken to be zero and sign of μ to be positive for all of the benchmark points.*

The first step in the extraction of polarisation information is to express some differential decay distributions of the τ^- in the laboratory frame. Let the polarisation information be denoted by P_τ, where $P_\tau = \pm 1$ correspond to taus with positive and negative helicity. Next, it is worthwhile to examine the laboratory frame variable z, defined as $z = E_{\pi,v}/E_\tau$, the fraction of the tau energy carried by the product meson. This variable can be related to θ, the angle between the direction of motion of the outgoing π^- or v^- and the axis of polarisation of the tau, which is taken to be along the direction of the tau momentum in the laboratory frame. In the limit $E_\tau >> m_\tau$,

$$\cos\theta = \frac{2z - 1 - c^2}{1 - c^2} \tag{7.14}$$

where $c = m_v/m_\tau$. The expression for the case where the tau decays to the pion and a ν_τ is obtained by setting $m_v = 0$ above.

The decay distributions in z for a τ^- in the laboratory frame are given by [23]

$$\frac{1}{\Gamma_\pi}\frac{d\Gamma_\pi}{dz} = [1 + P_\tau(2z - 1)] \tag{7.15}$$

$$\frac{1}{\Gamma_v}\frac{d\Gamma_{v_T}}{dz} = \frac{m_\tau^2 m_v^2}{(m_\tau^2 - m_v^2)(m_\tau^2 + 2m_v^2)}[\frac{m_\tau^2}{m_v^2}\sin^2\omega + 1 + \cos^2\omega + P_\tau\cos\theta \\ (\frac{m_\tau^2}{m_v^2}\sin^2\omega - \frac{m_\tau}{m_v}\sin 2\omega\tan\theta - 1 - \cos^2\omega)] \tag{7.16}$$

$$\frac{1}{\Gamma_v}\frac{d\Gamma_{v_L}}{dz} = \frac{m_\tau^2 m_v^2}{(m_\tau^2 - m_v^2)(m_\tau^2 + 2m_v^2)}[\frac{m_\tau^2}{m_v^2}\cos^2\omega + \sin^2\omega + P_\tau\cos\theta \\ (\frac{m_\tau^2}{m_v^2}\cos^2\omega + \frac{m_\tau}{m_v}\sin 2\omega\tan\theta - \sin^2\omega)] \tag{7.17}$$

where

$$\cos\omega = \frac{(m_\tau^2 - m_v^2) + (m_\tau^2 + m_v^2)\cos\theta}{(m_\tau^2 + m_v^2) + (m_\tau^2 - m_v^2)\cos\theta} \tag{7.18}$$

In the experiment, one looks for hard jets from the tau, which corresponds to large values of z. A close inspection of equations (7.15-7.17) shows that the energy distribution of the decay products from the decay of τ_L^- ($P_\tau = -1$) are in significant contrast to that from τ_R^- ($P_\tau = +1$) . When $P_\tau = +1$, the hard τ-jet consist largely of either a single pion or longitudinally polarised vector mesons (v_L). For $P_\tau = -1$, on the contrary, the hard τ-jet mostly comprises transversely polarised vector mesons only (v_T). This conclusion becomes almost self-evident in, for example, the extreme case of collinearity, with $\cos\omega = 1$ and $\sin\omega = 0$.

It should, however, be remembered that the quantity z is not amenable to actual measurement in the detector, and therefore the distinctions pointed out above are still somewhat theoretical in nature. It is therefore necessary to translate the distinction in terms of measurable quantities. The energy distribution among the pions arising from the decay of the ρ^- and a_1^- offer such a variable. It is the variable $R = E_\pi/E_\rho$, the fraction of the energy of v carried by the charged pion. For the case where the ρ^- is produced in τ^- decay, the distribution in R in the laboratory frame is given by [23]

$$\frac{d\Gamma(\rho_T \to 2\pi)}{dR} \sim 2R(1-R) - \frac{2m_\pi^2}{m_\rho^2} \tag{7.19}$$

$$\frac{d\Gamma(\rho_L \to 2\pi)}{dR} \sim (2R-1)^2 \tag{7.20}$$

The distribution for a_1^- is more complicated but has similar qualitative features. The reader is referred to [24] for the detailed expressions. The broad indication is that transversely polarised vector mesons favour even sharing of its momentum among the decay pions whereas longitudinally polarised ones favour uneven sharing of momentum among its decay products. Since the polarisation of the parent tau governs the level of polarisation of either type in the vector mesons v, the distribution in the variable R therefore is a reflection of the helicity of the tau whose signal one is concerned with.

Obviously, one always has $R = 1$ when the tau decays as $\tau^- \to \pi^-\nu_\tau$. What one must utilise, therefore, is the difference in R-distributions between the cases with v_T and v_L. When the decaying tau has p_τ = +1, one should mostly have v_L in the hard jets, in addition to the inconsequential single pions, giving its characteristic distribution on R. A contrast can be seen in the decay of a tau with p_τ = -1, where the hard tau-jets can be expected to be largely v_T, with a different distribution in R.

Hence, one can use the charged-pion spectra arising from the two-stage decays

$$\begin{aligned} \tau^- \to (\rho^-\nu_\tau) &\to \pi^-\pi^0\nu_\tau \\ \tau^- \to (a_1^-\nu_\tau) &\to \pi^-\pi^0\pi^0\nu_\tau \end{aligned}$$

to probe the polarisation of the parent tau. We utilise this possibility to identify the NUHM spectrum in cases the low-lying stau is of left chirality, which attaches similar chirality (same as helicity at high energy) to the taus either arising from stau-decay or produced in association with it. With this in view, we have selected tau-jets in our simulation with $p_T > 40GeV$ and $|\eta| < 2.5$, assuming a tau jet identification efficiency of 50%, with a fake tau jet rejection factor of 100 [12].

7.4 Lepton charge asymmetry

Another discriminator which is sensitive to the mass hierarchy between the right- and left-chiral sleptons is the charge asymmetry in the jet-lepton invariant mass distribution [14–16]. In the NUHM scenario (with large negative S), the lighter slepton mass eigenstate is dominated by the left-chiral component ($\tilde{l}_1 \sim \tilde{l}_L$). Hence, for $m_{\tilde{l}_1} < m_{\chi_2^0}$ (a criterion mostly satisfied by the 'extreme' NUHM scenario considered by us), the leptons produced in the decay of χ_2^0 will be mostly left-handed. In the usual mSUGRA scenario, on the other hand, one expects the leptons to be mostly right-handed as the lighter slepton mass eigenstate is dominantly right-chiral ($\tilde{l}_1 \sim \tilde{l}_R$) and the decay proceeds via the Bino component of χ_2^0.

This feature can be exploited to unmask NUHM by studying the charge asymmetry in the lepton-jet invariant mass (m_{jl_1}) distribution produced in the squark decay chains, where l_1 stands for the lepton reproduced in χ_2^0 decay. We shall consider sleptons of the first two generations only, for which left-right mixing is negligible, and the coupling of the leptons to the Higgsino components of a neutralino is also very small.

In this section we describe the spin correlation in the following decay chain

$$\tilde{q_L} \rightarrow q\chi_2^0 \rightarrow q l_1^{\pm} \tilde{l^{\mp}} \rightarrow q l_1^{\pm} l_2^{\mp} \chi_1^0 \tag{7.21}$$

where l_2 denotes the lepton produced in the subsequent step of the cascade. Due to the chiral structure of the squark-quark-neutralino coupling, the quark produced in the squark decay will be left-handed in the massless limit. The χ_2^0 produced in $\tilde{q}_L$ decay is also polarized having the same helicity as that of the quark as they are produced from the decay of a scalar.

In the rest frame of the squark produced in the initial hard scattering, a negatively charged lepton produced in the subsequent decay of the χ_2^0 will appear back-to-back or in the same direction as that of the quark depending on whether the slepton is left-chiral or right-chiral[2]. Exactly the opposite directional preferences hold for a (positively charged) antilepton vis-a-vis the quark produced in the chain. Therefore, we expect an asymmetry between the distributions $m_{jl_1^-}$ and $m_{jl_1^+}$. This can be utilised to define the following asymmetry parameter:

$$A_i = \frac{N_i(m_{jl_1^+}) - N_i(m_{jl_1^-})}{N_i(m_{jl_1^+}) + N_i(m_{jl_1^-})} \tag{7.22}$$

where i stands for the *ith* bin. A measurement of A_i should thus yield information on the chirality of the low-lying slepton produced in the chain.

[2]The other inputs that go into this argument are (a) The χ_2^0 produced in squark decay is sufficiently boosted, and (b) the χ_2^0 decays largely in the s-wave.

However, there are some experimental difficulties involved in the measurement of such an asymmetry–

1. In the decay of a $\tilde{q}_L^*$, the asymmetry in the lepton-jet invariant mass distribution has a sign opposite to that of the corresponding $\tilde{q}_L$. This is because the left antisquark decays via gaugino coupling into a right-handed antiquark. Since jets initiated by a quark or an antiquark are indistinguishable, it is impossible to disentangle the squark and antisquark production channels. However, the LHC is a pp machine where more squarks are produced than antisqaurks, a significant 'net' charge asymmetry in the m_{jl_1} distribution can finally survive. All one needs in order to measure this charge asymmetry is a substantial excess in the production of $\tilde{q}^{(*)}\tilde{g}$ and $\tilde{q}^{(*)}\tilde{q}^{(*)}$ over pairs containing squarks and antisquarks, and also gluino pairs.
2. In an experiment, it is not always possible to distinguish between the lepton (l_1) out of a χ_2^0 and the lepton (l_2) coming from slepton decay. We have taken the invariant mass distribution using the harder of the two leptons, a role in which l_1 fits in most of the time.

In NUHM, one expects negative charge asymmetries, whereas in the usual mSUGRA scenario they are expected to be positive, especially in the high invariant mass bins. However, in mSUGRA, depending on the mass hierarchy, the leptons produced in χ_2^0 decay can also be dominantly left-handed if $m_{\tilde{l}_1} < m_{\tilde{l}_2} < m_{\chi_2^0}$, as the diagonal component ($(U_N)_{22}$) of the neutralino mixing matrix wins over $(U_N)_{21}$. In that case, one would expect a dip in the asymmetry distribution at a lower value of m_{jl} and a peaking behaviour at the higher end. This is expected because the splitting between $m_{\chi_2^0}$ and $\tilde{l}_L$ is smaller than that between $m_{\chi_2^0}$ and $\tilde{l}_R$. One can use this feature to separate an mSUGRA-type scenario.

7.5 Collider simulation and numerical results

We have simulated events for $\sqrt{s}$ = 14 TeV, including initial-and final-state radiation, multiple scattering etc. We have used parton distribution functions CTEQL6L1 [25] for our analysis, with the renormalisation and factorisation scales set at the average mass of the final state particles.

7.5.1 Simulation strategy: ditau final states

To study the polarisation of the tau in SUSY cascade for both NUHM and mSUGRA scenario we have used the code TAUOLA (version 2.9) [26] interfaced with the event generator PYTHIA (version 6.4.16) [27]. The spectrum has been generated using SuSpect (version 2.41) [18]. TAUOLA has been suitably modified to incorporate the probability of producing left-or right-handed tau in the decay of SUSY

particles. For cases where the $\tilde{\nu_\tau}$ and/or the $\tilde{\tau}$ is lighter than the lightest neutralino, decay branching fractions of the lightest neutralino have been calculated using SDECAY (version 1.3b) [28] and fed into Pythia. The finite detector resolutions have been taken into account following the specifications listed in section 4.3.3.

The final state that we have considered is a pair of same-sign ditaus (SSDτ), together with at least three hard central jets and large missing E_T. Same-sign ditaus are preferred because they are less beset with SM backgrounds. We consider events where the taus have one-prong hadronic decays.

The following cuts have been imposed on each event–

- $p_T > 40$ GeV, $|\eta| < 2.5$ for each tau jet.
- $p_T > 100$, 100, 50 GeV, $|\eta| < 2.5$ for the three associated jets, in decreasing order of hardness.
- $\not{E}_T > 150$ GeV.

It should be reiterated that our main purpose is to obtain the observable difference between the NUHM scenario under consideration and an mSUGRA scenario. Situations in mSUGRA leading to tau-rich final states are most likely to fake NUHM phenomenology. Therefore, we have followed the criteria already mentioned in section 7.2.2, and isolated the regions where the total rate of $SSD\tau+ \geq 3\ jets + \not{E}_T$ is within $\pm$30% of the rate predicted for corresponding NUHM benchmark point.

7.5.2 Simulation strategy: lepton charge asymmetry

The charge asymmetry in the lepton-jet invariant mass distribution has been studied using the event generator HERWIG (version 6.5) [29] which takes into account the spin correlation in SUSY cascades. Spectra have been generated using ISAJET (version 7.78) [30] and the input parameters have been tuned in such a way that the spectrum generated is similar to that produced by SuSpect. A fast detector simulation has been done using AcerDET (version 1.0) [31] for reconstructing the isolated leptons, jets and $\not{E}_T$, which also takes into account the finite detector resolution of the visible momenta.

The final state under consideration is consists of a pair of isolated leptons of opposite charge and same flavour (OSSF) with more than three jets and missing E_T, i.e., $e^+e^- + \mu^+\mu^- + \geq 3\ jets\ + \not{E}_T$.

The preselection cuts [32,33] imposed in this case are the following–

- $p_{T_{l_1}} > 20$ GeV and $p_{T_{l_2}} > 10$ GeV, $|\eta| < 2.5$ for the two leptons.
- $p_T > 100$, 50, 50 GeV, $|\eta| < 2.5$ for the three associated jets, in decreasing order of hardness.

- $M_{eff} > 600$ GeV where, $M_{eff} = \not{E}_T + \Sigma|\vec{p}_T|$
  where, the summation is taken over all visible particles.
- $\not{E}_T > 0.2 M_{eff}$

The SUSY backgrounds come mainly from two independent $\chi_1^\pm$ decays. One can eliminate this by taking the flavour subtracted combination $e^+e^- + \mu^+\mu^- - e^\pm\mu^\mp$ and this cancels out the background contribution from the charginos up to statistical fluctuations. The Standard Model background, already small after imposing the above cuts, undergo further suppression in this process [33].

The leptons are combined with each of the two hardest jets and, for identifying the desired decay chain, the combination for which the jl^+l^- invariant mass is smaller has been selected . The $m_{jl^\pm}$ distribution for this subsample, for both the hard and soft lepton have been calculated. Depending on the mass splitting between the neutralino and slepton one of these leptons will be dominated by the 'correct' lepton, i.e., the one adjacent to the quark in the decay chain and will give the desired charge asymmetry in the jet-lepton invariant mass distribution.

7.5.3 Numerical results

Ditau final states:

We first present the numerical results of our analysis making use of the polarisation properties of the tau. In Table 7.3, we have tabulated the event rates for all the NUHM and the potentially faking mSUGRA points for the $SSD\tau$-channel. Event rates have been predicted for an integrated luminosity of 100 fb^{-1}. After applying all the cuts to suppress the SM background, one has similar event rates for both the NUHM and corresponding mSUGRA points, which is not surprising because we have identified the mSUGRA points following the criterion of similar event rate.

NUHM-1	**NUHM-2**	**NUHM-3**	**mSUGRA-1**	**mSUGRA-2**
31	51	28	41	46

Table 7.3: *Number of events in the $SSD\tau$ channel at an integrated luminosity of* 100 fb^{-1} *after applying the cuts listed in section 7.5.1, in addition to a cut on the R variable ($R >$ 0.2) for all of our benchmark points .*

For the benchmark point NUHM-1, $\tilde{\nu}_{\tau_L}$ is the LSP, and the lighter $\tilde{\tau}_1$ is dominantly left-chiral. Taus are mainly produced in the decay of $\chi_2^0 \to \tau\tilde{\tau}$(20.5%), $\chi_1^\pm \to \tau\tilde{\nu}_{\tau_L}$(26.5%) and $\tilde{\tau} \to \tau\chi_1^0$(100%) and therefore they are mostly left-handed.

The contributions from χ_3^0, χ_4^0, $\chi_2^\pm$ and $\tilde{\tau}_2$ are negligible as they are heavier in the spectrum. For NUHM-2 we similarly have lighter stau mass eigenstate dominated by the left-chiral component but here the mass hierarchy between the $\tilde{\tau}_1$ and the χ_1^0 is opposite to that of NUHM-1, i.e. $m_{\tilde{\tau}} < m_{\chi_1^0}$. At this benchmark point, χ_1^0 decays into $\tilde{l}l$ pair as well as $\tilde{\nu}\nu$ pair including the third generation. The mass difference between the lighter stau and tau-sneutrino is less than m_W, hence the decay proceed mainly via the two body decay mode $\tilde{\tau}_1^\pm \to \tilde{\nu}_\tau^* \pi^\pm$ and the three body decay $\tilde{\tau}_1^\pm \to \tilde{\nu}_\tau^{(*)} l^\pm \nu^{(-)}$. However, final states with higher pion multiplicities also have non-zero branching fractions, but we have not taken into account these modes, as they do not change our conclusion. In NUHM-3, the LSP is the lightest neutralino, however we still have a light enough $\tilde{\nu}_{\tau_L}$. The lighter $\tilde{\tau}_1$ is, of course, dominantly left-chiral here. The taus produced in SUSY cascade therefore are mostly left-chiral for all the NUHM points. The corresponding R-distributions (taking into account the SM contributions) for the respective benchmark points have been shown in Figure 7.2. Thus the distinction criterion set down by us is seen to survive the washouts caused by various extraneous SUSY cascades.

	NUHM-1	**NUHM-2**	**NUHM-3**	**mSUGRA-1**	**mSUGRA-2**
$\mathcal{O}_1(R < 0.8)$	0.77	0.77	0.76	0.71	0.72
$\mathcal{O}_2(R > 0.8)$	0.23	0.23	0.24	0.29	0.28
$r = \frac{\mathcal{O}_1(R<0.8)}{\mathcal{O}_2(R>0.8)}$	3.35	3.35	3.17	2.45	2.57

Table 7.4: *The ratio r for NUHM and corresponding mSUGRA scenario.*

In the corresponding mSUGRA benchmark points (mSUGRA-1 and mSUGRA-2), the lighter stau is dominantly right-chiral. However both the stau are heavier than the second lightest neutralino and lightest chargino. Taus are produced mainly via the decay of W and Z produced in the decay of $\chi_{3,4}^0 \to (\chi_1^\pm W^\mp), (\chi_2^0 h/Z)$, $\chi_2^\pm \to (\chi_{1,2}^0 W^\pm), (\chi_1^\pm h/Z)$ and $\chi_1^\pm \to \chi_1^0 W^\pm$. Hence the contributions to $SSD\tau$ channel come from two same sign W-decay produced in SUSY cascade or one from W-decay and one in Z decay, when one of the two tau out of a Z-decay is identified. Therefore, taus are mostly left-handed, with some right-handed admixtures. This shows up in the R-distribution for the corresponding mSUGRA points with a slight departure from that of the NUHM points.

Designating the total fraction of events for $0.2 < R < 0.8$ and $R > 0.8$ by $\mathcal{O}_1$ and $\mathcal{O}_2$ respectively, we find that the ratio $r = \mathcal{O}_1/\mathcal{O}_2$ is a rather effective discriminator between NUHM and a corresponding mSUGRA scenario yielding a similar number of same-sign ditau events. The values of this ratio for all the cases are listed in Table 7.4. For the NUHM points, this ratio turn out to be con-

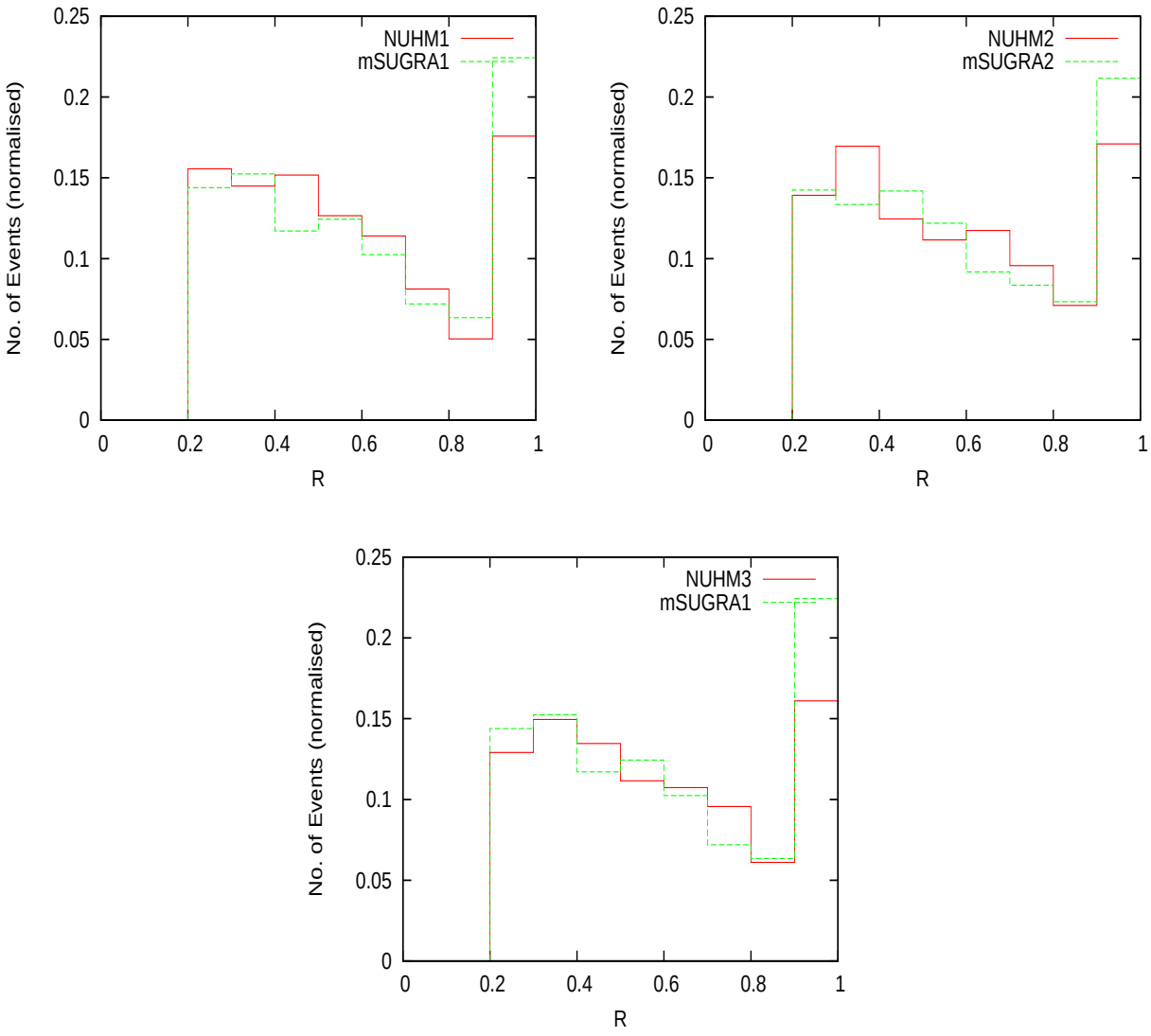

Figure 7.2: *R distribution (defined as $R = E_{\pi^-}/E_{\tau_j}$) for NUHM scenarios and corresponding mSUGRA points. A cut $R > 0.2$ has been applied in each of these distribution.*

sistently larger than the corresponding mSUGRA points, which is expected from the R-distribution given in Figure 7.2.

Lepton charge asymmetry:

The results of charge asymmetry in the jet-lepton invariant mass distribution have been shown in Figure 7.3 and 7.4. For both the NUHM-1 and NUHM-3 benchmark points, gluinos and left-chiral squarks have closely spaced masses. Therefore, the hard jets are produced either in the decay $\tilde{q}_L \to q\chi_2^0$ or in $\tilde{q}_R \to q\chi_1^0$, but not in whichever is allowed between $\tilde{g} \to q\tilde{q}_{L,R}$ or $\tilde{q}_{L,R} \to \tilde{g}q$. This is due to small mass splitting between them; even if the gluinos are lighter than the left-chiral squarks, the decay chain $\tilde{q}_L \to q\chi_2^0 \to ql_1^{\pm}\tilde{l}^{\mp} \to ql_1^{\pm}l_2^{\mp}\chi_1^0$ is still the dominant source of the opposite-sign-same-flavour dilepton signal, as the decay branching ratio of $\tilde{q}_L \to q\tilde{g}$ is very small ($\simeq$ 2% or less) due to phase-space suppression. The branching fraction for $\tilde{q}_L \to q\chi_2^0$ is $\simeq$ 32% and subsequently χ_2^0 decays into a $\tilde{l}^{\pm}l^{\mp}$ pair with a decay branching fraction ranging from 21%-29%, while the sleptons decay into a lepton and the lightest neutralino with 100% branching ratio.

It is clear from Figure 7.3a and 7.3b that both for NUHM-1 and NUHM-3 we get the desired charge asymmetry which is negative for increasing m_{jl}, since the lighter sleptons are dominantly left-chiral, and the leptons produced in χ_2^0 decay are mostly back-to-back with the quark while the antileptons are in the same direction to that of the quark, hence m_{jl^-} distribution has larger population than m_{jl^+} distribution near the end-point of m_{jl} invariant mass distribution.

The situation is somewhat more complicated for the corresponding mSUGRA points. For mSUGRA-1, the sleptons are heavier than the second lightest neutralino and the decay $\chi_2^0 \to \tilde{l}^{\pm}l^{\mp}$ is suppressed. Here the main source of the flavour subtracted opposite sign same flavour dilepton signal is the two step $\tilde{q}_L \to q\chi_2^0 \to ql^{\pm}l^{\mp}\chi_1^0$ decay chain rather than the three step decay chain considered earlier. In this case χ_2^0 decays into a $l^{\pm}l^{\mp}\chi_1^0$ pair via an off-shell slepton or Z. The sleptons are lighter than the second lightest neutralino and mostly dominated by the right-chiral component in mSUGRA-3. χ_2^0 follows its usual three step decay chain. The expected positive charge asymmetry is visible for both the mSUGRA-1 and mSUGRA-3 BP's (see Figure 7.4a and 7.4b).

7.6 Summary and conclusion

We have attempted a differentiation between mSUGRA and a scenario with non-universal Higgs masses. The extreme situation of large negative S, for which the characteristic features of the NUHM spectrum are most prominent, has been

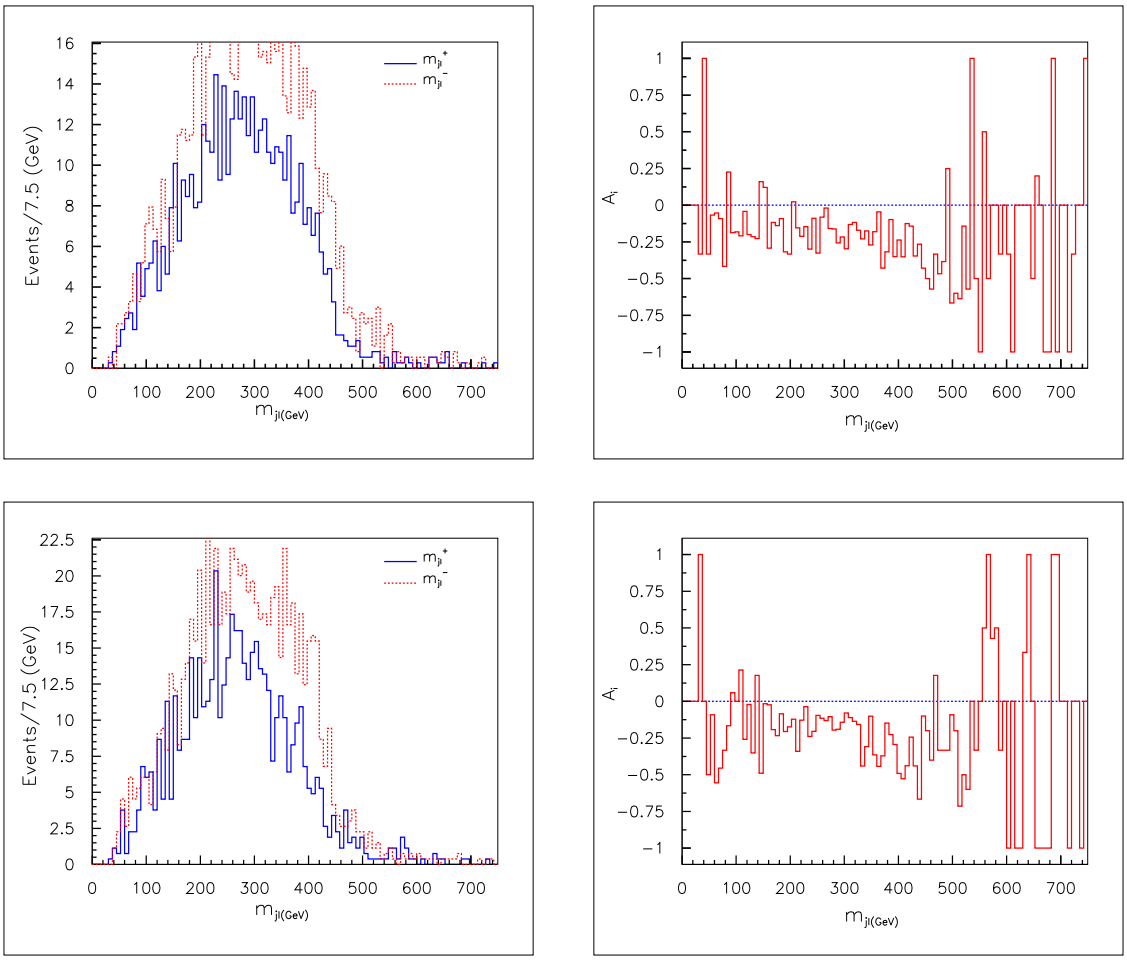

Figure 7.3: *a)* m_{jl} *(left) and b)* A_i *vs* m_{jl} *(right) distribution for NUHM BP1 (top) and NUHM BP3 (bottom). The event rates are predicted at an integrated luminosity of* 10 fb^{-1}.

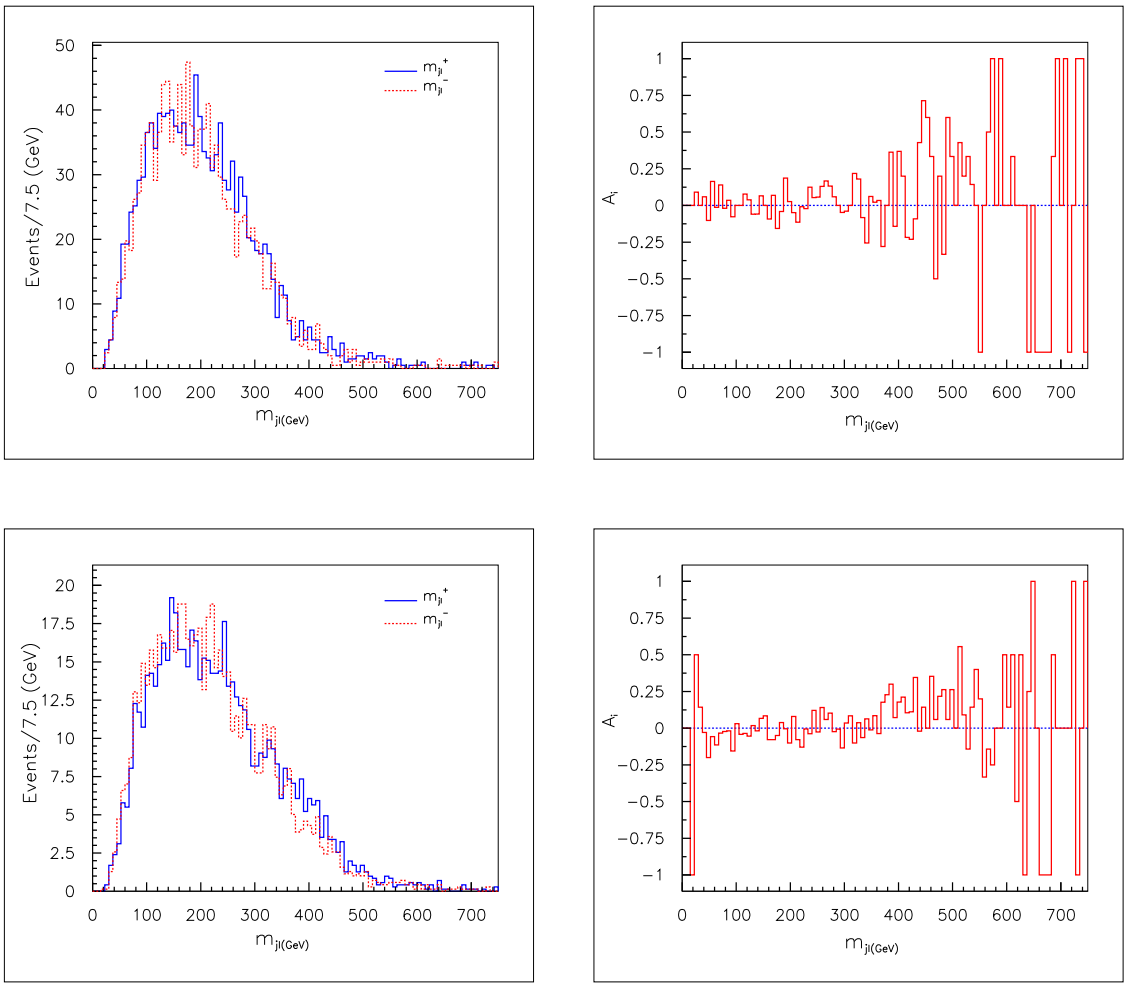

Figure 7.4: *a) m_{jl} (left) and b) A_i vs m_{jl} (right) distribution for mSUGRA points. The mSUGRA-1 (top) and mSUGRA-3 (bottom) corresponds to NUHM-1,and NUHM-3 benchmark points, respectively. The event rates are predicted at an integrated luminosity of* $10\ fb^{-1}$.

selected for this purpose, including three possible hierarchies among the masses of the lightest neutralino, the lighter stau and the tau-sneutrino. The primary channel of investigation being tau-rich, regions in the parameter spaces of both the scenarios, giving rise to similar ditau event rates, have been pitted against each other.

In the same-sign ditau channel, we find that the ratio defined as R, the fraction of the energy carried by the charged pion in a jet produced in one-prong tau-decays, is a rather useful differentiator. Because of the dependence of R on the polarisation of the tau, one ends up having different numbers of events for the two cases in the regions $R < 0.8$ and $R > 0.8$. The ratios of these two event numbers, in turn, display a concentration in different regions, depending on whether it is NUHM or mSUGRA.

We have further suggested the utilisation of signals involving leptons of the first two families, which are largely left chiral in NUHM. A bin-by-bin analysis of the of lepton-jet invariant masses exhibits a difference between the cases with negatively and positively charged leptons, whose general nature helps one distinguishing an NUHM scenario.

If SUSY is indeed discovered at the LHC, one will certainly wish to run the machine with large integrated luminosity, so as to reveal the nature of the underlying scenario. One important question to ask in this context will be whether Higgs mass(es) have different high-scale origins compared to masses of the other scalars, namely, squarks and sleptons. A study in the line suggested here, based on the polarisation study of tau as well as the first two family leptons, can be helpful in finding an answer to such a question.

Bibliography

[1] M. Dine, W. Fischler, Nucl. Phys. **B204**, 346 (1982); J. R. Ellis, L. E. Ibanez, G. G. Ross, Nucl. Phys. **B221**, 29-67 (1983); C. Kounnas, A. B. Lahanas, D. V. Nanopoulos, M. Quiros, Nucl. Phys. **B236**, 438 (1984); A. A. Anselm and A. A. Johansen, Phys. Lett. B **200** (1988) 331; N. Polonsky and A. Pomarol, Phys. Rev. Lett. **73** (1994) 2292 [arXiv:hep-ph/9406224]; R. Hempfling, Nucl. Phys. B **478** (1996) 3 [arXiv:hep-ph/9511288].

[2] J. R. Ellis, C. Kounnas and D. V. Nanopoulos, Nucl. Phys. B **247**, 373 (1984); J. R. Ellis, K. Enqvist, D. V. Nanopoulos and K. Tamvakis, Phys. Lett. B **155**, 381 (1985); M. Drees, Phys. Lett. B **158**, 409 (1985); A. Corsetti and P. Nath, Phys. Rev. D **64**, 125010 (2001) [arXiv:hep-ph/0003186]; S. Bhattacharya, A. Datta and B. Mukhopadhyaya, JHEP **0710**, 080 (2007) [arXiv:0708.2427 [hep-ph]]; S. Bhattacharya, A. Datta and B. Mukhopadhyaya, Phys. Rev. D **78**, 115018 (2008) [arXiv:0809.2012 [hep-ph]].

[3] N. Chamoun, C. -S. Huang, C. Liu, X. -H. Wu, Nucl. Phys. **B624**, 81-94 (2002) [hep-ph/0110332]; K. Huitu, J. Laamanen, Phys. Rev. **D79**, 085009 (2009) [arXiv:0901.0668 [hep-ph]]; S. P. Martin, Phys. Rev. D **79**, 095019 (2009) [arXiv:0903.3568 [hep-ph]]; S. Bhattacharya, J. Chakrabortty, Phys. Rev. **D81**, 015007 (2010) [arXiv:0903.4196 [hep-ph]].

[4] M. Drees, Phys. Lett. B **181** (1986) 279; J. S. Hagelin and S. Kelley, Nucl. Phys. B **342** (1990) 95; Y. Kawamura, H. Murayama and M. Yamaguchi, Phys. Lett. B **324** (1994) 52 [arXiv:hep-ph/9402254]; Y. Kawamura, H. Murayama and M. Yamaguchi, Phys. Rev. D **51** (1995) 1337 [arXiv:hep-ph/9406245]; A. Datta, A. Datta and M. K. Parida, Phys. Lett. B **431**, 347 (1998) [arXiv:hep-ph/9801242]; A. Datta, A. Datta, M. Drees, D. P. Roy, Phys. Rev. **D61**, 055003 (2000), [arXiv:hep-ph/9907444].

[5] F. Gabbiani, E. Gabrielli, A. Masiero and L. Silvestrini, Nucl. Phys. B **477**, 321 (1996) [arXiv:hep-ph/9604387]; M. Misiak, S. Pokorski and J. Rosiek, Adv. Ser. Direct. High Energy Phys. **15** (1998) 795 [arXiv:hep-ph/9703442]; J. Guasch and J. Sola, Nucl. Phys. B **562** (1999) 3 [arXiv:hep-ph/9906268].

[6] J. R. Ellis, K. A. Olive and Y. Santoso, Phys. Lett. B **539** (2002) 107, [arXiv:hep-ph/0204192]; J. R. Ellis, T. Falk, K. A. Olive and Y. Santoso, Nucl. Phys. B **652** (2003) 259, [arXiv:hep-ph/0210205].

[7] H. Baer, A. Mustafayev, S. Profumo, A. Belyaev and X. Tata, JHEP **0507**, 065

(2005), [arXiv:hep-ph/0504001]; J. R. Ellis, K. A. Olive and Y. Santoso, JHEP **0810** (2008) 005, [arXiv:0807.3736 [hep-ph]].

[8] A. Katz and B. Tweedie, Phys. Rev. D **81** (2010) 035012, [arXiv:0911.4132 [hep-ph]]; T. Figy, K. Rolbiecki and Y. Santoso, Phys. Rev. D **82**, 075016 (2010), [arXiv:1005.5136 [hep-ph]];

[9] U. Chattopadhyay and D. Das, Phys. Rev. D **79**, 035007 (2009) [arXiv:0809.4065 [hep-ph]]; S. Bhattacharya, U. Chattopadhyay, D. Choudhury, D. Das and B. Mukhopadhyaya, Phys. Rev. D **81**, 075009 (2010), [arXiv:0907.3428 [hep-ph]].

[10] S. Bhattacharya, S. Biswas, B. Mukhopadhyaya and M. M. Nojiri, arXiv:1105.3097 [hep-ph].

[11] M. M. Nojiri, Phys. Rev. D **51**, 6281 (1995), [arXiv:hep-ph/9412374].

[12] R. M. Godbole, M. Guchait and D. P. Roy, Phys. Lett. B **618**, 193 (2005), [arXiv:hep-ph/0411306]; R. M. Godbole, M. Guchait and D. P. Roy, Phys. Rev. D **79**, 095015 (2009), [arXiv:0807.2390 [hep-ph]]; M. Guchait and D. P. Roy, arXiv:0808.0438 [hep-ph].

[13] S. Y. Choi, K. Hagiwara, Y. G. Kim, K. Mawatari and P. M. Zerwas, Phys. Lett. B **648**, 207 (2007), [arXiv:hep-ph/0612237].

[14] P. Richardson, JHEP **0111**, 029 (2001), [hep-ph/0110108].

[15] A. J. Barr, Phys. Lett. B **596**, 205 (2004), [arXiv:hep-ph/0405052].

[16] T. Goto, K. Kawagoe, M. M. Nojiri, Phys. Rev. **D70**, 075016 (2004), [hep-ph/0406317]; S. K. Mandal, M. Nojiri, M. Sudano and T. T. Yanagida, JHEP **1101**, 131 (2011), [arXiv:1004.4164 [hep-ph]].

[17] S. P. Martin, arXiv:hep-ph/9709356, and references therein.

[18] A. Djouadi, J. L. Kneur and G. Moultaka, Comput. Phys. Commun. **176**, 426 (2007), [arXiv:hep-ph/0211331].

[19] C. Amsler *et al.* [Particle Data Group], Phys. Lett. B **667**, 1 (2008).

[20] A. Djouadi, M. Drees and J. L. Kneur, JHEP **0603**, 033 (2006), [arXiv:hep-ph/0602001].

[21] E. Komatsu *et al.* [WMAP Collaboration], Astrophys. J. Suppl. **192**, 18 (2011), [arXiv:1001.4538 [astro-ph.CO]].

[22] J. R. Ellis, K. A. Olive, Y. Santoso and V. C. Spanos, Phys. Lett. B **588**, 7 (2004), [arXiv:hep-ph/0312262]; J. L. Feng, S. Su and F. Takayama, Phys. Rev. D **70**, 075019 (2004), [arXiv:hep-ph/0404231].

[23] K. Hagiwara, A. D. Martin and D. Zeppenfeld, Phys. Lett. B **235**, 198 (1990); B. K. Bullock, K. Hagiwara and A. D. Martin, Phys. Rev. Lett. **67**, 3055 (1991).

[24] S. Raychaudhuri and D. P. Roy, Phys. Rev. D **52**, 1556 (1995), [arXiv:hep-ph/9503251].

[25] H. L. Lai *et al.* [CTEQ Collaboration], Eur. Phys. J. C **12**, 375 (2000), [arXiv:hep-ph/9903282].

[26] S. Jadach, J. H. Kuhn, Z. Was, Comput. Phys. Commun. **64**, 275-299 (1990); Z. Was, P. Golonka, Nucl. Phys. Proc. Suppl. **144**, 88-94 (2005), [hep-ph/0411377]; P. Golonka, B. Kersevan, T. Pierzchala, E. Richter-Was, Z. Was, M. Worek, Comput. Phys. Commun. **174**, 818-835 (2006), [hep-ph/0312240].

[27] T. Sjostrand, S. Mrenna and P. Skands, JHEP **0605**, 026 (2006), [arXiv:hep-ph/0603175].

[28] M. Muhlleitner, A. Djouadi and Y. Mambrini, Comput. Phys. Commun. **168**, 46 (2005) [arXiv:hep-ph/0311167].

[29] G. Marchesini, B. R. Webber, G. Abbiendi, I. G. Knowles, M. H. Seymour and L. Stanco, Comput. Phys. Commun. **67**, 465 (1992); G. Corcella *et al.*, JHEP **0101**, 010 (2001), [arXiv:hep-ph/0011363]; S. Moretti, K. Odagiri, P. Richardson, M. H. Seymour and B. R. Webber, JHEP **0204**, 028 (2002), [arXiv:hep-ph/0204123].

[30] F. E. Paige, S. D. Protopopescu, H. Baer and X. Tata, arXiv:hep-ph/0312045.

[31] E. Richter-Was, arXiv:hep-ph/0207355.

[32] The CMS Collaboration, CMS-TDR-8.1, CERN/LHCC 2006-001.

[33] G. Aad *et al.* [The ATLAS Collaboration], [arXiv:0901.0512].

Chapter 8

Summary and conclusions of the thesis

This thesis has aimed to study the collider aspects of some new physics scenarios in context of the Large Hadron Collider using various properties of tau-leptons. In chapter 1 we have tried to outline the existing standard model of particle physics and pointed out both its theoretical and experimental inadequacies. Supersymmetry which is a prototype of new physics scenario, has been discussed in detail in chapter 2.

Chapter 3 contains the cosmological and collider aspects of supersymmetric theories with a right-chiral neutrino superfield for each generation in order to incorporate the non-vanishing neutrino masses and mixings. We consider a supergravity (SUGRA) scenario, with universal scalar and gaugino masses at high scale. Such a scenario can have a lightest supersymmetric particle (LSP) dominated by the right sneutrino and a stau as the next-to lightest supersymmetric particle (NLSP). Since decays of all particles into the LSP are suppressed by the neutrino Yukawa coupling, the signal of supersymmetry consists in charged tracks of stable particles in the muon chamber.

In chapter 4, we demonstrate how neutralinos can be fully reconstructed over substantial areas in the SUGRA parameter space. To reconstruct the neutralino we have considered pair production of neutralinos in SUSY cascades. It further decays into a $\tilde{\tau}\tau$ pair. The final state consists of $2\tau_j + 2\tilde{\tau} + \not{E}_T + X$, where, X comprises of all the hard jets arising from SUSY cascades. Reconstruction of the neutralino requires the knowledge of four-momenta of tau as well as stau. We first reconstruct the two taus in the final state from the knowledge of total

$\not{E}_T$ of that event. The four-momentum of the stau (which shows up as a charged track in the muon chamber) is not completely known. From the bending of the track only its three momentum can be measured. To measure the mass of the particle (lighter stau) associated with the charged track we have prescribed a method of extracting it on a event-by-event basis. Then the mass of the neutralino can be obtained from the invariant mass distribution of the $\tilde{\tau}\tau$ pair.

Chapter 5 discusses the reconstruction of the lighter chargino considering the associated production of it with the neutralinos in SUSY cascades. The chargino further decays into a $\tilde{\tau}\nu_\tau$ pair and the neutralino on the other side decays into a $\tilde{\tau}\tau$ pair. The final state in this case consists of $\tau_j + 2\tilde{\tau} + \not{E}_T + X$. However, this final state can be faked by other SUSY processes. We have suggested a way of reducing these SUSY backgrounds imposing various cuts. The chargino mass, can then be found from the transverse mass distribution of the $\tilde{\tau}\nu_\tau$-pair, where we have also prescribed a way to find the transverse component of the four-momenta of the neutrino out of a chargino decay.

The reconstruction of the left-chiral tau sneutrino ($\tilde{\nu}_{\tau_L}$) has been discussed in chapter 6 in a way similar to that for the chargino. $\tilde{\nu}_{\tau_L}$ is predominantly produced in SUSY cascade via the decay of second lightest neutralino or the chargino and it further decays into a $\tilde{\tau}W$ pair. Therefore, we have an additional W in the final state in addition to that considered for chargino case, namely, $\tau_j + W + 2\tilde{\tau} + \not{E}_T + X$. We have suggested two different methods for reconstructing the mass of the left-chiral tau sneutrino. One of them is independent of the mass of the other SUSY particles whereas, the other one is more model dependent but has better signal to background ratio.

In all the above three cases, we conclude that using the available kinematic information of quasistable charged tracks and making use of various properties of tau-jets, it is possible to reconstruct faithfully the masses of the neutralinos, chargino and left-chiral tau-sneutrino. In some cases, the assumed luminosity is not too large, so that it is possible to explore some region of the parameter space even at the early phase of LHC run.

Chapter 7 discusses large non-universality in the Higgs sector at high scale in supersymmetric theories, in the context of the Large Hadron Collider (LHC). In particular, we note that if ${m_{H_u}}^2 - {m_{H_d}}^2$ is large and negative ($\simeq 10^6$ GeV^2) at high scale, the lighter slepton mass eigenstates at the electroweak scale are mostly left chiral, in contrast to a minimal supergravity (mSUGRA) scenario. We use this feature to distinguish between non-universal Higgs masses (NUHM) and mSUGRA by two methods. First, we study final states with same-sign ditaus. We find that an asymmetry parameter reflecting the polarisation of the taus provides a notable distinction. In addition, we study a charge asymmetry in the jet-lepton invariant mass distribution, arising from decay chains of left-chiral squarks leading to leptons of the first two families, which sets apart such an NUHM scenario.